

เอสเทอร์พีเคชั่นของโซลคีทาลและกรดเลวูลินิกบนตัวเร่งปฏิกิริยาวิวิธพันธุ์ชนิดกรด



บทคัดย่อและแฟ้มข้อมูลฉบับเต็มของวิทยานิพนธ์ตั้งแต่ปีการศึกษา 2554 ที่ให้บริการในคลังปัญญาจุฬาฯ (CUIR)  
เป็นแฟ้มข้อมูลของนิสิตเจ้าของวิทยานิพนธ์ ที่ส่งผ่านทางบัณฑิตวิทยาลัย

The abstract and full text of theses from the academic year 2011 in Chulalongkorn University Intellectual Repository (CUIR)  
are the thesis authors' files submitted through the University Graduate School.

วิทยานิพนธ์นี้เป็นส่วนหนึ่งของการศึกษาตามหลักสูตรปริญญาวิทยาศาสตรมหาบัณฑิต  
สาขาวิชาปิโตรเคมีและวิทยาศาสตร์พอลิเมอร์  
คณะวิทยาศาสตร์ จุฬาลงกรณ์มหาวิทยาลัย  
ปีการศึกษา 2559  
ลิขสิทธิ์ของจุฬาลงกรณ์มหาวิทยาลัย

ESTERIFICATION OF SOLKETAL AND LEVULINIC ACID OVER HETEROGENEOUS ACID CATALYSTS



A Thesis Submitted in Partial Fulfillment of the Requirements  
for the Degree of Master of Science Program in Petrochemistry and Polymer Science

Faculty of Science

Chulalongkorn University

Academic Year 2016

Copyright of Chulalongkorn University



สรกานต์ สุทินโน : เอสเทอร์ฟิเคชันของโซลคิตาลและกรดเลวูลินิกบนตัวเร่งปฏิกิริยาวิวิธพันธุ์ชนิดกรด (ESTERIFICATION OF SOLKETAL AND LEVULINIC ACID OVER HETEROGENEOUS ACID CATALYSTS) อ.ที่ปรึกษาวิทยานิพนธ์หลัก: รศ. ดร. ขวลิต งามจรัสศรีวิชัย, 99 หน้า.

งานวิจัยนี้ศึกษาเอสเทอร์ฟิเคชันของโซลคิตาลและกรดเลวูลินิกบนตัวเร่งปฏิกิริยาวิวิธพันธุ์ชนิดกรด ได้แก่ Amberlyst 15, Amberlyst 36 wet, HUSY zeolite, HMS-SO<sub>3</sub>H และ NR/HMS-SO<sub>3</sub>H ศึกษาผลของภาวะในการทำปฏิกิริยาต่อการเปลี่ยนของสารตั้งต้นและการกระจายตัวของผลิตภัณฑ์ โดยตัวแปรที่ศึกษา ได้แก่ เวลาในการทำปฏิกิริยา ชนิดของตัวเร่งปฏิกิริยา สัดส่วนโดยโมลของโซลคิตาลต่อกรดเลวูลินิก อุณหภูมิในการทำปฏิกิริยา และปริมาณของตัวเร่งปฏิกิริยา สำหรับการหาโครงสร้างทางเคมีของผลิตภัณฑ์รวมไปถึงผลิตภัณฑ์รวมที่เกิดขึ้นใช้เทคนิคแก๊สโครมาโทกราฟี-แมสสเปคโตรมิเตอร์ (GC-MS) ซึ่งผลิตภัณฑ์ประกอบด้วย โซลคิตาลเลวูลิเนต (SL) เฮมิแอซิทาลของโซลคิตาลเลวูลิเนต (H-SL) กรีเซอรอลเลวูลิเนต (GL) และโอลิโกเมอร์ (LGO) โซลคิตาลเลวูลิเนตถูกจัดให้เป็นผลิตภัณฑ์ปฐมภูมิ จากการวิเคราะห์ด้วยเทคนิคนิวเคลียร์แมกเนติกเรแนนซ์สเปคโตรสโคปี (NMR) แสดงให้เห็นว่า โอลิโกเมอร์มีโครงสร้างที่ถูกยุติสายโซ่ (Termination) ด้วยหมู่ที่ปลายของสายโซ่ (End group) ที่แตกต่างกันสามหมู่ ได้แก่ หมู่คีโท (KT), หมู่กลีเซอรอลคิตาล (GKT) และหมู่กลีเซอรอลเอสเทอร์ (GET) อย่างไรก็ตามน้ำที่อยู่ในตัวเร่งปฏิกิริยาและที่เกิดขึ้นจากปฏิกิริยาเอสเทอร์ฟิเคชัน เป็นสาเหตุของปฏิกิริยาไฮโดรไลซิสของโซลคิตาล ทำให้พบกลีเซอรอลในทุกการทดลอง และยังส่งผลให้เกิดผลิตภัณฑ์อื่นอีกหลายชนิด เนื่องจากเอสเทอร์ฟิเคชันเป็นปฏิกิริยาที่สามารถเกิดขึ้นได้เอง แต่การเปลี่ยนของสารตั้งต้นและผลได้ของผลิตภัณฑ์นั้นไม่สูงมากและใช้เวลานานในการทำปฏิกิริยา ดังนั้นตัวเร่งปฏิกิริยาชนิดกรดจึงถูกนำมาใช้ ปฏิกิริยาเอสเทอร์ฟิเคชันเป็นปฏิกิริยาคูดความร้อน ดังนั้นการเพิ่มอุณหภูมิทำให้การเปลี่ยนของสารตั้งต้นและผลได้ของผลิตภัณฑ์ให้สูงขึ้น อิทธิพลของสัดส่วนโดยโมลของโซลคิตาลต่อกรดเลวูลินิกทำให้ปฏิกิริยาดำเนินไปข้างหน้า และพบ LGO ในปริมาณมาก ในขณะที่อิทธิพลของปริมาณตัวเร่งปฏิกิริยา พบว่าสามารถควบคุมความจำเพาะของผลิตภัณฑ์ได้ ซึ่งภาวะที่เหมาะสมสำหรับปฏิกิริยาเอสเทอร์ฟิเคชันของโซลคิตาลและกรดเลวูลินิก คือ การใช้ Amberlyst 15 เป็นตัวเร่งปฏิกิริยา โดยใช้ปริมาณตัวเร่งปฏิกิริยาที่ 5 % เทียบกับน้ำหนักของกรดเลวูลินิก อุณหภูมิในการทำปฏิกิริยาที่ 120 องศาเซลเซียส เป็นเวลา 5 ชั่วโมง ซึ่งทำให้การเปลี่ยนของสารตั้งต้นสูง และลดการเกิดกลีเซอรอลอีกด้วย

สาขาวิชา ปิโตรเคมีและวิทยาศาสตร์พอลิเมอร์ ลายมือชื่อนิสิต .....

ปีการศึกษา 2559

ลายมือชื่อ อ.ที่ปรึกษาหลัก .....

# # 5672213123 : MAJOR PETROCHEMISTRY AND POLYMER SCIENCE

KEYWORDS: LEVULINIC ACID / ESTERIFICATION / SOLKETAL

SORRAKAN SUTINNO: ESTERIFICATION OF SOLKETAL AND LEVULINIC ACID OVER HETEROGENEOUS ACID CATALYSTS. ADVISOR: ASSOC. PROF. CHAWALIT NGAMCHARUSSRIVICHAI, Ph.D., 99 pp.

This work studied the esterification of solketal (SK) and levulinic acid (LA) over heterogeneous acid catalysts, including Amberlyst 15, Amberlyst 36 wet, HUSY zeolite, HMS-SO<sub>3</sub>H and NR/HMS-SO<sub>3</sub>H. The effect of reaction conditions on the reactants conversion and products distribution were studied such as reaction time, molar ratio of SK: LA, reaction temperature and catalyst loading. Gas chromatography with mass spectroscopy (GC-MS) was used to identify the chemical structure all of components in the products mixture. The products mixture is composed of solketal levulinate (SL), hemiacetal of solketal levulinate (H-SL), glycerol levulinate (H-SL) and oligomers (LGO). SL is considered as the primary product. Nuclear magnetic resonance (NMR) was used to identify the chemical structure of LGO. These oligomers was terminated by three different end groups, including keto terminal (KT), glycerol-ketal terminal (GKT), and glycerol-ester terminal (GET). However, water which located inside the catalyst and generated from esterification cause of hydrolysis and other larger products formation. Glycerol was found in all of experiments. It was obtained from SK hydrolysis. Typically, esterification is a spontaneous reaction but it was provided a low of the reactants conversion and products yield, and also takes long reaction time so adding acid catalyst is used. Esterification is an endothermic reaction so increasing the reaction temperature, the reactants conversion and product yield was increased. The effect of SK: LA molar ratio was enhanced the reaction forward and LGO was found as a major component. The effect of catalyst loading can be controlled the product selectivity. The optimum reaction conditions were used Amberlyst 15 as a catalyst at 5 wt.% respect to LA and reaction temperature at 120 °C for 5 h to achieve the higher conversion and minimize the glycerol formation.

Field of Study: Petrochemistry and Polymer Student's Signature .....

Science

Advisor's Signature .....

Academic Year: 2016

## ACKNOWLEDGEMENTS

I would like to take this opportunity to express my deepest gratitude to all those persons who have given their invaluable support and assistance.

I would like to express my sincere gratitude to advisor, Assoc. Prof. Dr. Chawalit Ngamcharussrivichai for his patience and guidance that I have been able to complete my study. I would like to thank for his encouragement and valuable comments.

I also would like to acknowledge Assist. Prof. Dr. Warinthorn Chavasiri, Dr. Varagorn Hengpunya, and Assist. Prof. Dr. Thongthai Witoon for serving as the chairman and members of thesis committee, respectively and for their worthy comments and suggestions.

Many thanks are going to all of instruments and equipments of the Department of Chemical Technology, Chulalongkorn University. I gratefully acknowledge the funding support from Program in Petrochemistry and Polymer Science and Graduate School Thesis Grant, Chulalongkorn University.

Finally, I would like to express my gratitude to my beloved family for their love, understanding and great support in my study. Also, special thanks are expended to my relation friends for their help and encouragement.

## CONTENTS

	Page
THAI ABSTRACT .....	iv
ENGLISH ABSTRACT .....	v
ACKNOWLEDGEMENTS .....	vi
CONTENTS .....	vii
LIST OF TABLE .....	x
LIST OF FIGURES .....	xi
CHAPTER I INTRODUCTION .....	1
1.1 The State of Problem.....	1
1.2 Objectives of the Research Work .....	4
1.3 Scope of the Research Work.....	5
CHAPTER II THEORY AND LITERATURE REVIEWS .....	6
2.1 Levulinic Acid.....	6
2.2 Solketal.....	14
2.3 Esterification of Alcohol and Carboxylic Acid.....	18
2.4 Acid Catalysts.....	21
2.5 Alkyl Levulinate Esters (ALs) .....	28
2.6 Literature Reviews.....	32
2.6.1 Levulinic acid.....	32
2.6.2 Solketal .....	33
2.6.3 Alkyl levulinate esters.....	33
2.6.4 Levulinic acid–glycerol ketal–ester oligomers.....	34
CHAPTER III EXPERIMENT AND ANALYTICAL METHOD .....	36

3.1 Materials and Chemical Reagents.....	36
3.1.1 Commercial catalysts used for esterification .....	36
3.1.2 Chemical reagents for preparation of HMS-SO <sub>3</sub> H and NR/HMS-SO <sub>3</sub> H.....	36
3.1.3 Chemical Reagents for esterification.....	36
3.1.4 Chemical reagents for products characterization using gas chromatography.....	37
3.2 Equipments and Apparatus.....	37
3.3 Catalyst Characterization .....	38
3.3.1 X-ray Powder diffraction (XRD).....	38
3.3.2 N <sub>2</sub> adsorption-desorption measurement .....	39
3.3.3 Thermogravimetric/differential thermal analysis (TG/DTA).....	40
3.4 Catalyst Preparation.....	41
3.5 Esterification of SK and LA over Heterogeneous Acid Catalysts.....	45
3.6 Products Characterization.....	47
CHAPTER IV RESULTS AND DISCUSSION.....	52
4.1 Catalyst Characterization .....	52
4.1.1 Structural properties .....	52
4.1.2 Textural Properties .....	54
4.1.3 Sulfur content and acidity .....	56
4.2 Esterification of Solketal and Levulinic Acid.....	58
4.2.1 Identification of reaction products.....	58
4.2.2 Effects of reaction conditions.....	63
4.2.2.1 Effect of reaction time.....	63



	Page
4.2.2.2 Effect of catalyst type .....	64
4.2.2.3 Effect of SK: LA molar ratio .....	69
4.2.2.4 Effect of reaction temperature .....	73
4.2.2.5 Effect of catalyst loading .....	75
4.2.2.6 Elimination of water in the reaction.....	78
4.2.3 Plausible the reaction pathway .....	78
4.2.4 Deactivation of Amberlyst 15 catalyst .....	80
CHAPTER V CONCLUSION AND RECOMMENDATIONS .....	83
5.1 Conclusion .....	83
5.1 Recommendations .....	84
REFERENCES .....	85
APPENDICES.....	92
Appendix A The Calibration Curves of Solketal and Levulinic acid .....	93
Appendix B The Calibration Curves of Glycerol .....	95
Appendix C Fragmentation Ions patterns .....	96
VITA.....	99

## LIST OF TABLE

<b>Table 1.1</b> The reaction conditions used for esterification SK and LA over heterogeneous acid catalysts.....	5
<b>Table 2.1</b> Physical properties of LA.....	7
<b>Table 2.2</b> Homogeneous acid catalysis of various bio-based feedstock for LA production.....	11
<b>Table 2.3</b> Heterogeneous acid catalysis of various bio-based feedstock for LA production.....	12
<b>Table 2.4</b> The physical properties of SK.....	15
<b>Table 2.5</b> Summary of catalysts and reaction conditions used for SK production.....	17
<b>Table 2.6</b> The major differences between homogeneous and heterogeneous catalysts [36].....	22
<b>Table 2.7</b> Synthesis of alkyl levulinates (ALs) from levulinic acid over heterogeneous acid catalysts.....	31
<b>Table 3.1</b> The analysis conditions of GC Agilent Technologies 7890A GC equipped with DB-5 HT column.....	49
<b>Table 3.2</b> The analysis conditions of GC-MS Agilent Technologies 7890B GC equipped with HP-5 column.....	50
<b>Table 4.1</b> Physicochemical properties of heterogeneous acid catalysts used in this work.....	57
<b>Table 4.2</b> Assignment of peaks observed from GC-MS chromatogram.....	59
<b>Table A1</b> The molar ratio and peak area ratio of SK to internal standard for plot the calibration curve of SK.....	93
<b>Table A2</b> The molar ratio and peak area ratio of LA to internal standard for plot the calibration curve of LA.....	93
<b>Table B1</b> The molar ratio and peak area ratio of glycerol to internal standard for plot the calibration curve of glycerol.....	95

## LIST OF FIGURES

<b>Figure 1.1</b> Top 12 value-added chemicals derived from biomass [1]. .....	1
<b>Figure 1.2</b> Acid-catalyzed synthesis and application of alkyl levulinates [3]. .....	3
<b>Figure 1.3</b> Ketalization of glycerol with acetone in the presence of acid catalyst [7, 8]. .....	3
<b>Figure 1.4</b> Esterification of solketal and levilinic acid over heterogeneous acid catalyst. ....	4
<b>Figure 2.1</b> Chemical structure of LA. ....	7
<b>Figure 2.2</b> Production of LA in the presence of hydrochloric acid [11]. ....	8
<b>Figure 2.3</b> Reaction pathway for conversion of hexose sugar to LA [9]. ....	9
<b>Figure 2.4</b> Synthesis of LA from pentose sugar [9]. ....	9
<b>Figure 2.5</b> LA as a platform molecule for producing other industrial chemicals and products [12]. ....	14
<b>Figure 2.6</b> Ketalization of glycerol with acetone in the presence of acid catalyst. ....	14
<b>Figure 2.7</b> General esterification of alcohol and carboxylic acid in presence of catalyst. ....	19
<b>Figure 2.8</b> The model of seven steps of heterogeneous catalytic reaction [36]. ....	23
<b>Figure 2.9</b> (A) The schematic structure and (B) SEM image of Amberlyst 15 [39, 40]. ....	25
<b>Figure 2.10</b> HUSY zeolite. ....	26
<b>Figure 2.11</b> The HMS-SO <sub>3</sub> H catalyst. ....	27
<b>Figure 2.12</b> The NR/HMS-SO <sub>3</sub> H catalyst. ....	28
<b>Figure 2.13</b> Esterification synthesis of alkyl levulinates. ....	29

<b>Figure 3.1</b> X-ray diffractometer of (A) Rigaku Ultima III and (B). Bruker D8 Discover. ..	39
<b>Figure 3.2</b> Micromeritics ASAP 2020 surface area and porosity analyzer.....	40
<b>Figure 3.3</b> Perkin Elmer Pyris Diamond Thermogravimetric/differential thermal analyzer. ....	41
<b>Figure 3.4</b> The proposed pathway for synthesis of HMS-SO <sub>3</sub> H [41]. ....	42
<b>Figure 3.5</b> The flowchart diagram for synthesis of HMS-SO <sub>3</sub> H. The inset table shows the molar ratio was used. ....	43
<b>Figure 3.6</b> The proposed pathway for synthesis of NR/HMS-SO <sub>3</sub> H [41].....	44
<b>Figure 3.7</b> The flowchart diagram for synthesis of NR/HMS-SO <sub>3</sub> H. The inset table shows the molar ratio was used. ....	45
<b>Figure 3.8</b> The equipment set up for esterification.....	46
<b>Figure 3.9</b> Flow diagram of the esterification. ....	47
<b>Figure 3.10</b> The flowchart diagram of sample preparation for GC analysis. ....	48
<b>Figure 3.11</b> GC Agilent Technologies 7890A GC system equipped with DB-5 HT column.....	49
<b>Figure 3.12</b> GC Agilent Technologies 7890B GC-MS system equipped with HP-5 column.....	50
<b>Figure 3.13</b> The temperature program for analyzing products from esterification of SK and LA. ....	51
<b>Figure 4.1</b> XRD patterns of HMS-SO <sub>3</sub> H and NR/HMS-SO <sub>3</sub> H. The inset table shows structural data of both materials.	52
<b>Figure 4.2</b> XRD patterns of HUSY zeolites. ....	53
<b>Figure 4.3</b> N <sub>2</sub> adsorption-desorption isotherms of HMS-SO <sub>3</sub> H and NR/HMS-SO <sub>3</sub> H.....	54
<b>Figure 4.4</b> BJH pore size distribution of HMS-SO <sub>3</sub> H and NR/HMS-SO <sub>3</sub> H.....	55
<b>Figure 4.5</b> N <sub>2</sub> adsorption-desorption isotherm of calcined HUSY zeolite. ....	56

<b>Figure 4.6</b> Representative GC-MS chromatogram of the reaction mixture obtained from the esterification of LA and SK. ....	58
<b>Figure 4.7</b> (A) $^1\text{H}$ and (B) $^{13}\text{C}$ NMR spectra of reaction mixture. (C) shows an enlarged $^{13}\text{C}$ spectrum in the $\delta$ range of 60–80 ppm. ....	61
<b>Figure 4.8</b> Assignment of $^{13}\text{C}$ NMR signals of the oligo(levulinic acid-co-glycerol) repeating unit (RU) with different terminal groups: keto terminal (KT), glycerol-ketal terminal (GKT), and glycerol-ester terminal (GET). ....	62
<b>Figure 4.9</b> Conversion of (▲) SK and (●) LA in the esterification of SK and LA over Amberlyst 15 (solid line) and blank (dash line). Reaction conditions: SK: LA molar ratio, 1:1; reaction temperature, 120 °C; Amberlyst 15 loading, 5 wt.% respect to LA. ....	63
<b>Figure 4.10</b> Conversion of SK and LA in the esterification of SK and LA in the presence of different acid catalysts. The amount of sulfuric acid used was 0.05 wt.% respect to LA. Reaction conditions: SK: LA molar ratio, 1:1; catalyst loading, 5 wt.%; temperature, 120 °C; time, 5 h. ....	66
<b>Figure 4.11</b> Products distribution in the esterification of SK and LA in the presence of r different acid catalysts. The amount of sulfuric acid used was 0.05 wt.% respect to LA. Reaction conditions: SK: LA molar ratio, 1:1; catalyst loading, 5 wt.%; temperature, 120 °C; time, 5 h. ....	66
<b>Figure 4.12</b> The glycerol yield obtained from the esterification of SK and LA in the presence of r different acid catalysts. The amount of sulfuric acid used was 0.05 wt.% respect to LA. Reaction conditions: SK: LA molar ratio, 1:1; catalyst loading, 5 wt.%; temperature, 120 °C; time, 5 h. ....	67
<b>Figure 4.13</b> Hydrolysis of SL. ....	68
<b>Figure 4.14</b> Ketolization/esterification of glycerol and LA in the presence of acid catalyst. ....	68

- Figure 4.15** The glycerol yield obtained from the esterification of SK and LA Amberlyst 15. A SK: LA molar ratio was varied at, (◆) 3:1, (▲) 1:1, (■) 1:2, and (●) 1:3. Other reaction conditions: catalyst loading, 5 wt.%; temperature, 120 °C. ... 70
- Figure 4.16** Effect of SK: LA molar ratio on the products distribution obtained from the esterification of SK and LA over Amberlyst 15. Reaction conditions: catalyst loading, 5 wt.%; time, 5 h; temperature, 120 °C. .... 71
- Figure 4.17** Effect of reaction temperature on the conversion of SK (open symbol) and LA (filled symbol) attained from the esterification of SK and LA over Amberlyst 15. Reaction conditions: SK: LA molar ratio, 1:1; catalyst loading, 5 wt.% respect to LA. The reaction temperature was varied at (triangle) 65 °C, (square) 80 °C, and (circle) 120 °C. .... 73
- Figure 4.18** The glycerol yield obtained from the esterification of SK and LA over Amberlyst 15 at (triangle) 65 °C, (square) 80 °C, and (circle) 120 °C. Reaction conditions: SK: LA molar ratio, 1:1; catalyst loading, 5 wt.% respect to LA. .... 74
- Figure 4.19** The products distribution obtained from the esterification of SK and LA over Amberlyst 15. Reaction conditions: SK: LA molar ratio, 1:1; catalyst loading, 5 wt.% respect to LA. The reaction temperature was varied at at (▧) 65 °C, (▣) 80 °C, and (▢) 120 °C. .... 75
- Figure 4.20** Effect of catalyst loading on the SK and LA conversion obtained from the esterification of SK and LA over Amberlyst 15. Reaction conditions: SK: LA molar ratio, 1:1; temperature, 120 °C; time, 5 h. .... 76
- Figure 4.21** Effect of catalyst loading on the glycerol yield obtained from the esterification of SK and LA over Amberlyst 15. Reaction conditions: SK: LA molar ratio, 1:1; temperature, 120 °C; time, 5 h. .... 77
- Figure 4.22** Effect of catalyst loading on the products distribution obtained from the esterification of SK and LA over Amberlyst 15. Reaction conditions: SK: LA molar ratio, 1:1; temperature, 120 °C; time, 5 h. .... 77

<b>Figure 4.23</b> The proposed reaction pathway in the esterification of SK and LA to various products. ....	78
<b>Figure 4.24</b> Weight loss and DTG curves of (A) fresh Amberlyst 15 and (B) deconvolution of DTG curve. ....	81
<b>Figure 4.25</b> Weight loss and DTG curves of (A) spent Amberlyst 15 and (B) deconvolution of DTG curve. ....	82
<b>Figure A1</b> The calibration curve of SK. ....	94
<b>Figure A2</b> The calibration curve of LA. ....	94
<b>Figure B1</b> The calibration curve of glycerol. ....	95
<b>Figure C1</b> Fragmentation pattern of SK. ....	96
<b>Figure C2</b> Fragmentation pattern of LA. ....	96
<b>Figure C3</b> Fragmentation pattern of glycerol. ....	97
<b>Figure C4</b> Fragmentation pattern of SL. ....	97
<b>Figure C5</b> Fragmentation pattern of H-SL. ....	98
<b>Figure C6</b> Fragmentation pattern of GL. ....	98

## CHAPTER I

### INTRODUCTION

#### 1.1 The State of Problem

Ester-based lubricant oil is a class of synthetic lubricants with excellent properties for preventing corrosion and decreasing friction force. Because of a high polarity of oxygen atoms containing in the ester group, the ester oil has a high adhesion to metal surface with positive charge. Moreover, the synthetic esters have various advantages, such as nontoxicity, biodegradability, high pour point and high viscosity index. Monoester is a kind of ester-based lubricant oil, which can be produced by esterification of alcohol with long-chain carboxylic acid in the presence of acid catalyst. This ester oil has a good performance in various applications because it has lower flow resistance, resulted from a high viscosity index. The monoester-based lubricants are also used as base oils for formulating engine oil, hydraulic oil, drilling mud fluids, additive carrier and grease.

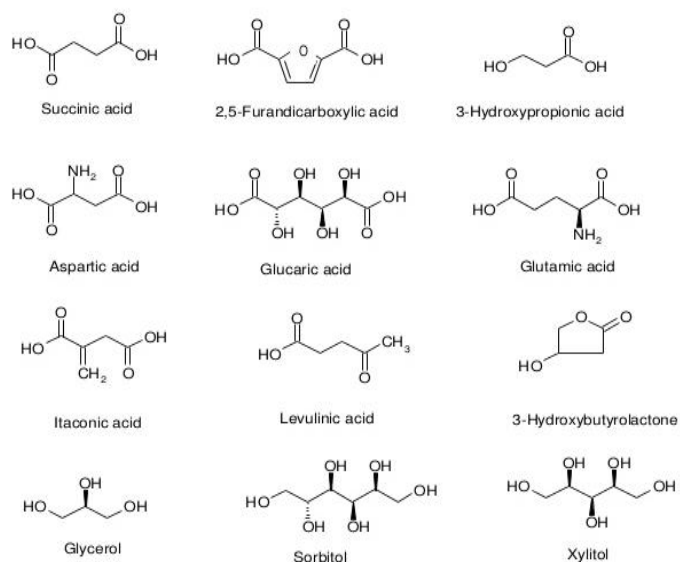


**Figure 1.1** Top 12 value-added chemicals derived from biomass [1].

Over the past few years, public awareness on issues, such as environmental pollution, public health aspects and energy crisis, have increased. A substantial



amount of research is currently being carried out worldwide to identify attractive chemical transformations of biomass into bulk organic chemicals. According to the report by the Pacific Northwest National Laboratory (PNNL) and the National Renewable Energy Laboratory (NREL), Department of Energy, USA, in 2004, *Top Value Added Chemicals from Biomass Volume I—Results of Screening for Potential Candidates from Sugars and Synthesis Gas*, there are 12 bio-based chemicals, which are potentially used as platform molecules for producing high value products and specialties, including 4-oxopentanoic acid (levulinic acid) and glycerol [1]. Figure 1.1 shows the top 12 bio-based chemicals screened by PNNL and NREL.

4-Oxapentanoic acid, well-known as levulinic acid (LA) is a sugar-based platform molecule produced via hydrolysis of cellulose and hemicellulose. It can be converted to higher value-added chemicals, such as 1,4-pentanediol,  $\gamma$ -valerolactone and diphenolic acid [2]. Moreover, LA is an important substance for synthesis of alkyl levulinates (ALs). Around 150 years ago, the synthesis of ALs from esterification of LA with methanol, ethanol and propanol was studied [3]. Later, around 40 years, Sah and Schuette reported about the synthesis of ALs using several alcohols as reactants in the presence of HCl [4, 5]. The ALs produced can be used as diesel and biodiesel additives or applied to flavor and fragrance industries. The ALs synthesized with long chain alcohols are potential biolubricants [6]. Nowadays, there are many routes for the synthesis of ALs, from different types of bio-based chemicals such as carbohydrate and furfuryl alcohol, in the presence of acid catalysts. Figure 1.2 shows the acid catalyzed synthesis and the application of ALs.

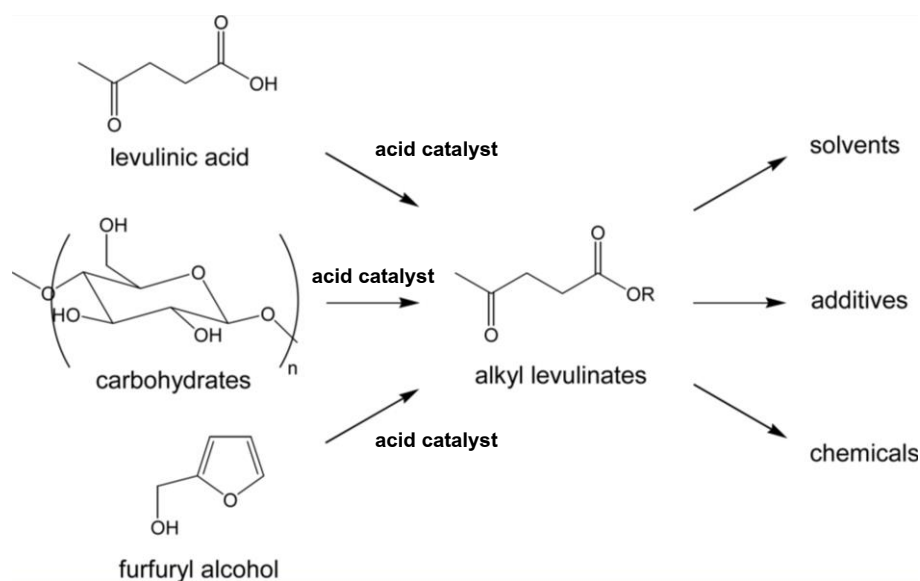


**Figure 1.2** Acid-catalyzed synthesis and application of alkyl levulinates [3].

Glycerol is a colorless, viscous and hygroscopic trihydric alcohol. It is a by-product from biodiesel production. The transesterification of triglycerides with methanol is currently route for the biodiesel production to generate fatty acid methyl esters (FAMES) and glycerol. Typically, around 10 kg of glycerol was generated from 100 kg of biodiesel produced. Glycerol is a potential precursor for synthesis of various high value-added chemicals and products used in the area of fuels, detergents, pharmaceuticals, food and cosmetics. It has an excellent biodegradability and low toxicity to aquatic organism. (2,2-Dimethyl-1,3-dioxolan-4-yl)methanol or DL-1,2-isopropylidenglycerol or solketal (SK) is obtained by ketalization of glycerol with acetone in the presence of acid catalyst as shown in Figure 1.3. It can be used as a fuel additive to improve octane number up to 2.5 points and reduce gum formation in gasoline, to improve cold flow properties in diesel fuel, surfactant, and to reduce particles emission [7, 8].

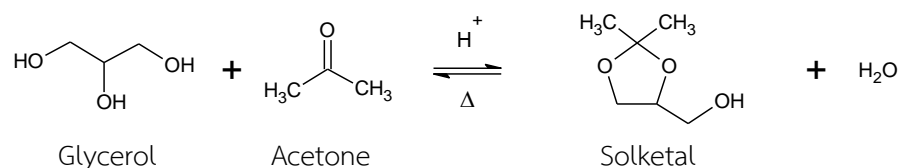


**Figure 1.3** Ketalization of glycerol with acetone in the presence of acid catalyst [7, 8].

Normally, homogeneous acid catalyst was commonly used such as  $\text{H}_2\text{SO}_4$ ,  $\text{HCl}$ , *p*-Toluenesulfonic acid (*p*-TSA) and  $\text{HNO}_3$  etc. These acids have drawbacks, which are corrosive to the reactor, neutralize after reaction requirement and difficultly separation from the products mixture. Alternatively, heterogeneous acid catalyst such as, zeolite, heteropoly acid, ion-exchanged resins or activated carbon, etc. were found in the industrial application because their advantages for example, selective and easy to handle, reduced reactor corrosive and easily separated and recycled.

This research was focused on the synthesis of solketal levulinate (SL) *via* the esterification of SK with LA by using various solid acid catalysts, including acidic ion-exchanged resins, HUSY,  $\text{HMS-SO}_3\text{H}$  and  $\text{NR/HMS-SO}_3\text{H}$ . The influences of reaction temperature, reaction time, molar ratio of SK to LA and catalyst loading on the reactants conversion and the products selectivity were studied. Figure 1.4 shows the esterification of SK and LA over heterogeneous acid catalyst to produce SL. The SL obtained is expected to be a new class of ester-based lubricants.

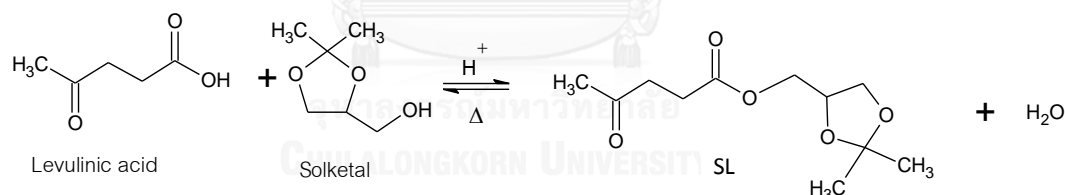


**Figure 1.4** Esterification of solketal and levulinic acid over heterogeneous acid catalyst.

## 1.2 Objectives of the Research Work

1. To study the esterification of solketal and levulinic acid over heterogeneous acid catalysts
2. To investigate effects of reaction conditions on the esterification of solketal and levulinic acid over heterogeneous acid catalysts

### 1.3 Scope of the Research Work

This study was separated into 5 parts.

1. Study the physicochemical properties of various heterogeneous acid catalysts, including crystallinity, thermal stability, and specific surface area and porosity by using following techniques:
  - Crystallinity : X-ray powder diffraction (XRD)
  - Thermal stability : Nitrogen (N<sub>2</sub>) adsorption-desorption measurement
  - Specific surface area and porosity : Thermogravimetric/differential-thermal analysis (TG/DTA)
2. Study the reaction conditions used for esterification of SK and LA over heterogeneous acid catalysts following Table 1.1

**Table 1.1** The reaction conditions used for esterification SK and LA over heterogeneous acid catalysts

Parameter	Value
Reaction temperature	65 °C–120 °C
Reaction time	0–5 h
Amount of catalyst loading <sup>1</sup>	1–8 wt.%
Molar ratio of SK to LA	1:1–3:1

<sup>1</sup>Respect to weight of LA used

3. Identify the reaction products by gas chromatography with mass spectrometer (GC-MS) and Nuclear magnetic resonance (NMR). The reaction pathways for the formation of different products are proposed.
4. Evaluate the conversion of LA and SK, yield and products distribution of products after the esterification by gas chromatography (GC)
5. Summation of the results and write thesis

## CHAPTER II

### THEORY AND LITERATURE REVIEWS

Due to the declining of petroleum resources and the world energy crisis in this century, biomass is potentially an alternative and environmentally friendly resource for sustainable energy production. Biomass can be converted to various chemicals and products in a broad range of applications, such as fine chemicals, pharmaceuticals, food, cosmetics, and petroleum-substituted fuels. Lignocellulose is one of the most economic raw materials derived from biomass. It is composed of lignin, cellulose and hemicellulose. Lignin is recognized as a source of aromatic molecules, presenting in form of three-dimensional polymeric network of methoxylated phenyl propane units. Moreover, cellulose and hemicellulose are carbohydrate-type polymers, which are constituted of glucose and different types of sugar, respectively. Depolymerization of cellulose and hemicellulose gives sugars, such as xylose, mannose, glucose and etc. It can be transformed to commodity platform chemicals (e.g., sorbitol, furans) [3].

#### 2.1 Levulinic Acid

4-oxopentanoic acid or levulinic acid (LA) is a sugar-derived platform chemical, which can be produced from hydrolysis of hexose sugars in the presence of acid catalyst. It is consisted of ketone group and acidic carboxyl group in the same molecule. LA is a colorless with a caramellic odor and soluble in water. It has molecular weight of  $116 \text{ g mol}^{-1}$ , boiling point of  $245 \text{ }^\circ\text{C}$ , melting point of  $33 \text{ }^\circ\text{C}$  and density around  $1.1447 \text{ g cm}^{-3}$  [9, 10]. LA has a high solubility in water, ethanol, ether, acids, chloroform, 1,4-dioxane, DMSO, etc. Moreover, it has a pKa of 4.59 in water at  $25 \text{ }^\circ\text{C}$  [10]. Figure 2.1 shows the chemical structure of LA. Table 2.1 summaries the properties of LA.

In 2004, National Renewable Energy Laboratory (NREL, USA) classified top 12 bio-based chemicals potentially being used as platform molecules, including LA, glycerol and their derivatives [1].

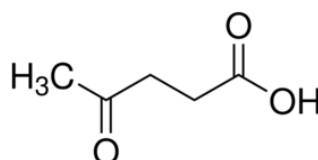


**Figure 2.1** Chemical structure of LA.

**Table 2.1** Physical properties of LA

Properties	
Chemical formula	$C_5H_8O_3$
Molar mass	$116.11 \text{ g mol}^{-1}$
Density	$1.1447 \text{ g cm}^{-3}$
Melting point	33 to 35°C (91 to 95°F; 306 to 308 K)
Boiling point	245 to 246°C (473 to 475°F; 518 to 519 K)

In 1840, the Dutch professor of chemistry, Dr. Gerardus Johannes Mulder (1802-1880), had reported the synthesis of LA by boiling fructose in HCl solution. 5-hydroxymethylfurfural (HMF) was assumed as an intermediate. The production of LA in the presence of hydrochloric acid is shown in Figure 2.2 [11]. According to the production of LA from hexose sugar, formic acid was formed as a by-product. It is a low-value commodity chemical, which is used for production of formaldehyde, rubber, plasticizers, pharmaceuticals and textiles [9].

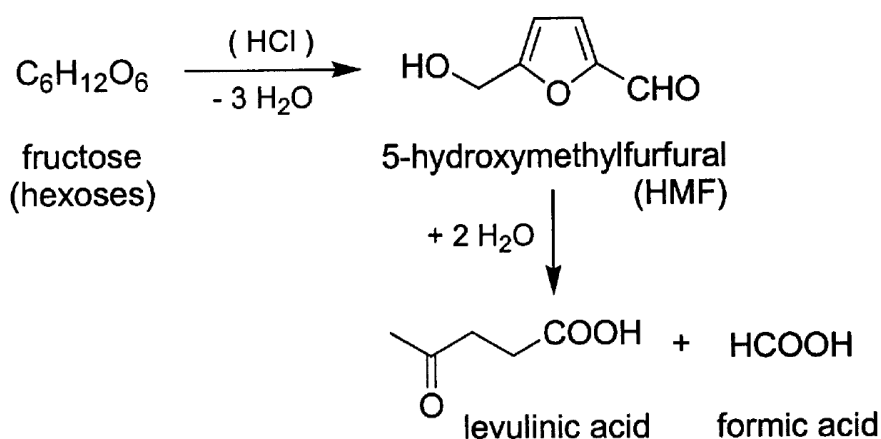


**Figure 2.2** Production of LA in the presence of hydrochloric acid [11].

In laboratory scale, LA is produced via two pathways in which hexose or pentose are used as reactants. Firstly, the reaction pathway for conversion of hexose or sugar to LA is shown in Figure 2.3 [9]. The hexose sugars (e.g. D-glucose, and D-fructose) are hydrolyzed in the acid condition to become HMF, which is considered as intermediate. D-glucose can be isomerized into D-fructose prior to its conversion to HMF. Furthermore, the hydrolysis of HMF gives LA and formic acid. Formic acid is formed as a by-product [9]. Alternatively, pentose sugars are hydrolyzed to generate furfural. In this pathway, furfuryl alcohol is obtained by hydrogenation of furfural. For LA, it is formed by hydrolysis of furfuryl alcohol. The synthesis of LA from pentose sugars is shown in Figure 2.4 [9].

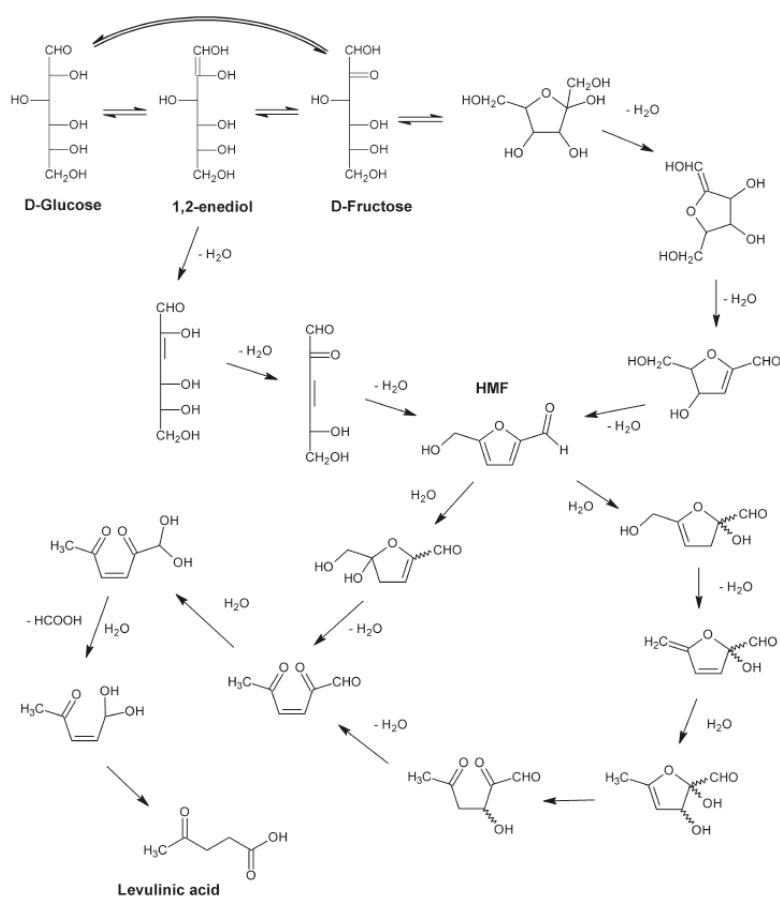


Figure 2.3 Reaction pathway for conversion of hexose sugar to LA [9].

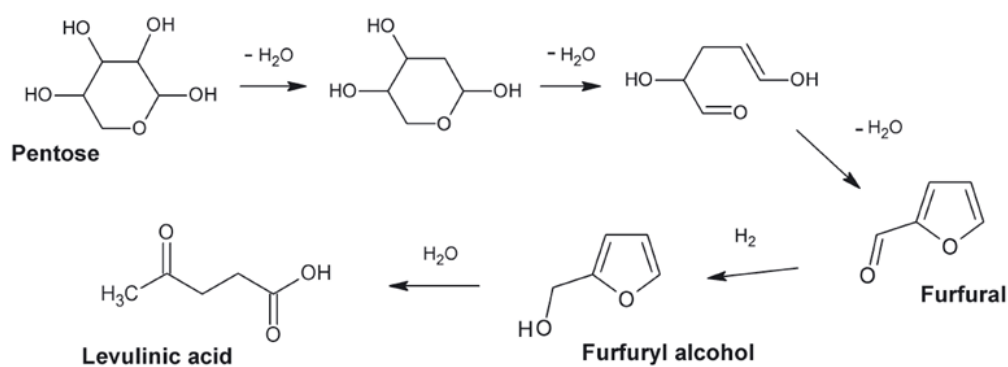


Figure 2.4 Synthesis of LA from pentose sugar [9].

Several researches on LA production from sugars, cellulose and biomass have been performed using mineral acid catalysts (HCl and H<sub>2</sub>SO<sub>4</sub>). Table 2.2 summarizes the homogeneous acid catalysts and reaction conditions used for LA production. The LA yield was obtained around 80 mol% under the optimized reaction conditions



when using sugars (fructose and glucose) and other raw materials (pulp residues, wheat straw, and bagasse) as feedstock. Except for sugars and starch, pretreatment is required in order to depolymerization of biomass to access the cellulose. According to the literature, the effect of processing conditions, including, acid concentration (3.5–10 wt.%) and temperature (95–220 °C), on LA production was investigated. Interestingly, the commercial process of LA production currently uses pulp residue as raw material, so called Biofine™ technology. This technology involves a two-stage acid-catalyzed reaction process. In the first stage, a plug flow reactor is used to dehydrate feed to HMF at temperature between 210–230 °C and pressure <3 MPa for very short time (30 s). LA is then produced in the second reactor at 195–215° C (around 1.5 MPa) for 15 to 30 min. At the second stage, formic acid and furfural are kept in the vapour phase in order to purify the product. The cost of LA can be reduced to approximately US\$ 0.2/kg by expanding the production of the Biofine™ technology. However these costs do not include the recovery of capital investment [9, 12].

Alternatively, heterogeneous acid catalysts are used for the LA synthesis from lignocellulosic biomass feedstock because they are selective, easy to handle, non-corrosive, easily separated and recycled [10, 13]. Table 2.3 summarizes the heterogeneous acid catalysts and reaction conditions used for the LA production from various feedstock. Sugars (fructose, glucose and sucrose) were used as feedstock for the LA synthesis. The solid catalysts studied included Amberlite IR–120 [14], LZY zeolite [15], Clay catalyst [16], HY zeolite, and Resin–Dowex [17]. In this case, using of 50 wt.% LZY zeolite catalyst for the production of LA from fructose achieved the highest yield of up to 43 mol% at 140 °C for 15 h. On the other hand, for cellulose as feedstock, Nafion SAC–13 was used as solid acid catalyst [18]. It give a low LA yield of 9 mol% although a high temperature (190 °C) and long reaction time (24 h) were used. In 2007, Buana et al. proposed the synthesis of LA by transformation of HMF at a high yield of 70 mol% when the process was conducted at 116 °C for 2 h over 5 wt.% ZSM-5 [19].

**Table 2.2** Homogeneous acid catalysis of various bio-based feedstock for LA production

Feedstock	Catalyst	Concentration (wt.%)	Operating temperature (°C)	Yield (mol%)	Ref.
Fructose	HCl	3.6-7.2	95	80	[12]
Glucose	H <sub>2</sub> SO <sub>4</sub>	5	170	80	[9]
Starch	H <sub>2</sub> SO <sub>4</sub>	6	200	66	[9]
Paper	H <sub>2</sub> SO <sub>4</sub>	5	<240	60	[9]
Pulp residues	H <sub>2</sub> SO <sub>4</sub>	1-5	1 <sup>st</sup> stage : 210 - 230	70-80	[9]
			2 <sup>nd</sup> stage : 195 - 215		
Wheat straw	H <sub>2</sub> SO <sub>4</sub>	3.5	210	68	[9]
	HCl	4.5	220	79	[12]
Sorghum grain	H <sub>2</sub> SO <sub>4</sub>	8	200	45	[9]
Bagasse	HCl	4.5	220	82	[12]
Water hyacinth	H <sub>2</sub> SO <sub>4</sub>	10	175	53	[9]

**Table 2.3** Heterogeneous acid catalysis of various bio-based feedstock for LA production

Feedstock	Catalyst	Catalyst loading (wt.%)	Process conditions		Yield (mol%)	Ref.
			Temperature (°C)	Time (h)		
Fructose	Amberlite IR-120	19	25	27	23	[14]
	LZY zeolite	50	140	15	43	[15]
Glucose	Amberlite IR-120	19	25	124	5	[14]
	Clay catalyst	3	150	24	12	[16]
	HY zeolite	3	150	24	6	[16]
Sucrose	Amberlite IR-120	19	25	41	15	[14]
	Resin-Dowex	6	100	24	24	[17]
Cellulose	Nafion SAC-13	3	190	24	9	[18]
HMF	ZSM-5	5	116	2	70	[19]

LA is recognized as a potential building block for production of a broad range of compounds [1]. Figure 2.5 displays some possible derivatives of LA.

The family of LA derivatives is quite broad, such as diphenolic acid (DPA), 5-aminolevulinic acid,  $\gamma$ -valerolactone (GVL), 2-methyltetrahydrofuran, and levulinate esters, etc. DPA or 4,4-bis-(4-hydroxyphenyl)pentanoic acid is prepared by the condensation of LA with two molecules of phenol. DPA is expected as a substitute for bisphenol A, a primary raw material of epoxy resin and polycarbonates, which is widely used as a chemical intermediate in the paint formulation, protective and decorative coatings [13]. 5-aminolevulinic acid is a natural substance presenting in plant and animal cells. It is used as an ingredient of herbicides. Moreover, it has also been used as an insecticide and for cancer treatment [18].  $\gamma$ -valerolactone (GVL) is proposed to be used as fuel additive. It has low melting point (-31 °C), high boiling point (207 °C) and low flash point (96 °C). GVL has similar properties to ethanol in fuel additive applications [14]. 2-Methyltetrahydrofuran is an organic compound, which has a highly flammable mobile liquid. It was reported for blending 70% (w/w) in gasoline [13]. Levulinate esters are produced by esterification of LA and alcohols. By using short-chain alcohols such as ethanol, methanol, butanol, etc., the levulinate esters obtained have similar properties to fatty acid methyl esters (FAME) as biodiesel [10]. On the other hand, the esterification of LA with long-chain alcohols, is a way to produce long-chain ester with lubricity properties [6, 20].

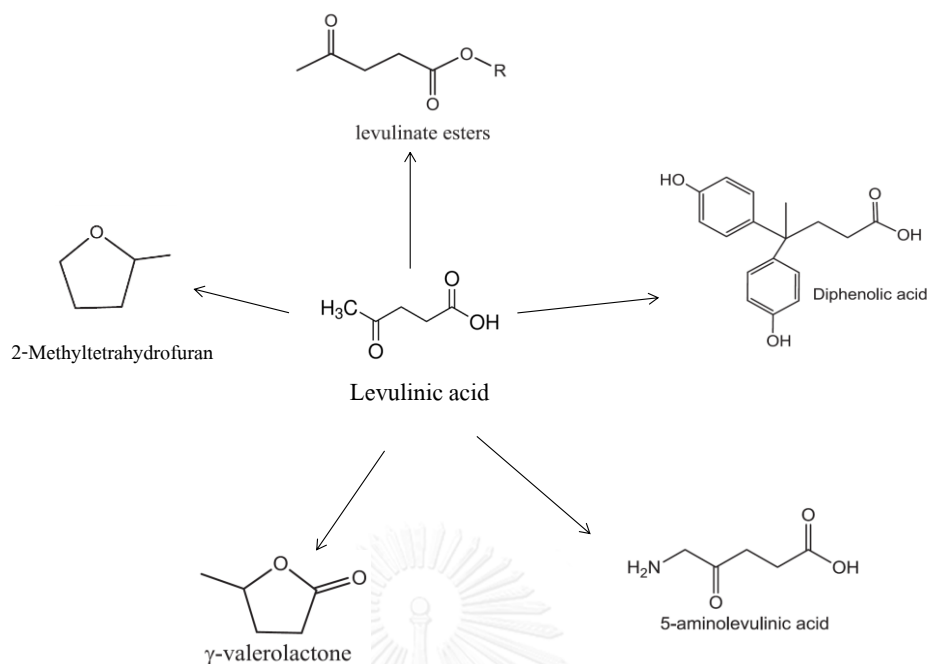


**Figure 2.5** LA as a platform molecule for producing other industrial chemicals and products [12].

## 2.2 Solketal

2,2-Dimethyl-1,3-dioxolane-4-methanol, D,L-1,2-isopropylidene glycerol isopropylidene glycerol, better known industrially as solketal (SK), is the major product obtained from ketalization of glycerol with acetone in the presence of acid catalyst as shown in Figure 2.6. Table 2.4 summarizes the physical properties of SK.

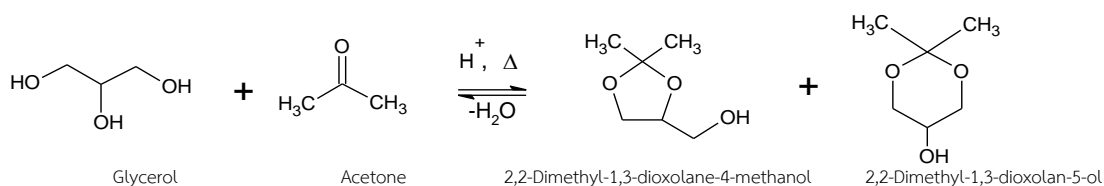


**Figure 2.6** Ketalization of glycerol with acetone in the presence of acid catalyst.

**Table 2.4** The physical properties of SK

Properties	
Chemical formula	$C_6H_{12}O_3$
Molar mass	$132.16 \text{ g mol}^{-1}$
Density	$1.062 \text{ g cm}^{-3}$ at $25^\circ\text{C}$
Boiling point	188 to $189^\circ\text{C}$ ( $370$ to $372^\circ\text{F}$ ; 461 to 462 K)
Appearance	clear colorless liquid
Flash point	$80^\circ\text{C}$ ( $176^\circ\text{F}$ ; 353 K)
Solubility in water	Miscible
Solubility	Miscible in most organic solvents (alcohols, ethers, hydrocarbons)

Ketalization of glycerol and acetone gives a high selectivity around 98 % to SK, which is a five-membered ring isomer. Furthermore, the formation of 2,2-dimethyl-1,3-dioxan-5-ol, as a six-membered ring isomer, is much less selective (<2%). Several studies had reported that SK has a significant potential for being applied as fuel additives and biofuels. It may be suitably used as additive for the formation of gasoline, diesel and biodiesel. Moreover, it can be used to improve fuel properties, decrease viscosity, and obtain standard requirements of biodiesel flash point and oxidation stability [21]. Interestingly, the esterification of SK with long-chain fatty acids, for example caprylic acid, lauric acid, palmitic acid, and stearic acid in the presence of 5 wt.% *p*-toluenesulfonic acid was performed successfully at 80-99 mol% yield of the fatty acid solketal esters (FASEs). These compounds have an excellent lubricity [22].

The SK synthesis has been investigated using homogeneous acid catalysts ( $H_2SO_4$ , HCl, and PTSA) or heterogeneous acid catalysts (zeolites, clays, and Amberlyst resins) [4-6, 9, 21, 23-30]. Table 2.5 summarizes the catalysts and reaction conditions used for the SK synthesis.

In 2011, Suriyaprapadilok et al. [7] proposed the synthesis of SK by using 1 wt.% PTSA as Brønsted acid at glycerol: acetone the molar ratio of 1:6 at 100 °C for 8 h. This reaction gave 80 mol% of glycerol conversion. Later, in 2013, Menezes et al. [23] studied the synthesis of SK by using SnCl<sub>2</sub> as Lewis acid catalyst at room temperature under solvent-free conditions. This system gave the glycerol conversion and the SK selectivity of 81 and 98 mol%, respectively. Recently, several studies had proposed the heterogeneous acid catalysts for the ketalization of glycerol and acetone. H-Beta zeolite [31], activated carbon [8], and Al-SBA-15 [29] exhibited the glycerol conversion of 86, 64, 75 mol%, and the SK selectivity of 98, 94, 99 mol%, respectively. In 2014, Nanda et al. [24] reported the new continuous-flow process for the ketalization of glycerol and acetone and screening the solid catalysts, for example Amberlyst 35, Amberlyst 36 wet, zeolite beta (CP 814 C), montmorillonite (K10), zirconium sulphate hydrate, and Polymax (845). The reaction was performed under continuous flow reactor at 1: 6 molar ratio of glycerol: acetone at 40 °C and 600 psi for 4 h. By comparing the glycerol conversion, the catalytic activity was ranked in the following decreasing order: Amberlyst 36 wet (89) > Amberlyst 35 > zeolite beta (CP 814 C) > zirconium sulphate hydrate > montmorillonite (K10) > Polymax (845) as shown in Table 2.5. Nowadays, SK is synthesized in laboratory scale to find its applications.

**Table 2.5** Summary of catalysts and reaction conditions used for SK production

Catalyst	Ratio (glycerol: acetone)	Conditions				Glycerol conversion (mol%)	SK yield (mol%)	SK selectivity (mol%)	Ref.
		Temperature (°C)	Time (h)	Pressure (psi)	Catalyst loading (wt.%)				
<i>p</i> -Toluenesulfonic acid	1:06	100	8	N/A	1	80	N/A	N/A	[7]
H-Beta zeolite	1:02	room temp.	1	N/A	5	86	N/A	98	[31]
Activated carbon	1:01	80	6	N/A	2.7	64	N/A	94	[8]
SnCl <sub>2</sub>	1:04	25	1.5	N/A	1	81	N/A	98	[23]
Amberlyst 35 dry	1:06	40	4	600	N/A	88	86	N/A	[24]
Amberlyst 36 wet	1:06	40	4	600	N/A	89	88	N/A	
Zeolite beta (CP 814 C)	1:06	40	4	600	N/A	85	84	N/A	
Montmorillonite (K10)	1:06	40	4	600	N/A	69	68	N/A	
Zirconium sulphate hydrate	1:06	40	4	600	N/A	79	77	N/A	
Polymax (845)	1:06	40	4	600	N/A	61	60	N/A	
Al-SBA-15	1:01	100	4	N/A	N/A	75	N/A	99	[29]

N/A. = not available.



### 2.3 Esterification of Alcohol and Carboxylic Acid

Esterification is an important reaction, which is widely used in various industries, such as fragrances, cosmetics, pharmaceuticals, foods and flavors, etc. The main product obtained from this reaction is an ester compound. For example, isoamyl acetate, also known as isopentyl acetate, is synthesized from isoamyl alcohol and acetic acid. It is colorless and slightly soluble in water but very soluble in organic solvents. Isoamyl acetate has a strong odor, which is similar to both banana and pear. It is added as a banana flavor in food [32]. Moreover, esterification is an initial step in synthesis of ester-based polymers (i.e. poly(ethylene terephthalate) or PET), which is an important material for textile and food packaging industries [33]. Recently, fatty acid solketal ester (FASEs) which has interesting properties as fuel additives such as better ignition and/or lubricity was synthesized by esterification of fatty acid (palmitic acid and stearic acid) with SK in the presence of 5 wt.% of PTSA at 60 °C [22].

Esterification can be performed without adding catalysts due to the weak acidity of carboxylic acids themselves. But the reaction is extremely slow and requires several days to reach equilibrium at typical reaction conditions. Using of acid catalyst promotes the protonation of the carbonyl oxygen on the carboxylic group, thereby activating nucleophilic attack by an alcohol to form a tetrahedral intermediate [34].

Generally, esterification is conducted by heating the alcohol ( $R'-OH$ ) and carboxylic acid ( $R-COOH$ ) to obtain the ester product ( $R-COO-R'$ ) with using acid catalyst. It is performed under batch conditions in the presence of homogeneous acid catalyst. A strong Bronsted acid, such as sulfuric acid and hydrochloric acid, is commonly used. The general esterification of alcohol and carboxylic acid in presence of catalyst is shown in Figure 2.7.

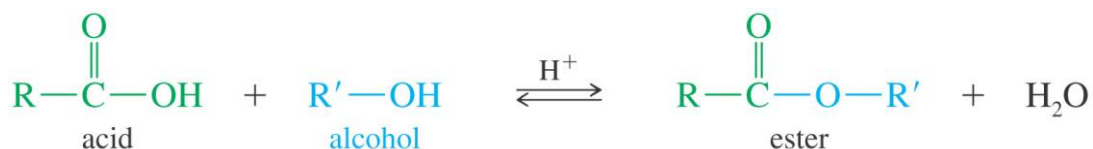
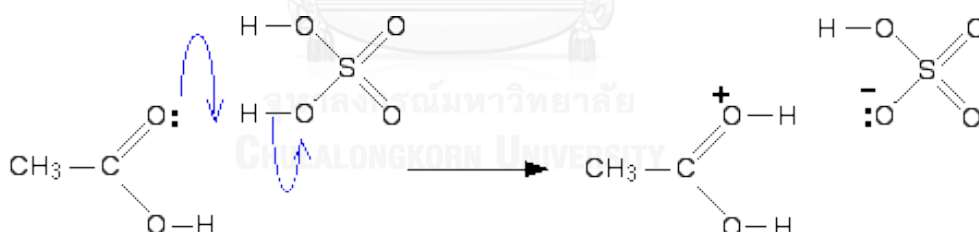


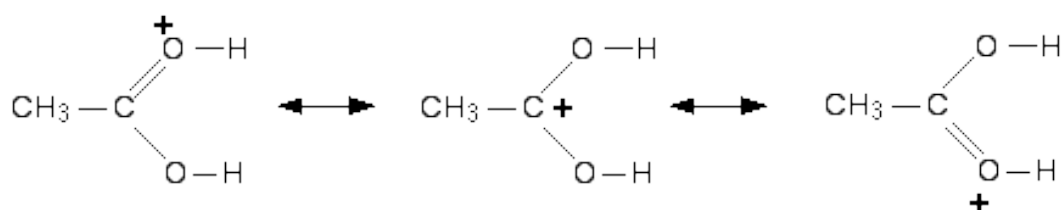
**Figure 2.7** General esterification of alcohol and carboxylic acid in presence of catalyst.

The proposed mechanism of esterification (ethanol react with acetic acid in the presence of sulfuric acid) is shown below [34]. For all of the steps in the mechanism below, they are expressed as one-way reactions in order to avoid the mechanism look less confusing. The reverse reaction is actually done sufficiently differently that it affects the way the mechanism is written below;

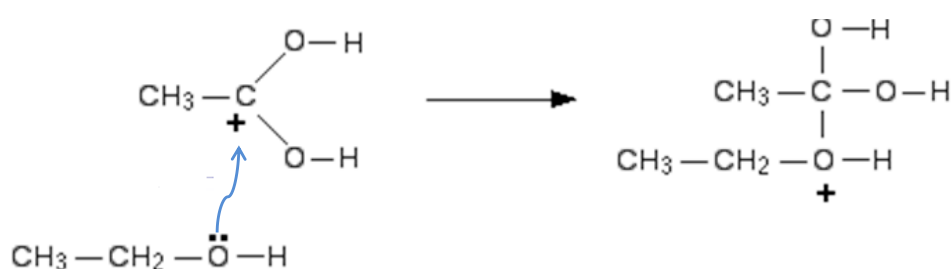
- Step 1: Acetic acid takes a proton (a hydrogen ion) from the concentrated sulfuric acid. The proton becomes attached to one of the lone pairs on the oxygen which is double-bonded to the carbon.



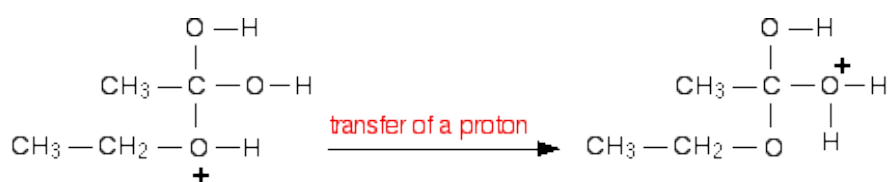
Then, the protonated carboxylic acid is delocalized in order to form the carbocation. The double headed arrows are considered that each of the individual structures makes a contribution to the real structure of the ion. The delocalized structures are known as resonance structures or canonical forms.



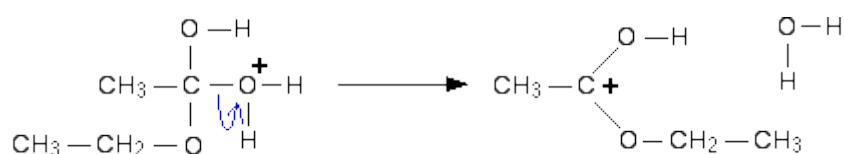
- Step 2: The lone pair electron of ethanol is attacked at the positive charge of the carbocation of protonated acetic acid. The tetrahedral intermediate is obtained. This step is the rate determining step of esterification.



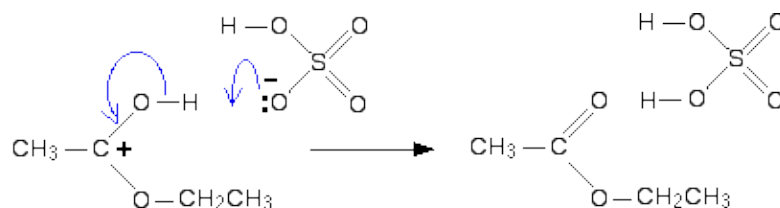
- Step 3: This step is occurred by the rearrangement of the intermediate which is transferring of a proton. A proton (a hydrogen ion) gets transferred from the bottom oxygen atom to one of the others. It gets picked off by one of the other substances in the mixture (for example, by attaching to a lone pair on an unreacted ethanol molecule), and then dump back onto one of the oxygen more or less at random.



- Step 4: Water molecule is eliminated from the carbocation. It was considered as by-product of esterification.



- Step 5: The lone pair electron from the acid catalyst attacks to the hydrogen atom in the carbocation. The carbocation which loosing proton is rearranged to become the ester product (ethyl acetate). Moreover, the catalyst not only consumed in the reaction but also can be catalyzed again.



## 2.4 Acid Catalysts

Catalyst is a substance, which assists the reaction to achieve a higher conversion and yield and accelerates the rate of a chemical reaction. Although some reactions are spontaneous, catalyst is used in order to increase the reaction rate to reach the reaction equilibrium faster. It is not consumed and does not appear in the overall reaction equation. It is written above the reaction arrow as shown in Figure 2.7. This indicates that a catalyst is needed for the reaction to attain equilibrium and accelerates the rate of the reaction. For example, the esterification of carboxylic acids with alcohols takes place in the presence of acids catalyst and the hydrolysis of esters [32-35]. Catalysts were classified in 2 types which are homogeneous and heterogeneous catalysts. For homogeneous catalysis, it has the same phase as the reactants. Mineral acids, which is a type of homogeneous catalyst, it was commonly used in the industries and academic researches such as  $\text{H}_2\text{SO}_4$ ,  $\text{HCl}$ , PTSA and  $\text{HNO}_3$  etc. These acids have drawbacks which are corrosive to the reactor, neutralize after reaction requirement and difficultly separation from the products mixture etc., [32-38]. On the other hand, heterogeneous catalysis has a difference phase from the reactants. In this case, phase means solid, liquid, gas and also immiscible liquids, e.g. water and oil. However, using of heterogeneous acid catalyst can be separated from

the mixture products easily [38]. The major differences between homogeneous and heterogeneous catalysts are summarized in the Table 2.6.

**Table 2.6** The major differences between homogeneous and heterogeneous catalysts [36].

items	Catalyst	
	Homogeneous	Heterogeneous
Thermal stability	Mild (<250 °C)	High (250-500°C)
Activity	High	Moderate
Selectivity	High	Low
Active site	Single	Multiple
Diffusion	Easy	Difficult
Heat transfer	Easy	Difficult
Products separation	Difficult	Easy
Catalyst recovery	Difficult and expensive	Easy and cheap

According to the reaction catalyzed by solid catalysts occurs where the reactant molecules come in contact with the active sites, which are located inside the catalyst pores. The catalytic reaction occurs after the reactant molecules diffuse through the fluid layer surrounding the catalyst particles (external diffusion or film diffusion), then through the pore with in the particle (internal diffusion). However, the diffusion of molecules is not only hindered by the other molecules, but also by the physical hindrances. Generally, heterogeneous catalyst has seven step of mass transfer, which occurred in the surfaces of the catalysts [36, 37]. Figure 2.8 shows the classical seven steps for a heterogeneous catalytic reaction [36]. The classical seven steps for a catalytic reaction are described following;

First step, the reactant diffuses from the bulk phase (boundary layer) to the external surface of the catalyst pellet (film diffusion or interphase diffusion). This step is called external diffusion. Second step, it is called internal pore diffusion. The reactant from the pore mouth diffuses through the catalyst pores in to the internal

catalytic surface. These two steps are depended on the physical of the reactant. Next, this step is adsorption of reactants on the inner catalytic surface. The reactant is adsorbed on the active site of the catalyst. Next step, the chemical reaction is performed on the surface of the catalyst. This step is considered as reactant changed to product. After that, product from the inner surface is desorbed from the active site on the surface of the catalyst. Then, the product diffuses from the internal surface of the catalyst to the pore mouth (external surface of the catalyst). Finally, the product from the external surface diffuses to the bulk mixture [36, 37].

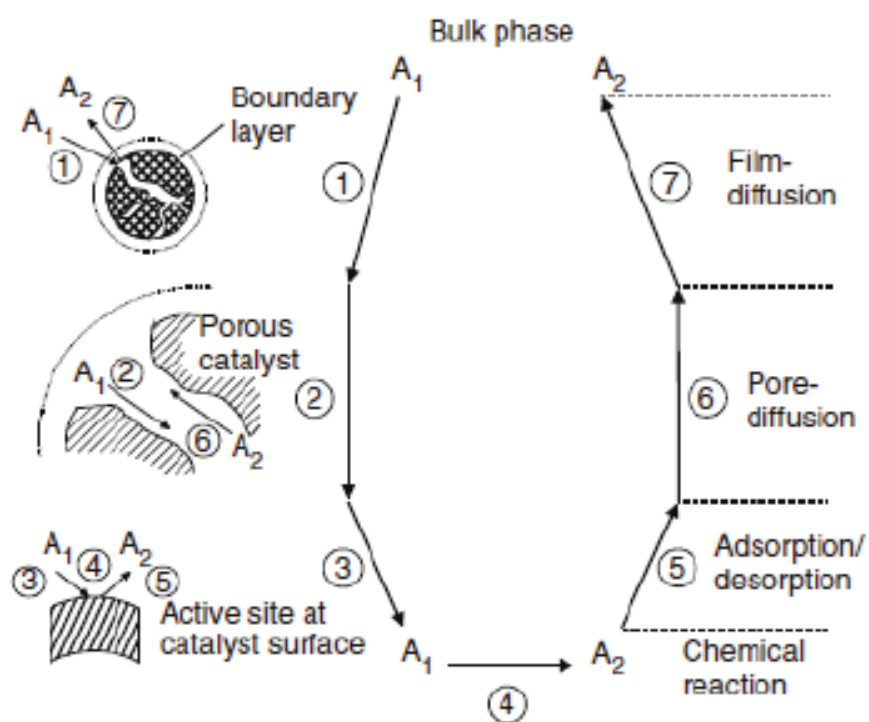


**Figure 2.8** The model of seven steps of heterogeneous catalytic reaction [36].

Typically, the catalyst is composed of two components which are active part and supporter or carrier. Hence, the best supporter should have high surface area and high stability in reaction temperature and pressure. However, a few of catalysts have only active part, so it can be promoted by adding promoter in order to increase the activity and selectivity of the catalyst. The active part is classified in four groups by

their functions which are metal, metal oxide, bifunctional catalyst and acid catalyst [36, 37].

Because of the several advantages of heterogeneous catalysts for example high reaction temperature and pressure resistance, easily for the separation from product mixture, and high mechanical strength. Heterogeneous catalyst is widely used in the industries which generally in the solid form. It is always use in the reaction of liquid and gas reactant.

In the reaction of liquid reactant, it is added with the reactant in the reactor. After the reaction is completed, the catalyst is separated centrifugation. The product is purified by distillation or evaporator. Moreover, in the reaction of gas reactant, the catalyst is packed in the reactor in order to passing of gas reactant which is reacted on the surface of the catalyst. The product is obtained from the reaction is flowed in the other side.

This study is focused on the acid catalyst for the esterification of SK and LA. The interested acid catalysts are showed below;

- *Acidic ion-exchanged resins (Amberlyst<sup>®</sup> series)*

Acidic ion-exchanged resins or Amberlyst<sup>®</sup> series are composed of copolymer polystyrene crosslinked with divinyl benzene and sulfonation with olem sulfuric acid [35, 39] This copolymer is very stable and hardly dissolved in the solvent. Because of Amberlyst<sup>®</sup> series are solid catalyst with high acid content and strong acid site so were used in industries. Generally, Amberlyst<sup>®</sup> series are classified in two types, which are macroreticular and Amberlyst with gel in the center. For macroreticular, it has shape of pore constantly for example Amberlyst 15 and Amberlyst 35. The other type has the distribution in pore size such as Amberlyst 131 and Amberlyst 33.

For this work, Amberlyst 15 and Amberlyst 36 wet were used to study the esterification of SK and LA. For Amberlyst 15, it is able to resist at low reaction temperature around 120 °C thus it is not suitably used under severe conditions. It has acidity of 4.7 mmol H<sup>+</sup> g<sup>-1</sup>, specific surface area of 53 m<sup>2</sup> g<sup>-1</sup> and pore size of 30 nm. In the other hand, Amberlyst 36 wet has higher thermal stability than Amberlyst 15 (around 150 °C). It has acidity of 5.4 mmol H<sup>+</sup> g<sup>-1</sup>, specific surface area of 33 m<sup>2</sup> g<sup>-1</sup> and pore size of 24 nm. Figure 2.9 shows the schematic structure and SEM image of Amberlyst 15.

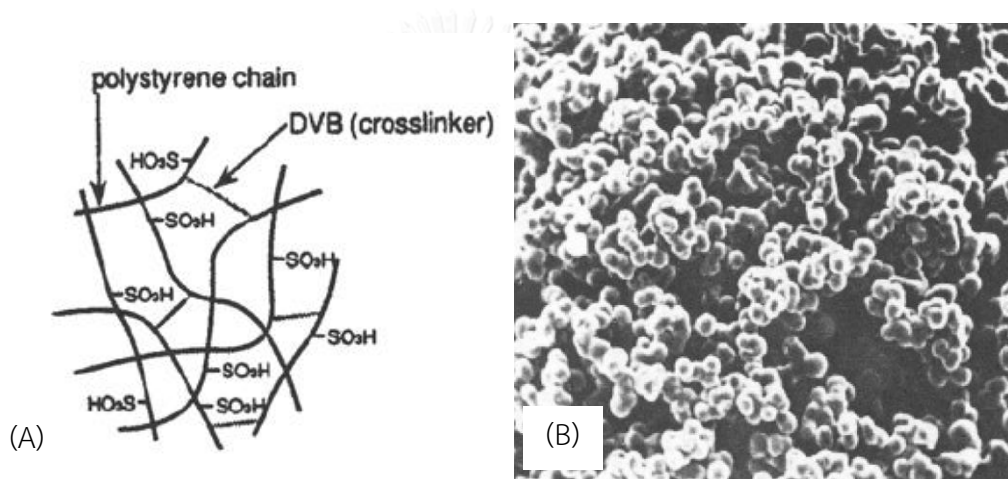


**Figure 2.9** (A) The schematic structure and (B) SEM image of Amberlyst 15 [39, 40].

CHULALONGKORN UNIVERSITY

#### - Zeolites

Zeolites are microporous material with well-defined crystalline structure. These materials are composed of silicon, aluminium and oxygen in their framework and accommodate a variety of cations such as Na<sup>+</sup>, K<sup>+</sup>, Ca<sup>2+</sup>, Mg<sup>2+</sup> and others. Because of the well-defined crystalline structure, zeolites are used in various applications in the chemical production industries. Recently, zeolite are used in petrochemical cracking, water purification (ion exchange for softening), in the chemical separation process and removal solvents and gases. Furthermore, they are used as molecular sieve. Some of common mineral zeolites are heulandite,



phillipsite, natrolite and stilbite, etc. Natural zeolites are formed where volcanic rocks and ash layers react with alkaline groundwater. Zeolites are prepared by mixing of alumina materials and silica in the hydrothermal process this reaction is catalyzed by base catalysts. Finally, they are precipitated slowly around 200°C. Today, synthetic zeolites are synthesized to serve in many reactions including fuel synthesis, crude oil cracking and isomerization in petroleum refinery industries. There are synthetic zeolites for example, Beta (BEA), ZSM-5 and zeolites A, etc. An example, Al-ZSM-5 with a  $\text{SiO}_2/\text{Al}_2\text{O}_3$  ratio of 50 is used for caprolactam production.

In this work, HUSY zeolite ( $\text{SiO}_2/\text{Al}_2\text{O}_3$  molar ratio of 10.6) which has acidity of  $1.04 \text{ mmolH}^+ \text{ g}^{-1}$ , specific surface area of  $637 \text{ m}^2 \text{ g}^{-1}$  and pore size of 2.54 nm., is used to study the catalytic performance. Figure 2.10 shows the HUSY zeolite.



**Figure 2.10** HUSY zeolite.

- *Propylsulfonic acid functionalized hexagonal mesoporous silica (HMS-SO<sub>3</sub>H) and acidic natural rubber/mesoporous silica composites (NR/HMS-SO<sub>3</sub>H)*

Propylsulfonic acid functionalized hexagonal mesoporous silica (HMS-SO<sub>3</sub>H) is a solid catalyst. It is prepared *via* an in situ sol-gel process of Tetraethyl orthosilicate (TEOS) as silica source and dodecylamine as organic template, followed by co-condensation of organo-sulfonic acid groups. The catalyst preparation is described in Chapter 3. This catalyst has high surface area and strength of sulfonic acid groups as shown in Table 4.1. Figure 2.11 shows the HMS-SO<sub>3</sub>H catalyst.



**Figure 2.11** The HMS-SO<sub>3</sub>H catalyst.

NR/HMS-SO<sub>3</sub>H is a solid catalyst composed of propylsulfonic acid functionalized HMS (HMS-SO<sub>3</sub>H) and NR as hydrophobicity improver. Unlike the conventional procedure for HMS synthesis, tetrahydrofuran (THF) is used as synthesis media in order to dissolve the NR in the synthesis mixture and to obtain a high dispersion level of the NR in the silica framework. This material has an excellent hydrophobic property which can assist the esterification of long-chain fatty acid (lauric acid) [41]. Figure 2.12 shows the NR/HMS-SO<sub>3</sub>H catalyst.



**Figure 2.12** The NR/HMS-SO<sub>3</sub>H catalyst.

This work, both of HMS-SO<sub>3</sub>H and NR/HMS-SO<sub>3</sub>H were used to study the catalytic performance in comparison with the commercial catalysts, including ion exchanged resins (Amberlyst 15, Amberlyst 36 wet) and zeolite (HUSY). Moreover, hydrophobic property of NR/HMS-SO<sub>3</sub>H could assist the esterification due to preventing of water adsorbed on the catalyst surface (poisoning).

## 2.5 Alkyl Levulinate Esters (ALs)

Alkyl levulinate esters (ALs) are obtained from biomass-derived products (levulinic acid) react with alcohol in the acid condition. Around 150 years ago, ALEs was studied the formation of methyl to propyl levulinate esters from purified levulinic acid. In 1930, Sah [4] and Schuette [5] et al. published the synthesis of ALs from esterification of LA and several alcohols in the presence of HCl [3]. Figure 2.13 shows the esterification synthesis of ALs via esterification of LA and alcohol in the acid condition.

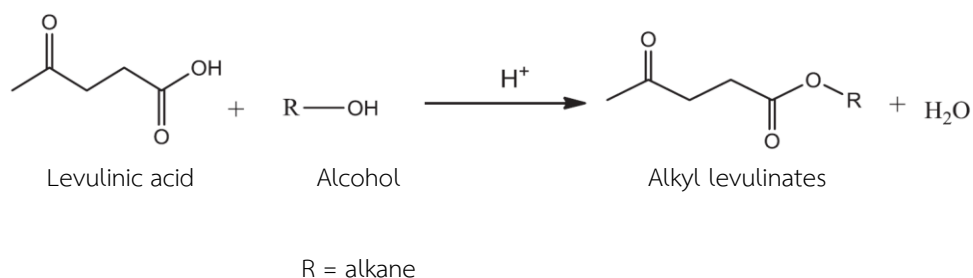


**Figure 2.13** Esterification synthesis of alkyl levulinates.

According to the esterification of ALs from LA, several studies are focused on the synthesis of LA with short chain alcohols, for example methanol, ethanol, propanol and butanol, etc. These levulinate esters, for example methyl levulinate, ethyl levulinate, and butyl levulinate, have similar properties to the biodiesel fatty acid methyl ester (FAME) [13]. Moreover, ALs have the excellent properties for used in gasoline additives, such as non-toxic, high lubricity, flashpoint stability and better flow properties under cold condition. They are recognized as important platform chemicals and wide range of applications. ALs can be used in the flavoring and fragrance industries [3, 13]. In 2013, Hu et al. [42], ethyl levulinate (EL) as an oxygenated additive was used to develop the diesel formulation by Biofine and Texaco. The effects of adding EL have been determined by studying on the cloud point, pour point, kinematic viscosity and flash point. The results showed the low temperature was improved compare to unblended sample of biodiesel. Interestingly, the 21:79 formulation of diesel, which is consists of 20% EL, 1% co-additive and 79% of diesel, it can be used in regular diesel engine.

However, heterogeneous acid catalysts were used for catalyze in esterification because easily separated from the reaction mixture in order to reuse and regenerate the catalyst. The synthesis of alkyl levulinate esters (ALs) from levulinic acid over heterogeneous acid catalysts are summarized in Table 2.7.

Recently, heteropoly acids (HPAs) and zeolites are preferred choices for esterification of LA with alcohols. Dharme et al. [28] reported the HPAs loading on montmorillonite K10 ( $H_3PW_{12}O_{40}/K10$ ) for synthesis of *n*-butyl levulinate. This catalyst

gives a high LA conversion at 97 mol% and 97 mol% of *n*-butyl levulinate yield. Similarly, Nandiwale et al. [43] deposited  $H_3PW_{12}O_{40}$  on desilicated ZSM-5 zeolite ( $H_3PW_{12}O_{40}/ZSM-5$ ) for esterification of LA with ethanol. This catalyst is performed at 78 °C with a high LA conversion and ethyl levulinate yield at 94 mol%. In 2011, Yan et al. [44] synthesized the mesoporous  $H_4SiW_{12}O_{40}-SiO_2$  catalyst for synthesis of both methyl levulinate (73% yield achieved at 79% conversion of levulinic acid) and ethyl levulinate (67% yield obtained at 75% conversion of levulinic acid). Cyclohexane was used as solvent. In 2013, Melero et al. [45] studied conversion of LA into alkyl levulinates catalyzed by sulfonic mesostructured silicas (SBA-15-( $CH_2$ )<sub>3</sub>-SO<sub>3</sub>H). This research were studied the esterification of LA with methanol, ethanol, isopropanol and butanol, respectively. The conversion of LA is achieve at 80-95 mol% as well as the product yield is obtained around 80-95 mol%. The LA conversion is decreased when increasing the chain of alcohol because the stearic hindrance and mass transfer limitation effects. Another report compared to the zeolites that showed very poor or even no activity for the synthesis of ethyl levulinate. Patil et al. [46] synthesized the EL over HBA zeolite. This catalyst gives low LA conversion and EL yield at 40 and 39 mol%, respectively. It can be conclude that the acidic nature and pore geometry are expected as the most important affect to the reaction of levulinate ester synthesis. On the other hand, nonporous material (sulfonated oxides) gives both of LA conversion and EL yield at 45 mol% because this material has low surface area and acidity [47].

Table 2.7 Synthesis of alkyl levulinates (ALs) from levulinic acid over heterogeneous acid catalysts

Catalyst	Alcohol	solvent	Conditions <sup>a</sup>				LA conversion		Ref.	
			Molar ratio (LA : alcohol)	Temperature (°C)	Time (h)	Catalyst loading (wt.%)	Reusability	(mol%) <sup>a</sup>		(mol%)
20 wt.% H <sub>3</sub> PW <sub>12</sub> O <sub>40</sub> /K10	butanol		1:6	120	4	10	3	97	Bu, 97	[28]
10 wt.% H <sub>3</sub> PW <sub>12</sub> O <sub>40</sub> /ZSM-5	ethanol		1:8	78	4	20	4	94	Et, 94	[43]
20 wt.% H <sub>4</sub> SiW <sub>12</sub> O <sub>40</sub> -SiO <sub>2</sub>	methanol	Cyclohexane	1:20	65-75	6	50	N/A	79	Me, 73	[48]
	ethanol	Cyclohexane	1:20	65-75	6	50	N/A	75	Et, 67	
SBA-15-(CH <sub>2</sub> ) <sub>3</sub> -SO <sub>3</sub> H	methanol		1:5	117	2-4	7	4	95	Me, 95	[45]
	ethanol		1:5	117	2-4	7	4	95	Et, 95	
	isopropanol		1:5	117	2-4	7	4	90	iPr, 90	
	butanol		1:5	117	2-4	7	4	80	Bu, 80	
HBA zeolite	ethanol		1:6	78	5	20	5	40	Et, 39	[46]
SnO <sub>2</sub> -SO <sub>3</sub> H	ethanol		1:5	70	10	2.5	1	45	Et, 45	[47]
ZrO <sub>2</sub> -SBA-15-SO <sub>3</sub> H	ethanol		1:10	70	24	5	5	80	Et, 80	[49]
Sulfonated carbon nanotubes	ethanol		1:5	70	5	2.5	N/A	55	Et, 35	[50]
Sulfonated carbon Starbons	ethanol	water	1:30	60	6	86	N/A	85	Et, 85	[51]
ZrO <sub>2</sub> -TiO <sub>2</sub> nanorods	ethanol		1:2.5	105	3.5	3	3	90	N/A	[52]

N/A = not available.

<sup>a</sup> The wt.% values is referenced to the amount of the levulinic acid.

## 2.6 Literature Reviews

### 2.6.1 Levulinic acid

Hayes *et al.* [11] reported the LA production from lignocellulosic biomass by bio-refinery process. It was performed by two acid-catalyzed steps, where hexose sugar was converted to HMF in the presence of 1-4 wt.%  $\text{H}_2\text{SO}_4$  at 200–230 °C and pressure of 20–25 bar for 30 s, for second step, HMF was transferred to the second reactor in order to further hydrolyzed HMF to LA at 190–220 °C and pressure of 10–15 bar for 30 min. Formic acid was considered as by-product while LA yield around 70–80 mol% was obtained. This process was a semi-commercial LA production. However, the main drawbacks of this process are inefficiency in separation and recovery LA from dilute aqueous solution.

Girisuta *et al.* [53] reported the classical method for chemical conversion of lignocellulosic biomass (sugars and starch) to LA synthesis. Typically, LA was produced by mineral acid ( $\text{HCl}$ ,  $\text{HNO}_3$ ,  $\text{H}_2\text{SO}_4$ ,  $\text{H}_3\text{PO}_4$  and etc.). These acid catalysts had highly effective to LA production depended on the concentration of acid used and their acid strength. However, using of mineral acid catalysts had several of drawbacks for example, undesired product formation (formic acid, humins), reactor corrosive, environmental pollution, and difficult catalyst recycle. This work focused on the kinetic experiments of LA synthesis from biomass. The kinetic were studied in the range of 150-200 °C,  $\text{H}_2\text{SO}_4$  concentrations between 0.05 and 1 M, and initial cellulose intakes between 1.7 and 14 wt %. This work found that the highest yield of levulinic was 60 mol %, obtained at a temperature of 150 °C, an initial cellulose intake of 1.7 wt %, and a sulfuric acid concentration of 1 M.

Mellmer *et al.* [54] studied the hydrolysis of high concentration furfuryl alcohol (1 M) to synthesis LA. The highest LA yields (>70 mol%) was obtained by using H-ZSM-5\_23 zeolite ( $\text{SiO}_2/\text{Al}_2\text{O}_3$  molar ratio of 23) as the catalyst in monophasic THF–water solvent systems. The zeolite H-ZSM-5\_23 was containing a 3-dimensional channel system with medium size pore/cage diameters (5.5 Å) and high acid site

density ( $650 \mu\text{mol g}^{-1}$ ). The solvent systems were varied in the range of 19:1–1:2 w/w. At the 4:1 of THF–water was suitable condition to achieve the LA yield at 74% mol.

### 2.6.2 Solketal

Suriyaprapadilok *et al.* [7] reported the synthesis of SK by acetalization of glycerol and acetone in the presence of 1 wt.% PTSA. At the 1: 4 of glycerol: acetone molar ratio and the reaction temperature of 120 °C were optimum conditions. After 8h, the glycerol conversion was found 87.2 wt.%. Interestingly, water was formed as by-product thus it should be removed in order to achieve a higher conversion of glycerol and avoid the reaction backward. The chemical products structure was confirmed by using GC-MS and FT-IR technique.

Manjunathan *et al.* [31] studied the synthesis of solketal at room temperature under batch condition reactor. Several types of heterogeneous acid catalysts including Amberlyst-15, H-ZSM-5, H-Modernite, H-Beta, H-Y, Montmorillonite,  $\text{MoO}_3/\text{SiO}_2$  and cesium salt of phosphotungstic acid were compared the catalyst performance. H-Beta zeolite was the best one. It gave the glycerol conversion and SK selectivity at 86 and 98.5 mol%, respectively. The optimum glycerol: acetone molar ratio was 1:2. On the other hand, decreasing the acetone concentration at 1:1 molar ratio, the SK yield was decreased to 66 mol%.

### 2.6.3 Alkyl levulinate esters

Pileidis *et al.* [27] reported the use of biomass–derived hydrothermal carbons (HTC) modified with sulfonic groups as heterogeneous catalysts for synthesis of ethyl levulinates. The raw materials of biomass in this study were including, cellulose, glucose and rye straw. The biomass precursor were placed in the 30 mL stainless steel autoclaves equipped with a Teflon inlet with HCl as catalyst, then heated in an oven at 230 °C for 24 h. After the hydrothermal reaction completely, the solid particles were removed by centrifuged at a speed of 1400 rpm, washed with ethanol



and dried overnight. After that, the HTC materials were suspended in  $\text{H}_2\text{SO}_4$  (99.999% purity, 10 mL acid per g of HTC material) and heated for 4 h at 80 °C. After sulfonation, the HTC materials were gently stirred overnight in 500 mL of water in order to remove the unreacted  $\text{H}_2\text{SO}_4$ . Finally, they were washed with distilled water until the pH of the supernatant was close to 7, and dried in a vacuum oven at 60 °C overnight. For esterification of LA and ethanol was performed in the batch reactor equipped with reflux apparatus at the LA: ethanol molar ratio of 1:5, reaction temperature of 60 °C for 3 h. HTC-Glu-S was obtained from glucose as precursor, which gave the highest both of LA conversion and ethyl levulinate selectivity at 97 mol%.

Dharne *et al.* [28] studied the esterification of LA and *n*-butanol over dodecatungstophosphoric acid (DTPA) supported on acid-treated clay montmorillonite (K10). The reaction was performed at the LA: *n*-butanol molar ratio of 1: 6, reaction temperature of 120 °C for 4 h. This material was optimized the catalyst loading of 20% w/w. The highest LA conversion was 97 mol%. Interestingly, this reaction provided the 100 mol% of *n*-butyl levulinate selectivity. Moreover, 20% (w/w) DTPA/K10 can be used for two cycles with the same activities.

Nandiwale *et al.* [6] studied the synthesis of octyl levulinate *via* esterification of LA and *n*-octanol over modified H-ZSM-5 (Meso-HZ-5) as catalyst. The reaction was performed by mixing LA and *n*-octanol in the batch reflux system at 100 °C for 5 h. The optimum LA: *n*-octanol molar ratio was 1:8. The octyl levulinate yield and selectivity was obtained at 60 and 99 mol%, respectively. This compound had the excellent lubricity property. This compound had potential to apply in biolubricant application.

#### 2.6.4 Levulinic acid–glycerol ketal–ester oligomers

Amarasekara *et al.* [55] studied the synthesis of levulinic acid–glycerol ketal–ester oligomers *via* ketalization of LA and glycerol in the presence of acid catalysts. Three different catalysts including  $\text{Sb}_2\text{O}_3$ , PTSA, and 1-(1-propylsulfonic)-3-methylimidazolium chloride were used in this study. For all of experiment, the LA:

glycerol molar ratio at 1: 1 was used. Because of LA had two carbonyl groups (ketone and carboxylic acid groups) in the same molecule so it can be reacted with polyols molecule like glycerol in two different reaction modes, where the keto group can be formed ketals with 1,2 or 1,3 hydroxyls, and the esterification. Bifunctional groups of LA was enhanced the opportunity for the synthesis of polymeric structures from levulinic acid–glycerol system. The reaction was performed by adding 1.0 mol% of catalyst into the mixture of levulinic acid and glycerol, then heated from room temperature to 210 °C, after that further heated under vacuum for 3–9 h. The oligomers were slightly yellow, transparent, highly viscous materials closer to solid state at room temperature. The highest average degree of oligomerization of the oligomer produced was 9.8 by using  $\text{Sb}_2\text{O}_3$  as acid catalyst. The structural characterization of oligomer was investigated using NMR spectroscopy. There were three types of end groups of oligomers, which were keto terminal (KT), glycerol–ketal terminal (GKT) and glycerol–ester terminal (GET). The  $^{13}\text{C}$  NMR spectrum of KT is observed at the chemical shift  $\delta = 206.58$  ppm, which was represent keto carbonyl in KT. For GKT end groups were confirmed by a small peak at (109.59 109.88), (76.22, 77.01), and (65.56, 65.97) from the dioxolane ring at C-2, C-4, C-5, respectively. Finally, GET end group was found  $^{13}\text{C}$  NMR at the chemical shift  $\delta = 63.25, 69.91,$  and 65.16 from C-1, C-2, and C-3, of the monosubstituted glycerol, respectively. Moreover, for TG–DTG curve of oligomer was confirmed the thermal degradation at around 380 °C.

## CHAPTER III EXPERIMENT AND ANALYTICAL METHOD

### 3.1 Materials and Chemical Reagents

#### 3.1.1 Commercial catalysts used for esterification

- Amberlyst 15 (Sigma Aldrich)
- Amberlyst 36 wet (Sigma Aldrich)
- HUSY with a  $\text{SiO}_2/\text{Al}_2\text{O}_3$  molar ratio of 10.6 (Tosoh Corporation)

#### 3.1.2 Chemical reagents for preparation of HMS-SO<sub>3</sub>H and NR/HMS-SO<sub>3</sub>H

- Tetraethyl orthosilicate (TEOS) ( $\text{SiC}_8\text{H}_{20}\text{O}_4$ ) (AR grade, 98%, Sigma Aldrich)
- Dodecylamine (DDA) ( $\text{CH}_3(\text{CH}_2)_{11}\text{NH}_2$ ) (AR grade, 98%, Sigma Aldrich)
- 3-Mercaptopropyltrimethoxysilane (MPTMS) ( $\text{HS}(\text{CH}_2)_3\text{Si}(\text{OCH}_3)_3$ ) (AR grade, 99%, Sigma Aldrich)
- Tetrahydrofuran (THF) ( $\text{C}_4\text{H}_8\text{O}$ ) (AR grade, Qrec)
- Hydrogen peroxide solution ( $\text{H}_2\text{O}_2$ ) (ACS grade, 30 wt.%, Fisher)
- Natural rubber (NR) STR-5L, Thai Hua Chumporn Natural Rubber Co, Ltd.)
- Sulfuric acid ( $\text{H}_2\text{SO}_4$ ) (AR grade, 95%, Merck)

#### 3.1.3 Chemical Reagents for esterification

- DL-1,2-Isopropylidenediglycerol ( $\text{C}_6\text{H}_{12}\text{O}_3$ ) (AR grade, 98%, Sigma Aldrich)
- Levulinic acid ( $\text{C}_5\text{H}_8\text{O}_3$ ) (AR grade, 98%, Sigma Aldrich)
- Glycerol ( $\text{C}_3\text{H}_8\text{O}_3$ ) (AR grade, 99%, Sigma Aldrich)

- Absolute ethanol (C<sub>2</sub>H<sub>5</sub>OH) (AR grade, 99%, Merck)

### 3.1.4 Chemical reagents for products characterization using gas chromatography

- 1,4-Dioxane (C<sub>4</sub>H<sub>8</sub>O<sub>2</sub>) (AR grade, 98%, Fisher)
- Methyl undecanoate (CH<sub>3</sub>(CH<sub>2</sub>)<sub>9</sub>CO<sub>2</sub>CH<sub>3</sub>) (GC grade, 98%, Sigma Aldrich)
- *N*-M ethyl-*N*-(trimethylsilyl)trifluoroacetamide (MSTFA) (CF<sub>3</sub>CON(CH<sub>3</sub>)Si(CH<sub>3</sub>)<sub>3</sub>) (AR grade, >98.5%, Sigma Aldrich)
- Sodium sulfate (Na<sub>2</sub>SO<sub>4</sub>) (AR grade, 99%, Sigma Aldrich)

### 3.2 Equipments and Apparatus

- Hot plate and magnetic stirrer
- Thermocouple (IKA, model: ETS-D5)
- Paraffin oil bath
- Reflux condenser
- Three-necked round bottom flask
- Magnetic bar
- Syringe (3 mL)
- Syringe filter (0.2 micron)
- Filter papers No.42 (Ø 90 mm)
- Beakers (20 and 50 mL)
- Volumetric flasks (10 and 25 mL)
- Dropper
- Spatula

- Test tube
- Micropipette
- Pipette tips (200 and 1000  $\mu\text{L}$ )
- Burette (50 mL)
- Crucible
- Electrical oven
- Desiccator
- Rotary evaporator
- Erlenmeyer flask (250 mL)
- Büchner funnel
- Büchner flask (500 mL)
- Universal indicator paper
- Vacuum pump
- Aspirator
- Petri dish

### 3.3 Catalyst Characterization

Physicochemical properties of all catalysts were characterized by following techniques;

#### 3.3.1 X-ray Powder diffraction (XRD)

X-ray powder diffraction (XRD) is the most widely used for the identification of unknown crystalline materials. By measuring the angles and intensities of these

diffracted beams. The XRD pattern was showed crystalline phase of sample which compared with library patterns database.

X-ray powder diffraction (XRD) patterns of both HMS-SO<sub>3</sub>H and NR/HMS-SO<sub>3</sub>H were obtained on a Rigaku Rint-Ultima III X-ray diffractometer employing Cu K $\alpha$  radiation and an X-ray power of 40 kV and 40 mA. The diffraction angle was studied in the range of  $2\Theta = 1\text{--}10^\circ$  with a scanning step of  $0.02^\circ$  and a count time at 1 sec. The repeating distance ( $a_0$ ) was calculate from the  $d$ -spacing of plane (100) ( $d_{100}$ ) by using the formula;  $a_0 = 2d_{100} / \sqrt{3}$

For as-recieved and calcined HUSY zeolite, the X-ray powder diffraction (XRD) patterns were obtained on a Bruker D8 Discover X-ray diffractometer employing Cu K $\alpha$  radiation at 40 kV and 40 mA. The diffraction angle were studied in the range of  $2\Theta = 5\text{--}80^\circ$  with a scanning step of  $0.02^\circ$  and a count time at 1 sec.

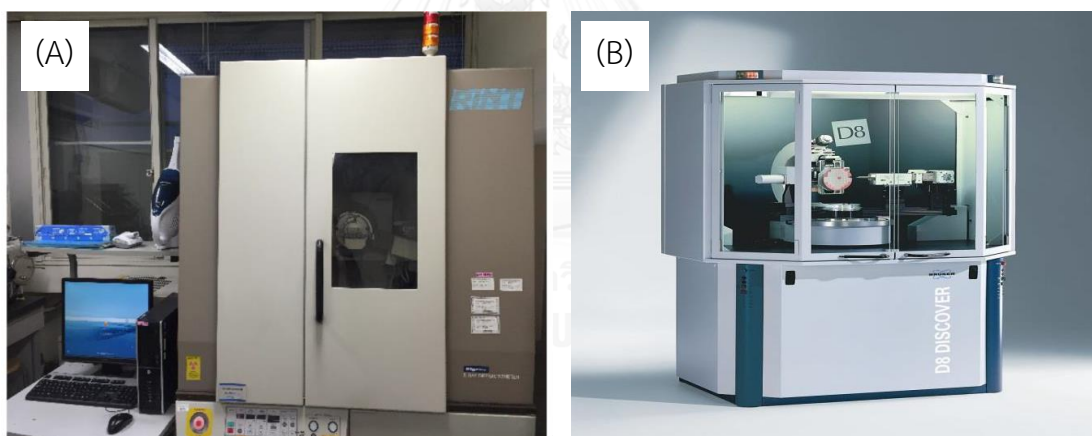


**Figure 3.1** X-ray diffractometer of (A) Rigaku Ultima III and (B). Bruker D8 Discover.

### 3.3.2 N<sub>2</sub> adsorption-desorption measurement

The textural properties of the HUSY zeolite, HMS-SO<sub>3</sub>H, and NR/HMS-SO<sub>3</sub>H were analyzed by Micromeritics ASAP 2020 nitrogen (N<sub>2</sub>) adsorption-desorption measurement. The Brunauer-Emmett-Teller (BET) method was employed to calculate the specific surface area ( $S_{\text{BET}}$ ) in the relative pressure ( $P/P_0$ ) range of 0.02–0.2 and the total pore volume ( $V_t$ ) was obtained from the accumulative volume of N<sub>2</sub> adsorbed at a  $P/P_0$  about 0.990. The N<sub>2</sub> adsorption-desorption measurement was

conducted at  $-196^{\circ}\text{C}$  using a BEL Japan BELSORP-mini II instrument. The weight of the sample used (initially around 40 mg) was measured exactly after pretreatment at  $150^{\circ}\text{C}$  for 2 h.



**Figure 3.2** Micromeritics ASAP 2020 surface area and porosity analyzer.

### 3.3.3 Thermogravimetric/differential thermal analysis (TG/DTA)

Thermogravimetric/differential thermal analysis (TG/DTA) was applied to investigate the amount of NR and/or silica content in the synthesis materials (HMS-SO<sub>3</sub>H and NR/HMS-SO<sub>3</sub>H) by using a Perkin Elmer Pyris Diamond Thermogravimetric/differential thermal analyzer. Around 10 mg of the sample was used and the temperature was heated from room temperature to  $1000^{\circ}\text{C}$  at a heating rate of  $10^{\circ}\text{C}/\text{min}$  under a dried air flow.

Moreover, TG/DTA was used to study the moisture contents, and thermal degradation behavior of organic compounds on the surface of Amberlyst 15 after esterification of SK and LA. Approximately 15 mg of sample was placed on the

sample holder (platinum pan) in the analyzer. The temperature was heated from room temperature to 900 °C with heating rate at 5 °C/min and a dried nitrogen flow (50 mL/min).



**Figure 3.3** Perkin Elmer Pyris Diamond Thermogravimetric/differential thermal analyzer.

จุฬาลงกรณ์มหาวิทยาลัย  
CHULALONGKORN UNIVERSITY

### 3.4 Catalyst Preparation

- *HUSY zeolite*

Before being used, HUSY was calcined at 500 °C for 5 h under the air atmosphere in the electrical furnace.



- Propylsulfonic acid functionalized hexagonal mesoporous silica (HMS-SO<sub>3</sub>H)

HMS-SO<sub>3</sub>H was synthesized by dissolve DDA in the solution of THF and deionized water with continuously stirring. Next step, the solution mixture was slowly added TEOS and then continuously stirring at 40°C for 30 min. Finally, the mixture was added slowly of MPTMS and H<sub>2</sub>O<sub>2</sub> and stirred at 40 °C for 1 h. The molar ratio of synthesis mixture is 0.100 TEOS: 0.040 DDA: 5.888 H<sub>2</sub>O: 0.370 THF: 0.024 MPTMS: 0.168 H<sub>2</sub>O<sub>2</sub>. When the solution becomes gel, it was aged at ambient temperature for 18 h. Next, the solid particles were obtained by precipitation in 100 mL of ethanol. The solid HMS-SO<sub>3</sub>H was collected by filtration and air dried overnight. Finally, the templates that accommodate in the pores of the composites were removed by extraction with H<sub>2</sub>SO<sub>4</sub> solution. After extraction completely, the white solid particles was washed with ethanol until pH equal to 7, dried and stored in the desiccator [41, 56]. The proposed pathway for synthesis of HMS-SO<sub>3</sub>H and the flowchart diagram are display in Figure 3.4 and 3.5, respectively.

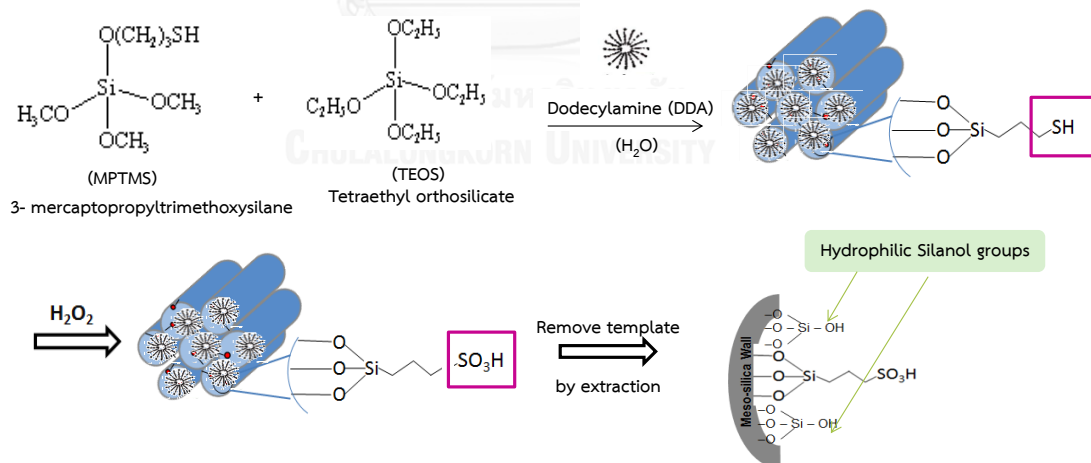
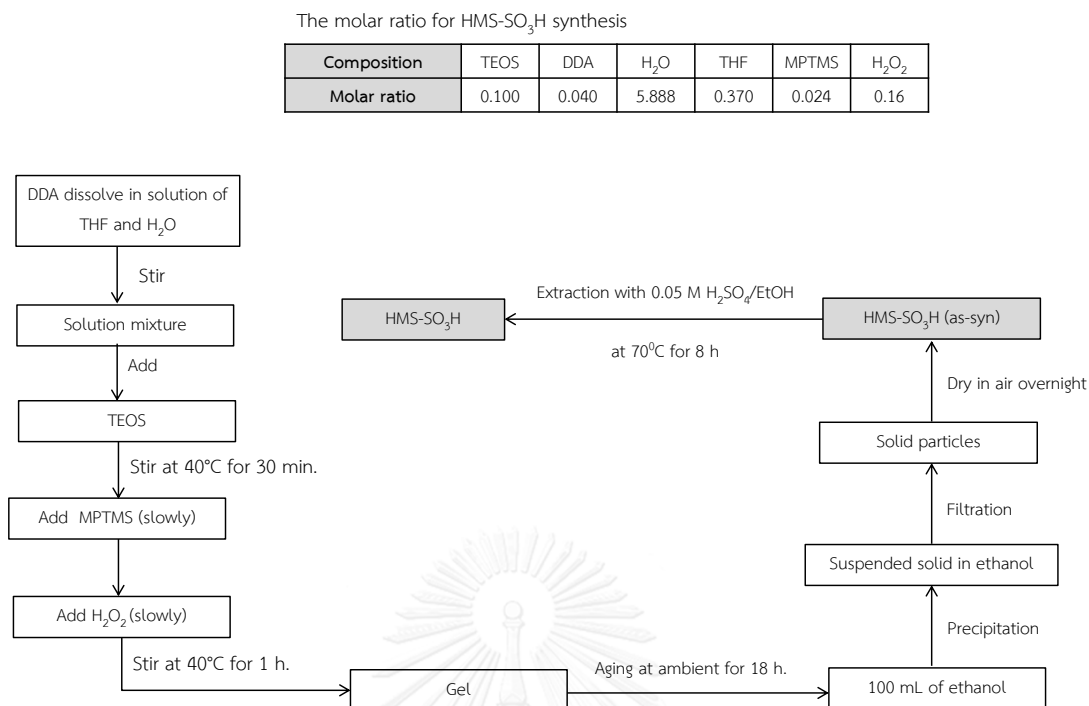


Figure 3.4 The proposed pathway for synthesis of HMS-SO<sub>3</sub>H [41].



**Figure 3.5** The flowchart diagram for synthesis of HMS-SO<sub>3</sub>H. The inset table shows the molar ratio was used.

- *Acidic natural rubber/mesoporous silica composites (NR/HMS-SO<sub>3</sub>H)*

NR/HMS-SO<sub>3</sub>H was prepared by in situ sol-gel method within THF as synthesis media. First step, 1 g of NR sheet was swollen in the TEOS at room temperature for 16 h. Next step, the swollen NR sheet was dissolved in THF in order to attain homogeneous solution. After that, the NR solution was mixed with DDA, followed by adding dropwise of TEOS with stirring for 1 h. Then, the mixture was added deionized water, 3-mercaptopropyltrimethoxysilane (MPTMS) and hydrogen peroxide sequentially with stirring at 40°C for 1 h. The molar ratio of synthesis mixture is 0.100 TEOS : 0.04 DDA : 5.888 H<sub>2</sub>O : 0.370 THF : 0.01 NR : 0.024 MPTMS : 0.168 H<sub>2</sub>O<sub>2</sub>. When the mixture was mixed completely, the gel was aged at 40 °C for 3 days. Next, the solid particles were obtained by precipitation in 100 mL of ethanol then filtration and drying under vacuum atmosphere at 60 °C for 2 h. Finally, the templates that accommodate in

the pores of the composites were removed by extraction with  $\text{H}_2\text{SO}_4$  solution. After extraction completely, the white solid particles was washed with ethanol until pH equal to 7, dried and stored in the desiccator [41, 56]. The proposed pathway for synthesis of NR/HMS- $\text{SO}_3\text{H}$  and the flowchart diagram are display in Figure 3.6 and 3.7, respectively.

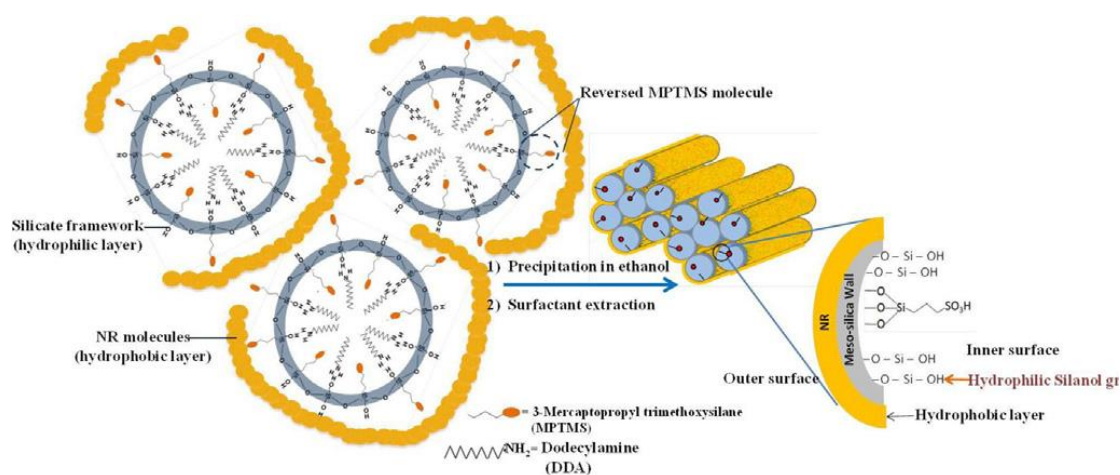
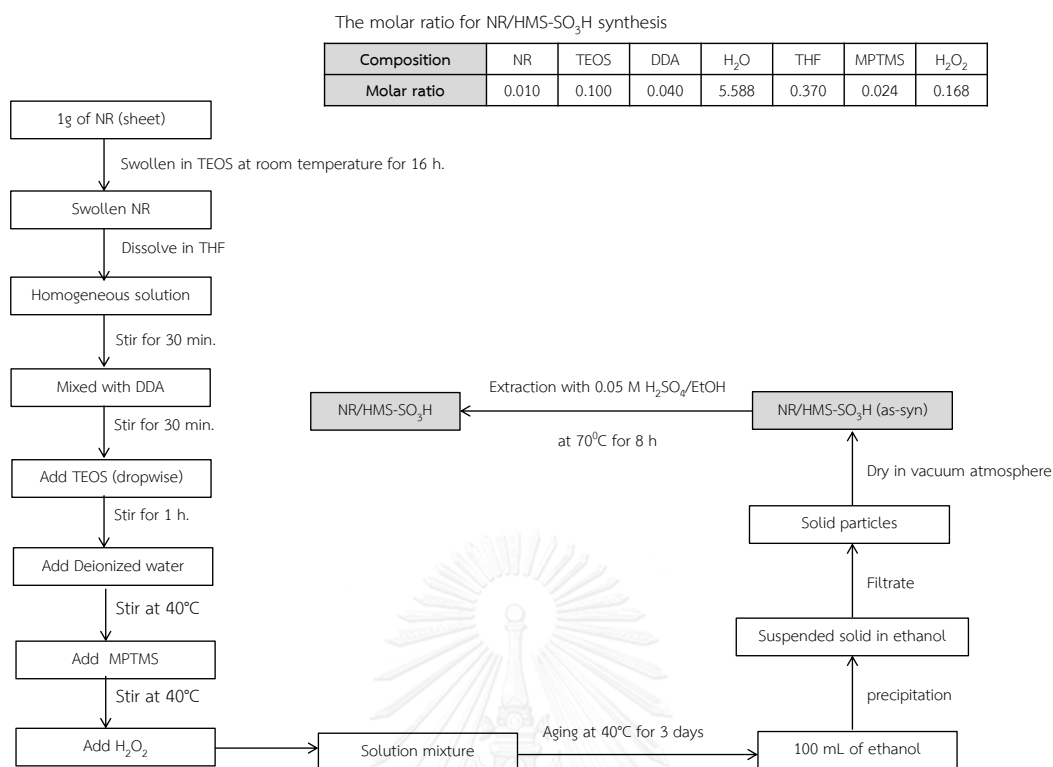


Figure 3.6 The proposed pathway for synthesis of NR/HMS- $\text{SO}_3\text{H}$  [41].



**Figure 3.7** The flowchart diagram for synthesis of NR/HMS-SO<sub>3</sub>H. The inset table shows the molar ratio was used.

Both of the functionalized materials, HMS-SO<sub>3</sub>H and NR/HMS-SO<sub>3</sub>H were dried in an oven at 100 °C for 2 h prior to use in the esterification of SK and LA.

### 3.5 Esterification of SK and LA over Heterogeneous Acid Catalysts

The esterification of SK and LA was studied to find the optimum conditions for synthesis of chemical products and also compared their catalytic performance. Figure 3.8 shows the equipment set up for esterification. The reaction was performed by 0.05 mol of solketal and levulinic acid placed in a 50-mL three-necked round bottom flask connected with a reflux condenser and a magnetic stirrer. The reaction temperature was controlled at the range of 65 °C–150 °C by a paraffin oil bath for 0–8 h. After the reaction complete, quench the reaction mixture in the ice bath until its cool down to the room temperature. When the solution mixture cooled, add 20 mL

of absolute ethanol into the reactor and then stir for 15 minutes. The solid catalyst was separated from the product solution mixture by filtrate with the filter paper No.42 (diameter = 90 mm) and aspirator. Figure 3.9 shows flow diagram of the esterification. After the reaction, the products was analyzed by gas chromatography (GC) using an Agilent Technology 7890A GC system equipped with a 15 m x 0.320 mm DB-5 HT column.

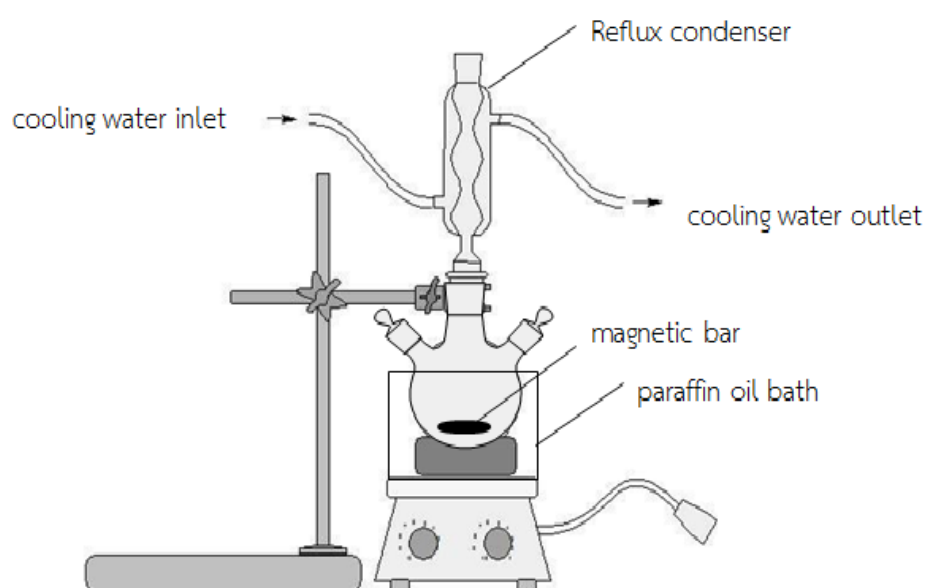
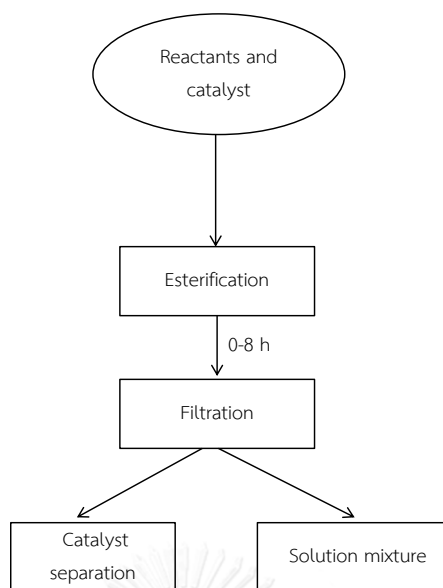


Figure 3.8 The equipment set up for esterification.



**Figure 3.9** Flow diagram of the esterification.

### 3.6 Products Characterization

According to the products analysis, the reactants (SK and LA) and glycerol were calculated by internal standardization method. For other products (SL, H-SL, GL and LGO) area-based method was used to calculate their distribution

To prepare the sample for GC analysis, 0.5 mL of solution mixture from the reaction was filtered by syringe filter (pore diameter = 0.2 micron). Then, 0.1 g of filtrate completely solution mixture was mixed with 1 g of 1,4-Dioxane. The filtrate was dried by the suspension of  $\text{Na}_2\text{SO}_4$  in order to removing of water. The 0.1 g of solution mixture was placed to a vial. After that, 100 microliter of MSTFA was used in preparation of volatile and thermally stable derivatives for GC and MS analysis. For the derivatization completely, the sample had to continuously shake for 3 min and let sample to the room temperature for 30 min. Then, 100 microliter of the internal standard which prepared by mixing of 0.3 g of methyl undecanoate with 25 mL of 1,4-Dioxane was added into the mixture. Finally, adjust volume to 1.5 mL in the vial by using 1,4-Dioxane. Figure 3.10 shows the flowchart diagram of sample preparation for GC analysis.

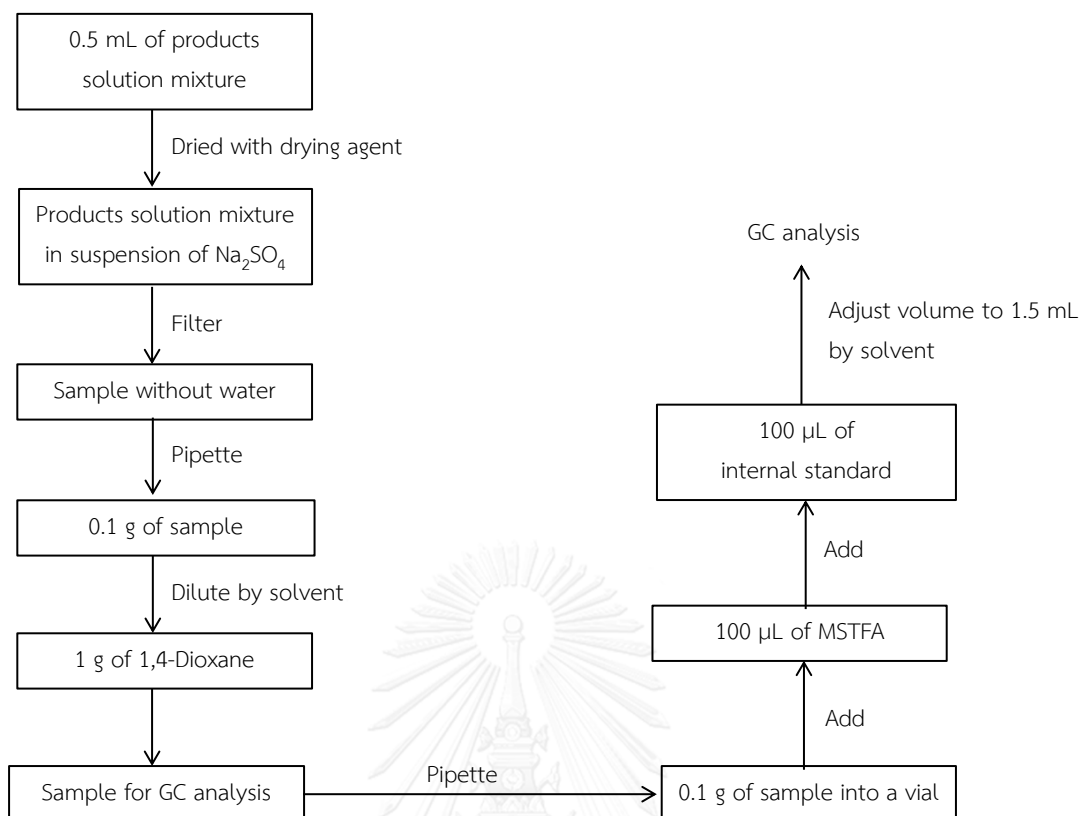


**Figure 3.10** The flowchart diagram of sample preparation for GC analysis.

The GC analysis conditions for analyzing are summarized in the table 3.1. The column temperature program started at 50 °C and held at this temperature for 2 min. Then, the temperature was increased to 130 °C at the constant heating rate of 10 °C/min. After that, the heating rate was changed to 30 °C/min for heating column from 130 °C to 320 °C and maintained the final temperature for 2 min. The schematic of column temperature program is shown in figure 3.13.

The reaction products were also confirmed for their chemical structures with an Agilent 7890B gas chromatograph equipped with a 30-m HP-5 ms capillary column and mass spectrometer detector (Figure 3.12) r. The analysis conditions for analyzing the reaction products structure are used similar to GC-FID (Table 3.2).



**Figure 3.11** GC Agilent Technologies 7890A GC system equipped with DB-5 HT column.

**Table 3.1** The analysis conditions of GC Agilent Technologies 7890A GC equipped with DB-5 HT column

Condition	Value
Carrier (He) flow rate	3 mL/min
Hydrogen flow rate (for FID)	30 mL/min
Air flow rate (for FID)	20 mL/min
Detector temperature (for FID)	350 °C
Injection mode	Cool on column (COC)
Injection port temperature	250 °C
Injection volume	0.1 $\mu$ L
Initial column temperature	50 °C
Final column temperature	320 °C





**Figure 3.12** GC Agilent Technologies 7890B GC-MS system equipped with HP-5 column.

**Table 3.2** The analysis conditions of GC-MS Agilent Technologies 7890B GC equipped with HP-5 column

Condition	Value
Carrier (He) flow rate	3 mL/min
Hydrogen flow rate (for FID)	30 mL/min
Air flow rate (for FID)	20 mL/min
Detector temperature (for FID)	300 °C
Injection mode	Split, split ratio 350:1
Injection port temperature	250 °C
Injection volume	0.1 $\mu$ L
Initial column temperature	50 °C
Final column temperature	300 °C

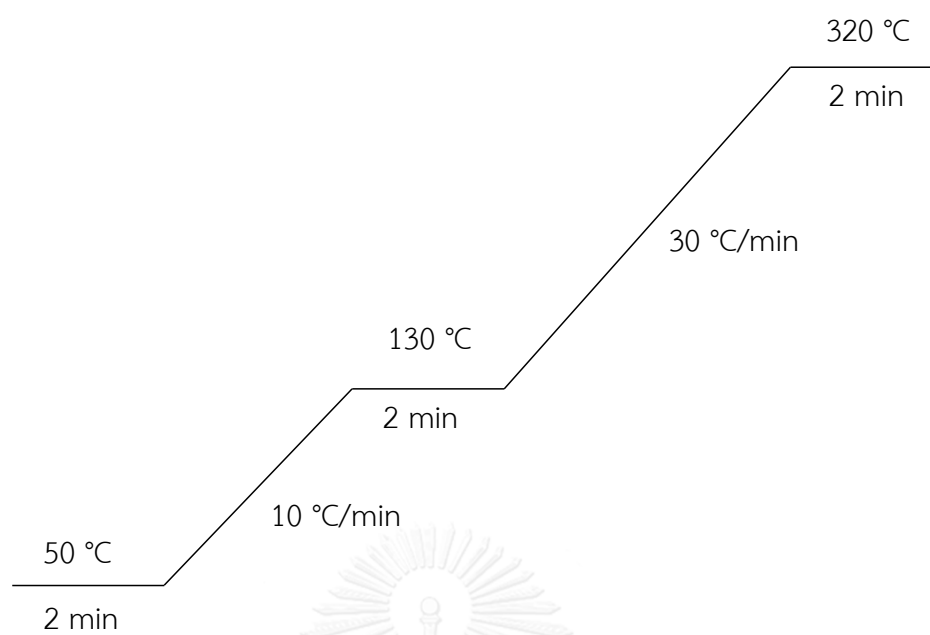


**Figure 3.13** The temperature program for analyzing products from esterification of SK and LA.



## CHAPTER IV

### RESULTS AND DISCUSSION

#### 4.1 Catalyst Characterization

##### 4.1.1 Structural properties

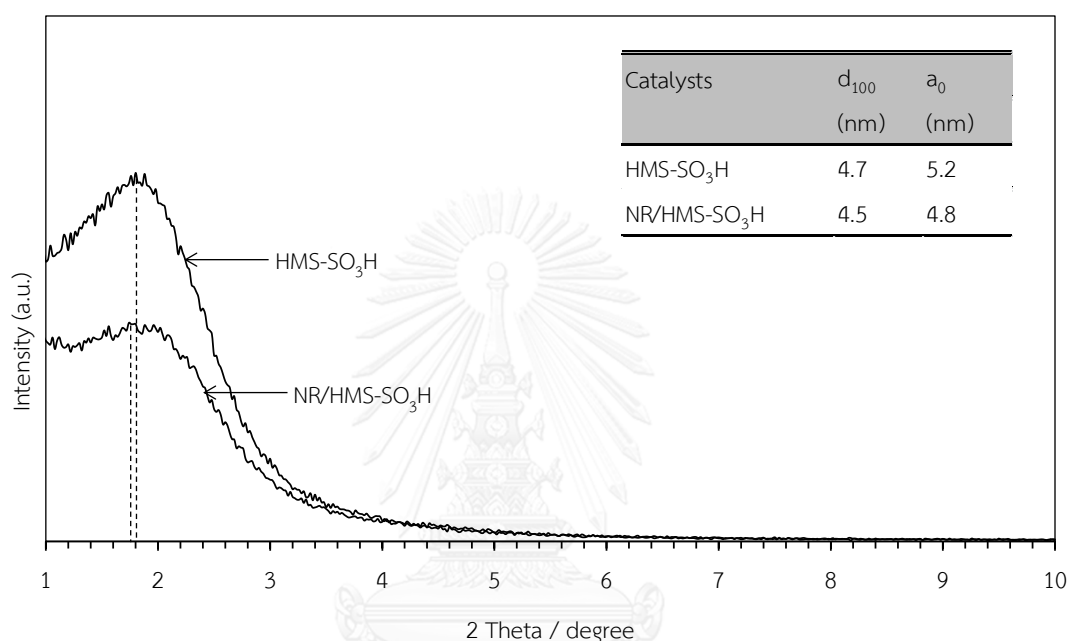


**Figure 4.1** XRD patterns of HMS-SO<sub>3</sub>H and NR/HMS-SO<sub>3</sub>H. The inset table shows structural data of both materials.

X-ray powder diffraction (XRD) was used to study the crystalline phase and structure of the heterogeneous acid catalysts. The XRD patterns of HMS-SO<sub>3</sub>H and NR/HMS-SO<sub>3</sub> after extraction of DDA template are shown in Figure 4.1. These materials were exhibited a strong diffraction peak at  $2\Theta = 4.7^\circ$  and  $4.5^\circ$  for HMS-SO<sub>3</sub>H and NR/HMS-SO<sub>3</sub>, respectively. These peaks are relating to characteristic (100) plane of hexagonal mesoporous structure with wormhole-like framework [41, 56]. The formation of nanocomposite decreased the structural ordering. The amount of NR containing in NR/HMS-SO<sub>3</sub>H was incorporated between the mesoporous channels

[41, 56]. As a result, the unit cell ( $a_0$ ) of NR/HMS-SO<sub>3</sub>H was smaller than that of HMS-SO<sub>3</sub>H (inset in Figure 4.1).

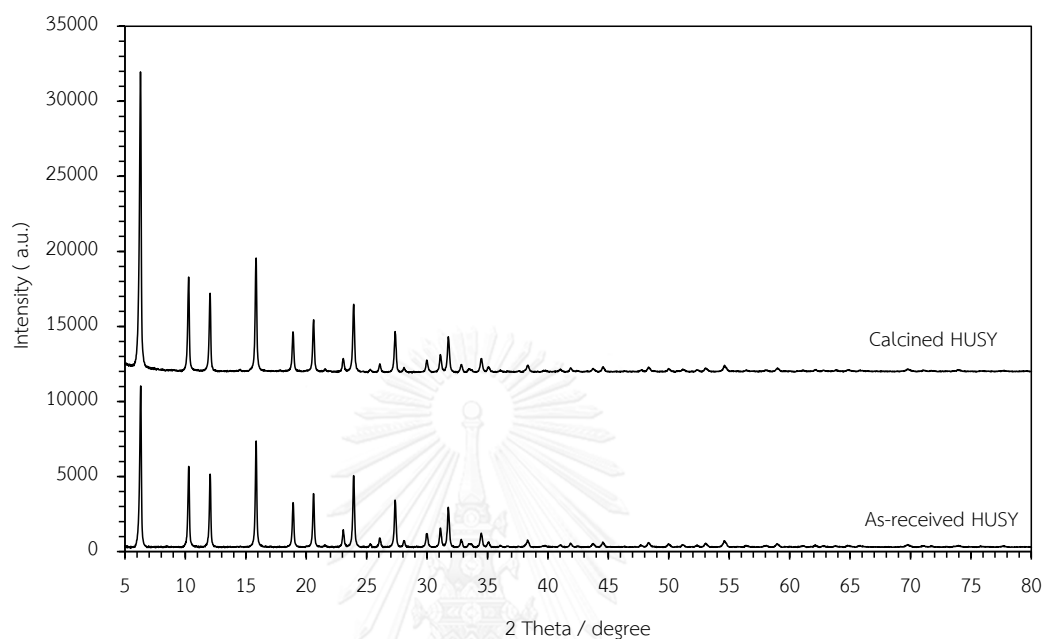


**Figure 4.2** XRD patterns of HUSY zeolites.

Figure 4.2 compares the XRD patterns of as-received and calcined HUSY zeolites. The as-received HUSY exhibited faujasite structure (JCPDS file: 01-088-2887) [57]. After calcination at 500 °C for 5 h, the XRD peaks became intense due to removal of moisture and organic compounds depositing on the zeolite surface. Thus, the crystal structure of HUSY catalyst was not changed by calcination.

#### 4.1.2 Textural Properties

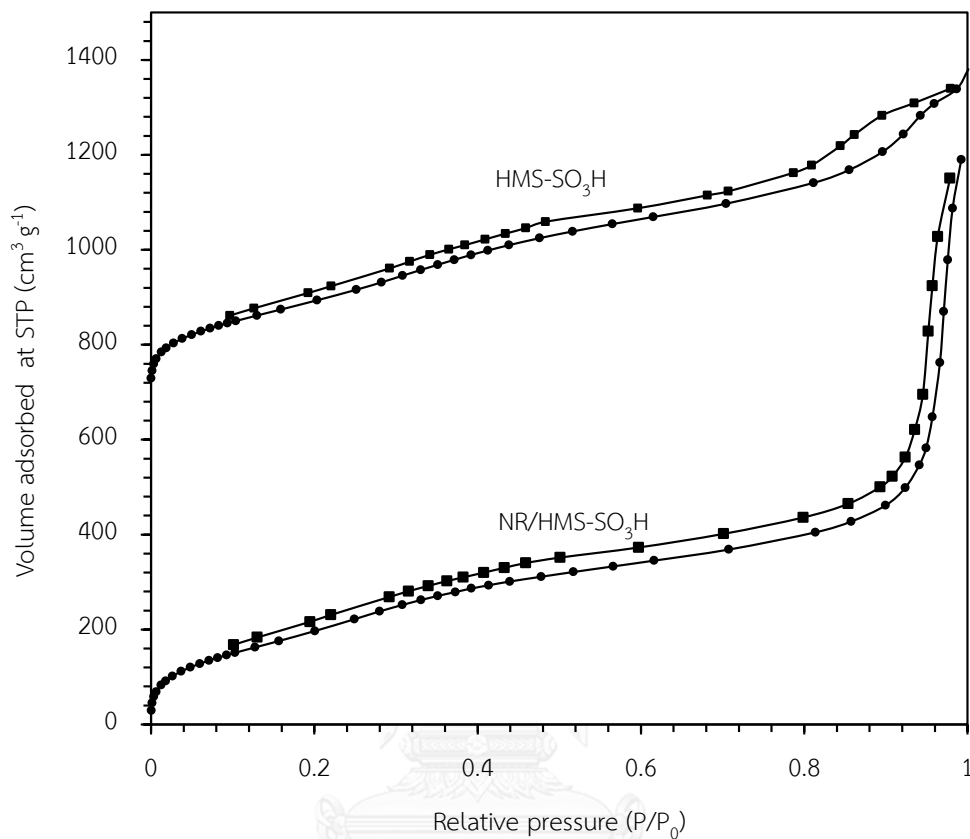


**Figure 4.3**  $N_2$  adsorption-desorption isotherms of  $HMS-SO_3H$  and  $NR/HMS-SO_3H$ .

Figure 4.3 shows  $N_2$  adsorption-desorption isotherms of  $HMS-SO_3H$  and  $NR/HMS-SO_3H$  after template removal. Both materials exhibited the isotherms of type IV according to the IUPAC classification. The presence of hysteresis loops at  $P/P_0$  in the range of 0.2 to 0.4 confirmed the mesoporous nature of these materials. The large hysteresis loop observed at  $P/P_0 > 0.8$  for these materials was related to  $N_2$  condensation inside the interparticle voids of particle agglomerates. The presence of rubber phase in the HMS framework enhanced the particles aggregation as deduced from larger hysteresis loop of  $NR/HMS-SO_3H$ .

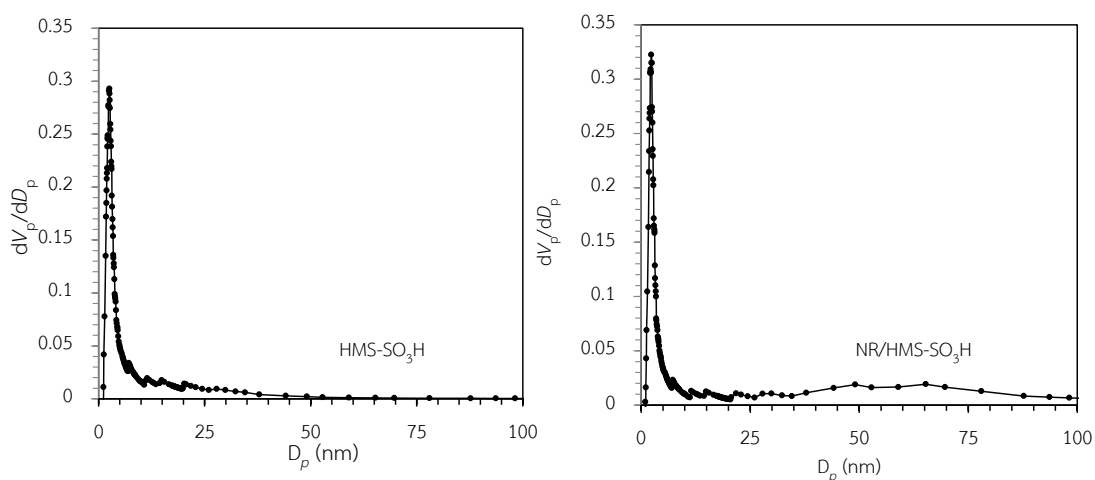


**Figure 4.4** BJH pore size distribution of HMS-SO<sub>3</sub>H and NR/HMS-SO<sub>3</sub>H.

The BJH pore size distribution of both materials is shown in Figure 4.4. The pore size of HMS-SO<sub>3</sub>H and NR/HMS-SO<sub>3</sub>H were 2.54 and 2.33 nm, respectively. The secondary pores as interparticle voids were observed for NR/HMS-SO<sub>3</sub>H, which collaborate with the large hysteresis loop at P/P<sub>0</sub> > 0.8 (Figure 4.3). Table 4.1 summaries the textural properties of acidic mesoporous catalysts. HMS-SO<sub>3</sub>H had higher specific surface area ( $S_{\text{BET}}$ ) and mesopore volume ( $V_p$ ) than NR/HMS-SO<sub>3</sub>H. It should be because some NR molecules covered on the HMS surface.

Figure 4.5 shows N<sub>2</sub> physisorption isotherm of calcined HUSY zeolite. This material exhibited the isotherm of type I according to the IUPAC classification. It had  $S_{\text{BET}}$  of 448 m<sup>2</sup> g<sup>-1</sup>. Its pore size was 0.8 nm as determined by the Horvath-Kawazoe (HK) method. In case of Amberlyst 15 and Amberlyst 36 wet, they had  $S_{\text{BET}}$  53 and 33 m<sup>2</sup> g<sup>-1</sup>, respectively, which was lower than that of the mesoporous and zeolite catalysts.

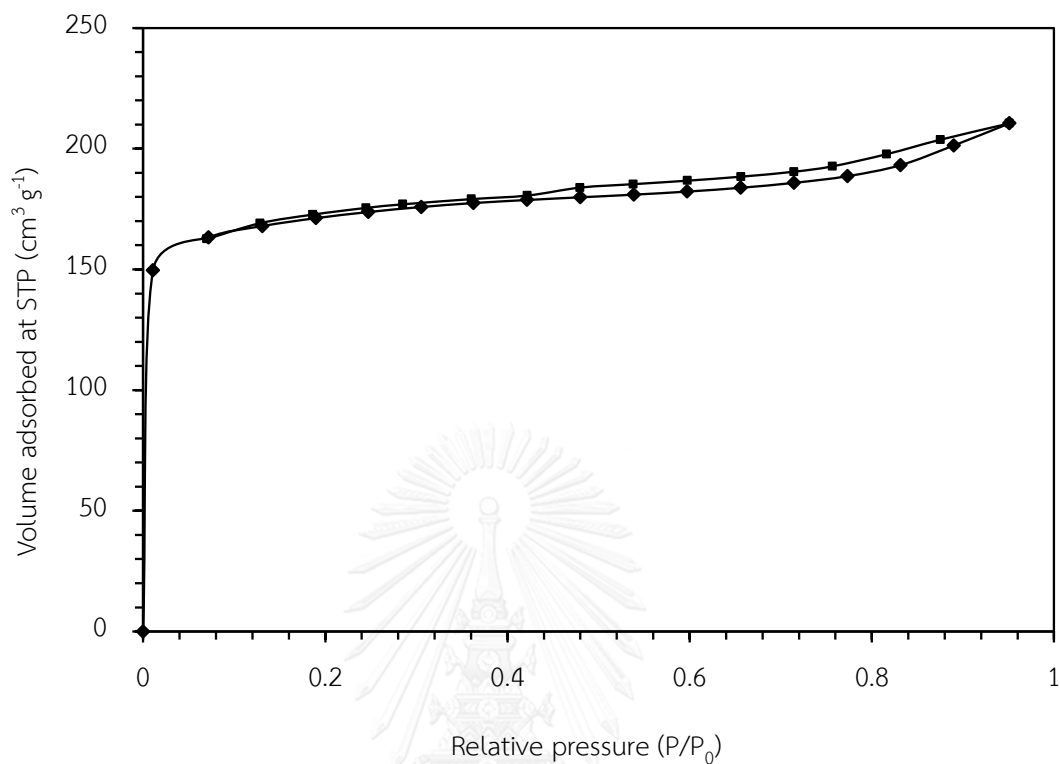


**Figure 4.5** N<sub>2</sub> adsorption-desorption isotherm of calcined HUSY zeolite.

#### 4.1.3 Sulfur content and acidity

The physicochemical properties of heterogeneous acid catalysts used in this study are summarized in Table 4.1. The total acidity of Amberlyst 15 and Amberlyst 36 wet was 4.70 and 5.40 mmol H<sup>+</sup> g<sup>-1</sup>, respectively. The mesoporous and zeolite catalysts had a similar range of total acidity (1.04–1.35 mmol H<sup>+</sup> g<sup>-1</sup>). Comparing the density of acid sites, it was found that the acid density was ranked in the following descending order : Amberlyst 36 wet > Amberlyst 15 > HUSY zeolite > NR/HMS-SO<sub>3</sub>H > HMS-SO<sub>3</sub>H.

**Table 4.1** Physicochemical properties of heterogeneous acid catalysts used in this work

Catalyst	Silica content (%)	Sulfur content (mmol g <sup>-1</sup> )	Acidity (mmol H <sup>+</sup> g <sup>-1</sup> )	S <sub>BET</sub> <sup>f</sup> (m <sup>2</sup> g <sup>-1</sup> )	D <sub>p</sub> <sup>g</sup> (nm)	V <sub>t</sub> <sup>h</sup> (cm <sup>3</sup> g <sup>-1</sup> )	V <sub>p</sub> <sup>i</sup> (cm <sup>3</sup> g <sup>-1</sup> )	Acid density (mmol H <sup>+</sup> m <sup>-2</sup> )
Amberlyst 15	N/A	4.6	4.7	53	30	0.4	N/A	0.0887
Amberlyst 36 wet	N/A	N/A	5.4	33	24	0.2	N/A	0.1636
HUSY	10.6 <sup>b</sup>	N/A	1.04 <sup>d</sup>	448	0.8	0.31	N/A	0.0023
HMS-SO <sub>3</sub> H	67.0 <sup>a</sup>	1.55 <sup>c</sup>	1.35 <sup>e</sup>	673	2.54	1	0.43	0.002
NR/HMS-SO <sub>3</sub> H	61.7 <sup>a</sup>	1.59 <sup>c</sup>	1.18 <sup>e</sup>	543	2.33	1.8	0.34	0.0021

N/A = not applicable.

<sup>a</sup> Determined by thermogravimetry technique

<sup>b</sup> Determined by ICP-AES

<sup>c</sup> Determined by CHNS analyzer

<sup>d</sup> Determined by TPD of NH<sub>3</sub>

<sup>e</sup> Determined by acid-base titration

<sup>f</sup> BET surface area

<sup>g</sup> Pore diameter calculated using the BJH method

<sup>h</sup> Total pore volume

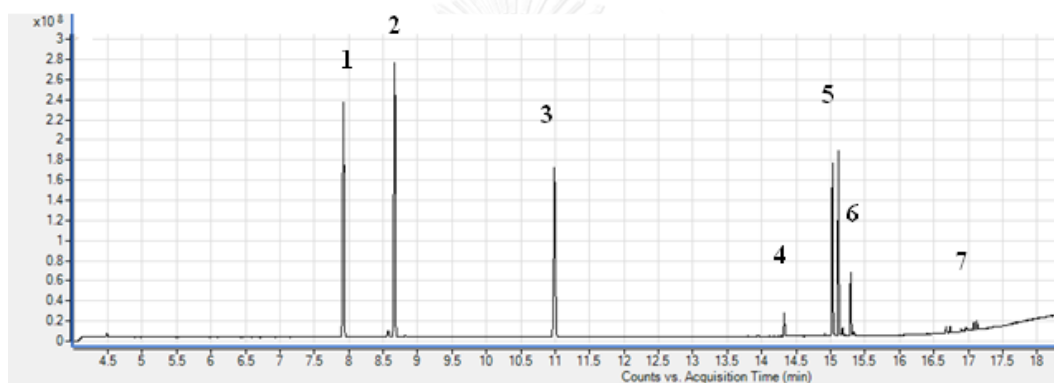
<sup>i</sup> Mesopore volume



## 4.2 Esterification of Solketal and Levulinic Acid

### 4.2.1 Identification of reaction products

Because there were various organic compounds formed as products in the reaction mixture, GC-MS was used to identify their chemical structures. The representative GC-MS chromatogram of the products mixture is shown in Figure 4.6. Table 4.2 summarizes the retention time and the chemical structure of organic compounds presenting in the reaction mixture. The fragmentation patterns in the mass spectra of these compounds are reported in Appendix C.

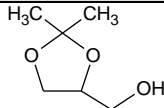
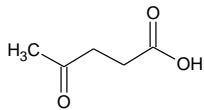
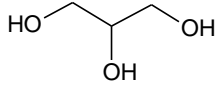
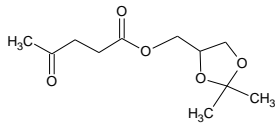
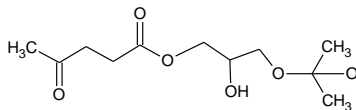
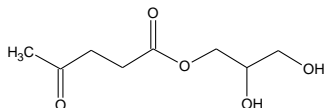
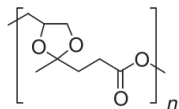


**Figure 4.6** Representative GC-MS chromatogram of the reaction mixture obtained from the esterification of LA and SK.

SK ( $m/z = 73, 101, 115, 131, 189$ ) and LA ( $m/z = 75, 99, 145, 173$ ) as reactants were observed at 7.92 and 8.66 min, respectively. There were at least 5 types of products formed in the reaction. Their appearance was in sequence based on the boiling point. Prior to the GC-MS analysis, MSTFA was used as derivatizing agent to reduce their polarity. Solketal levulinate (SL) ( $m/z = 99, 215$ ) was the primary product obtained from the esterification of LA and SK. The presence of glycerol ( $m/z = 73, 147, 205$ ) indicates that SK was hydrolyzed in the reaction system. Hemiacetal of solketal levulinate (H-SL) ( $m/z = 73, 99, 129, 131, 189, 231, 261, 319$ ) and glycerol levulinate (GL) ( $m/z = 73, 99, 147, 231$ ) would be generated via hydrolysis reaction.

Water produced as by-product from the esterification might participate in the hydrolysis of SK and SL. A group of large products formed as levulinic acid-glycerol ketal-ester oligomers (LGO) was observed at 16–17 min. The formation of these oligomers was related to the fact that LA has two reactive functional groups, i.e. ketone carbonyl (C=O) and acidic carboxyl (COOH) groups. However, identifying their chemical structures using the fragmentation patterns was not successful due to their complex structure.

**Table 4.2** Assignment of peaks observed from GC-MS chromatogram

Peak no.	Retention time (min)	Name	Chemical structure
1	7.92	Solketal (SK)	
2	8.66	Levulinic acid (LA)	
3	11.00	Glycerol	
4	14.33	Solketal levulinate (SL)	
5	15.00, 15.11	Hemiacetal of solketal levulinate (H-SL)	
6	15.30	Glycerol levulinate (GL)	
7	16.00-17.00	Levulinic acid-glycerol ketal-ester oligomers (LGO)	

The chemical structures of oligomers (LGO) were confirmed by  $^1\text{H}$  and  $^{13}\text{C}$  NMR spectroscopy (Figure 4.7).  $\text{CDCl}_3$  was employed as solvent, presenting in  $^{13}\text{C}$  NMR spectra at  $\delta = 78.00$  ppm. Amarasekara et al. reported the synthesis of LGO and identified the chemical structure of product using NMR spectroscopy [55]. The bifunctional groups of LA can react with glycerol in two different reaction modes, where the keto group forms ketals with 1,2 or 1,3 hydroxyls, and the carboxylic acid function undergoes the esterification. Based on the  $^{13}\text{C}$  NMR result [35], the oligomers obtained had oligo(levulinic acid-co-glycerol) as repeating unit (RU) and were consisted of three type of terminal groups, which are keto terminal (KT), glycerol-ketal terminal (GKT), and glycerol-ester terminal (GET). Figure 4.8 shows the chemical structures of LGO and the  $^{13}\text{C}$  NMR signal assignment.

In this work, the reaction mixture still contained the remaining reactants (LA and SK) and various types of products formed (SL, H-SL, GL and LGO). The purification of the products was difficult, and so only water was eliminated by rotary evaporator. According to the literature [58], SK was corresponded to the  $^1\text{H}$  at  $\delta = 4.11, 3.88, 3.68, 1.48$  ppm and the  $^{13}\text{C}$  signals at  $\delta = 110.10, 73.23, 67.68, 62.35, 25.60$  ppm. The  $^1\text{H}$  signals at  $\delta = 2.89, 2.61, 2.22$  ppm and the  $^{13}\text{C}$  signals at  $\delta = 214.19, 177.85, 38.27, 29.62, 28.33$  ppm were assigned to LA [59]. The presence of free glycerol was deduced from the  $^1\text{H}$  signals at  $\delta = 3.70, 3.50$  ppm and the  $^{13}\text{C}$  signals at  $\delta = 73.20, 63.80$  ppm [60]. The oligomers with different terminal groups were assigned in Figure 4.7. The RU was related to the  $^1\text{H}$  signal at  $\delta = 1.29$  ppm and the  $^{13}\text{C}$  signal at  $\delta = 110.18, 110.38$  ppm, corresponding to C-2 of 1,3-dioxolane ring [55]. These are terminated chain of oligomers by carbonyl ester of LA, levulinate-glycerol ketal structure and glycerol, respectively. The KT terminal with carbonyl ester end group was observed from the  $^1\text{H}$  signal at  $\delta = 1.29$  ppm and the  $^{13}\text{C}$  at  $\delta = 206.62, 26.99$  corresponding to C-4 and C-5 of KT, respectively. The  $^{13}\text{C}$  signals found at  $\delta = 76.22$  and  $62.35$  ppm were assigned to the GKT terminal with levulinate glycerol ketal end group [55]. Finally, the GET terminal was corresponded to the  $^{13}\text{C}$  signals at  $\delta = 69.94, 65.12, 63.12$  ppm, which were respectively assigned to C-2, C-3 and C-1 of glycerol end group of GET.

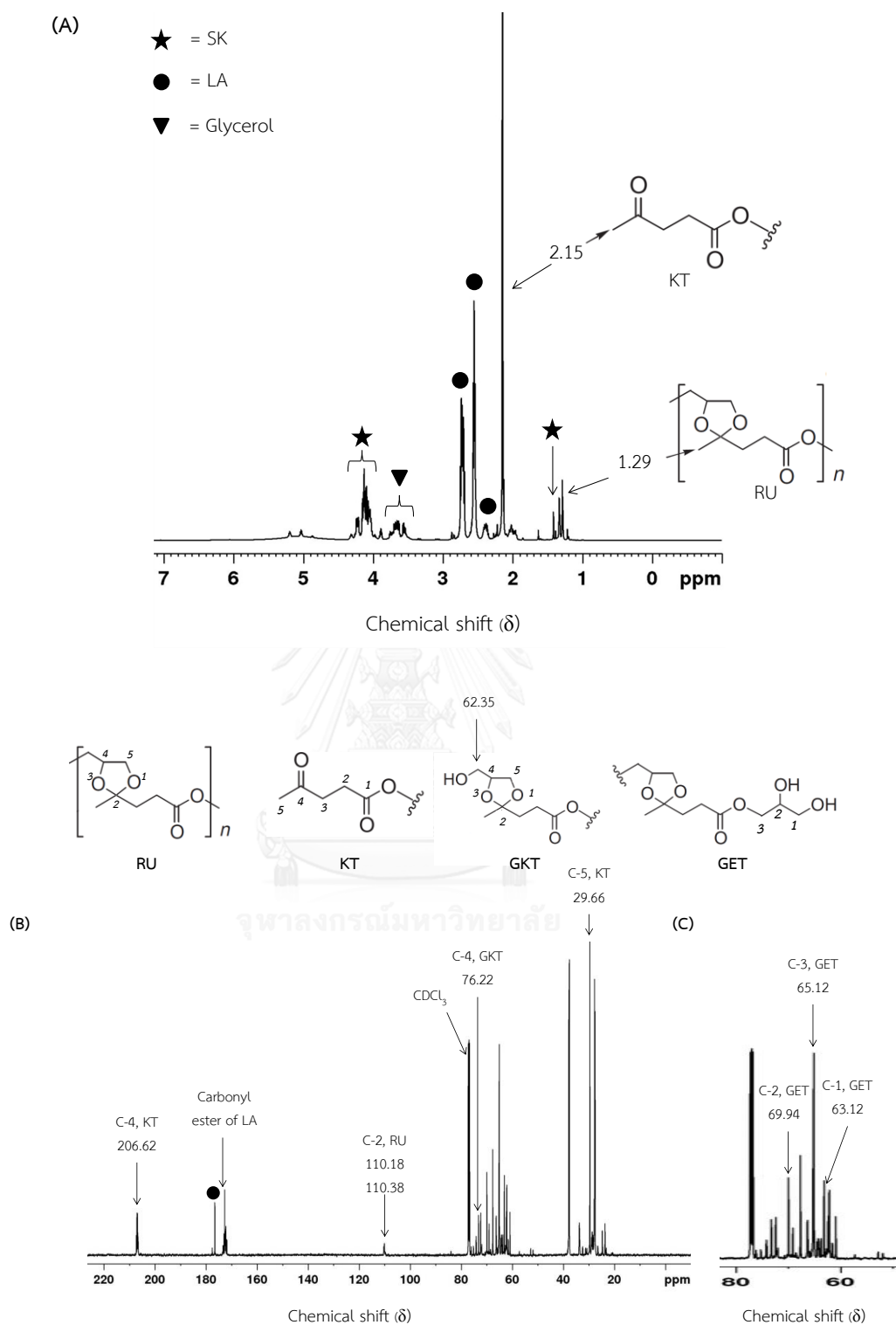


**Figure 4.7** (A)  $^1\text{H}$  and (B)  $^{13}\text{C}$  NMR spectra of reaction mixture. (C) shows an enlarged  $^{13}\text{C}$  spectrum in the  $\delta$  range of 60–80 ppm.

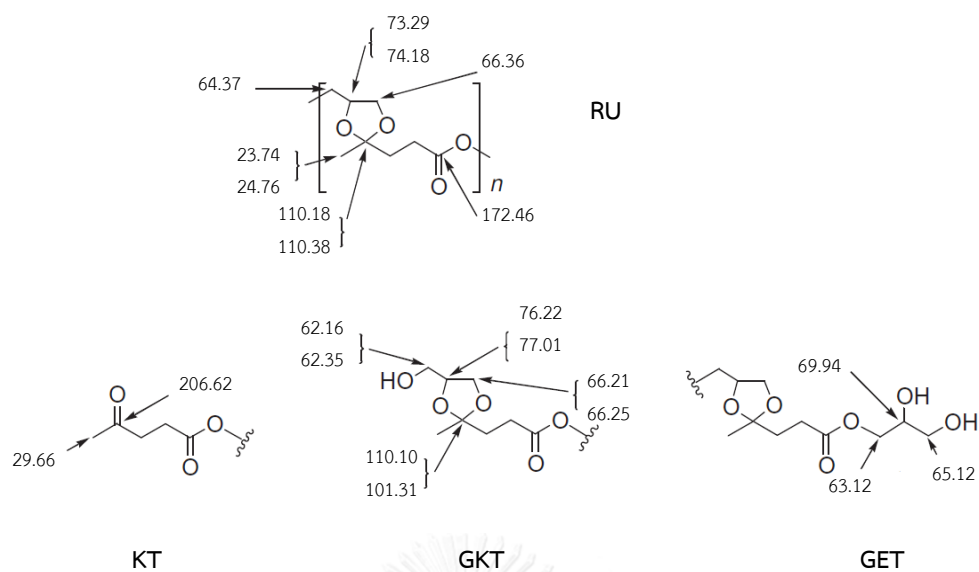


**Figure 4.8** Assignment of  $^{13}\text{C}$  NMR signals of the oligo(levulinic acid-co-glycerol) repeating unit (RU) with different terminal groups: keto terminal (KT), glycerol-ketal terminal (GKT), and glycerol-ester terminal (GET).

## 4.2.2 Effects of reaction conditions

### 4.2.2.1 Effect of reaction time

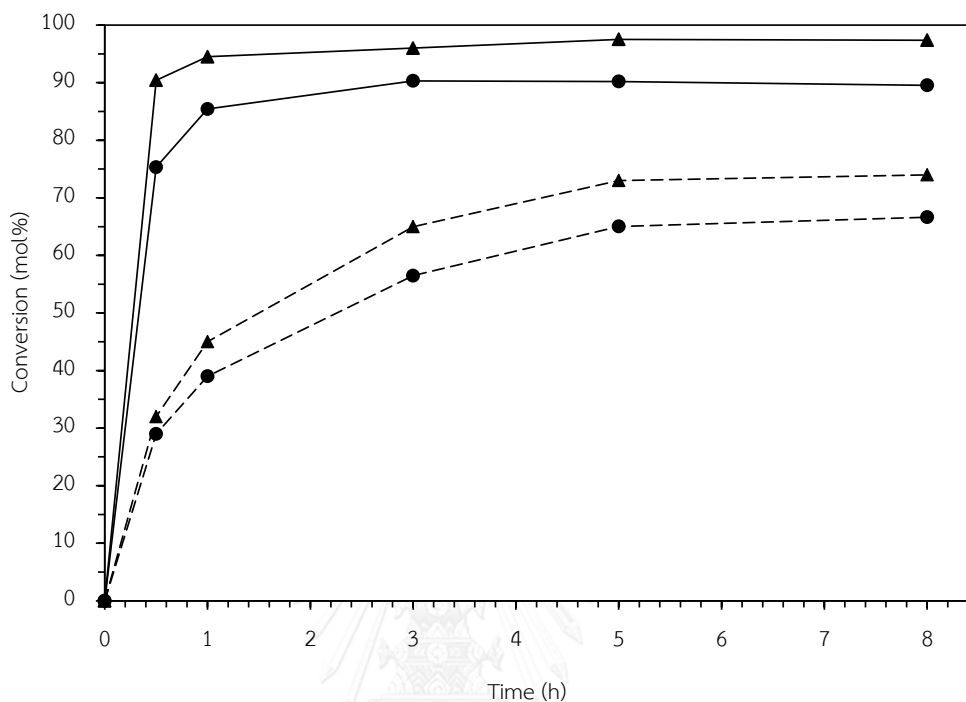


**Figure 4.9** Conversion of (▲) SK and (●) LA in the esterification of SK and LA over Amberlyst 15 (solid line) and blank (dash line). Reaction conditions: SK: LA molar ratio, 1:1; reaction temperature, 120 °C; Amberlyst 15 loading, 5 wt.% respect to LA.

The effect of reaction time on the LA and SK conversion was studied in the range of 0 to 8 h to find the optimum reaction condition. Figure 4.9 shows the conversion of SK and LA in the esterification of SK and LA over Amberlyst 15 in comparison with that attained from the reaction without any catalyst (blank). Both of LA and SK conversion increased with increasing the reaction time, especially from 0 to 1 h. At 1 h, the LA and SK conversion around 42 mol% was obtained in the absence of catalyst. It confirmed that the esterification of SK and LA is a spontaneous reaction. Adding Amberlyst 15 as an acidic catalyst promoted the conversion of LA and SK to 85 and 95 mol%, respectively. Since the reactants conversion over Amberlyst 15 was insignificantly changed from 3 to 8 h, the reaction approached the

equilibrium at 3 h as the optimum reaction time. At the 1:1 SK: LA molar ratio, the conversion of SK and LA was expected to be equal. However, the conversion of SK over Amberlyst 15 was 10 mol% higher than that of LA at 1 h. It was suspected that SK was converted to other products. As indicated by GC-MS result (Section 4.2.1), glycerol was a possible product derived from the SK hydrolysis [4, 8]. The product mixture obtained over Amberlyst 15 was transparent yellow solution and more viscous than that obtained from the blank test. Therefore, the formation of large products as oligomers was probably promoted in the presence of acid catalyst.

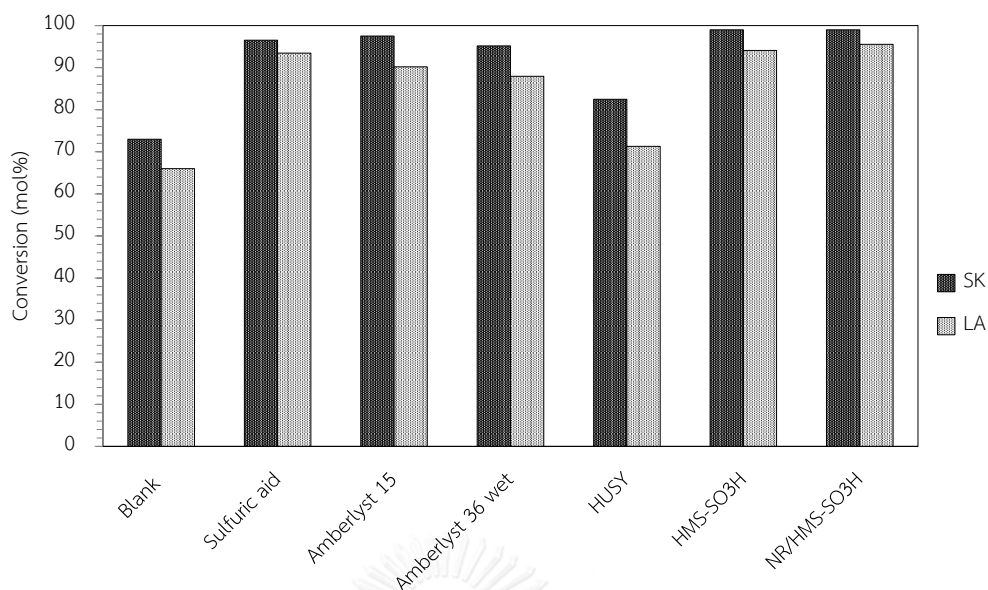
#### 4.2.2.2 Effect of catalyst type

Catalyst plays an important role in the esterification since it enhances the rate of reaction to achieve the higher reactant conversion in shorter period. Sulfuric acid is a mineral acid widely used as catalyst in the esterification process [23-28]. However, using heterogeneous acid catalysts instead of homogeneous acid catalyst has several advantages such as ease of separation from the products mixture. In this study, several types of heterogeneous acid catalysts, including Amberlyst 15, Amberlyst 36 wet, HUSY zeolite, HMS-SO<sub>3</sub>H and NR/HMS-SO<sub>3</sub>H, were studied for their catalytic performance to obtain the suitable catalyst for the esterification of SK and LA. Zeolite is a type of heterogeneous acid catalysts for production of petrochemicals and fine chemicals due to its high intrinsic acidity and thermal stability [57]. The Amberlyst<sup>®</sup> series are cationic-exchange resins with high proton activity. They are a class of organic-based catalysts used in the reaction of free fatty acids in low-cost oil feedstock for biodiesel production [35][16]. HMS-SO<sub>3</sub>H is a potential heterogeneous acid catalyst for the esterification of various carboxylic acids with ethanol because it has a large surface area and a high acidity of propylsulfonic acid group [41]. NR/HMS-SO<sub>3</sub>H is a solid catalyst composed of propylsulfonic acid-functionalized HMS (HMS-SO<sub>3</sub>H) and NR as hydrophobicity improver. Its enhanced

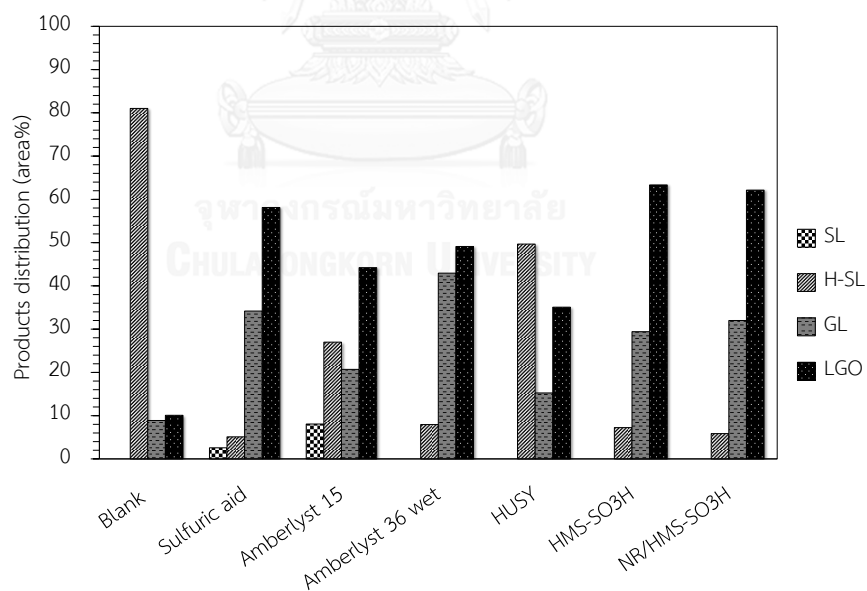
hydrophobic properties were proved to be beneficial for the esterification of medium-to-long chain fatty acids (octanoic acid and lauric acid) [41, 56].

Figure 4.10 shows the SK and LA conversion obtained from the esterification in the presence different acid catalysts. In the absence of any catalyst (blank), the conversion of SK and LA was 73 and 65 mol%, respectively. The amount of sulfuric acid used was 0.05 wt.% respect to LA, by which the SK and LA conversion of 97 and 93 mol%, respectively, was attained. For the ion-exchanged resin catalysts, Amberlyst 15 gave the conversion of both SK and LA (98 and 90 mol%, respectively) higher than Amberlyst 36 wet ( 95 and 88 mol%, respectively) although Amberlyst 15 had acidity ( $4.60 \text{ mmol H}^+ \text{ g}^{-1}$ ) lower than Amberlyst 36 wet ( $5.40 \text{ mmol H}^+ \text{ g}^{-1}$ ). This result should be ascribed to effect of surface area since Amberlyst 15 ( $53 \text{ m}^2 \text{ g}^{-1}$ ) had the surface area larger than Amberlyst 36 wet ( $33 \text{ m}^2 \text{ g}^{-1}$ ). The higher surface area promoted the reactants adsorption and increased the concentration of reactants on the catalyst surface, resulting in the higher conversion. It can be seen that HUSY zeolite yielded the lowest conversion of reactants (around 70–80 mol%) when compared to other heterogeneous acid catalysts. It should be because HUSY had the lowest acidity ( $1.08 \text{ mmol H}^+ \text{ g}^{-1}$ ) and the smallest pore diameter (0.8 nm). This material is classified as a microporous material, so the diffusion of reactant molecules into the interior surface and the reaction on the active sites were limited by its pore size. In heterogeneous catalysis, mass transfer limitation is an important factor to determine the catalytic activity. The HMS-SO<sub>3</sub>H catalyst gave LA conversion of 94 mol%, which was similar to that obtained over NR/HMS-SO<sub>3</sub>H (96 mol%). Since NR/HMS-SO<sub>3</sub>H had lower surface area and pore volume than HMS-SO<sub>3</sub>H (Table 4.1), the hydrophobicity of NR might compensate the reduced activity by promoting the mass transfer of reactant molecules.





**Figure 4.10** Conversion of SK and LA in the esterification of SK and LA in the presence of different acid catalysts. The amount of sulfuric acid used was 0.05 wt.% respect to LA. Reaction conditions: SK: LA molar ratio, 1:1; catalyst loading, 5 wt.%; temperature, 120 °C; time, 5 h.



**Figure 4.11** Products distribution in the esterification of SK and LA in the presence of r different acid catalysts. The amount of sulfuric acid used was 0.05 wt.% respect to LA. Reaction conditions: SK: LA molar ratio, 1:1; catalyst loading, 5 wt.%; temperature, 120 °C; time, 5 h.

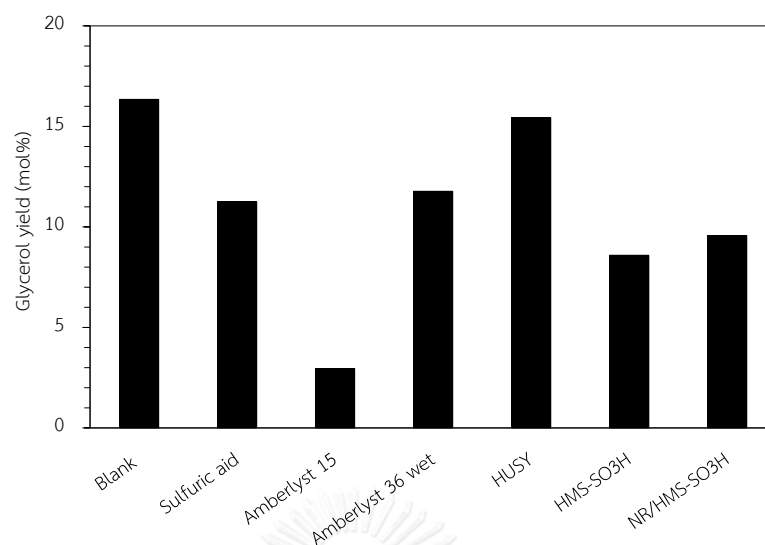


**Figure 4.12** The glycerol yield obtained from the esterification of SK and LA in the presence of different acid catalysts. The amount of sulfuric acid used was 0.05 wt.% respect to LA. Reaction conditions: SK: LA molar ratio, 1:1; catalyst loading, 5 wt.%; temperature, 120 °C; time, 5 h.

Figure 4.11 shows the products distribution obtained from the esterification of SK and LA in the presence of different acid catalysts. SL is defined as the primary esterification product. It was only found when the reaction was catalyzed by sulfuric acid (3%) and Amberlyst 15 (8%). For other solid acid catalysts, SL was not detected indicating that it was converted to other products. H-SL is a product derived from the hydrolysis of SL as shown in Figure 4.13. Water was generated as a by-product from the esterification of SK and LA, and so took place in the hydrolysis reaction. Interestingly, the reaction without any catalyst (blank) gave the highest selectivity to H-SL (81%). So, it was confirmed that, similarly to the esterification, the hydrolysis is a spontaneous reaction. Figure 4.12 compares the yield of glycerol obtained as a product from the SK hydrolysis. SK can be hydrolyzed backward to glycerol and acetone as shown in Figure 1.3. The highest glycerol yield (16 mol%) in the absence of catalyst collaborated with the highest selectivity to H-SL. In the blank test, the GL and oligomers (LGO) selectivities were ca. 9 % and 10 %, respectively. The formation of GL was related to the hydrolysis of H-SL and/or the esterification of glycerol with

LA. LGO was generated by multi-step ketolization/esterification of glycerol and LA as shown in Figure 4.14. The reaction of GL with glycerol and LA was also a possible route for the LGO formation. The low acidity of LA itself contributed the formation of GL and LGO at small extent.

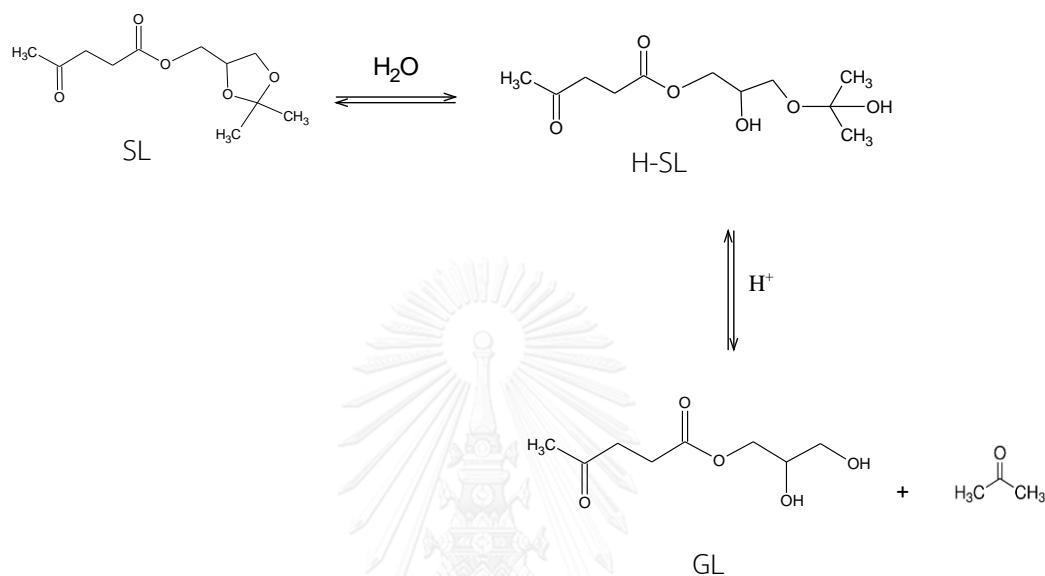


Figure 4.13 Hydrolysis of SL.

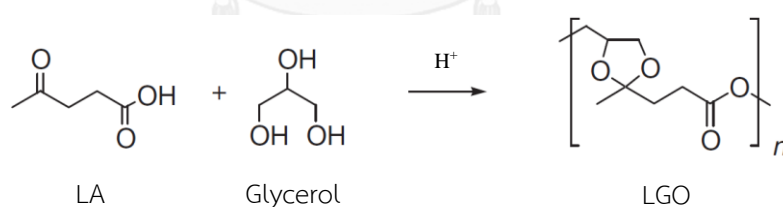


Figure 4.14 Ketolization/esterification of glycerol and LA in the presence of acid catalyst.

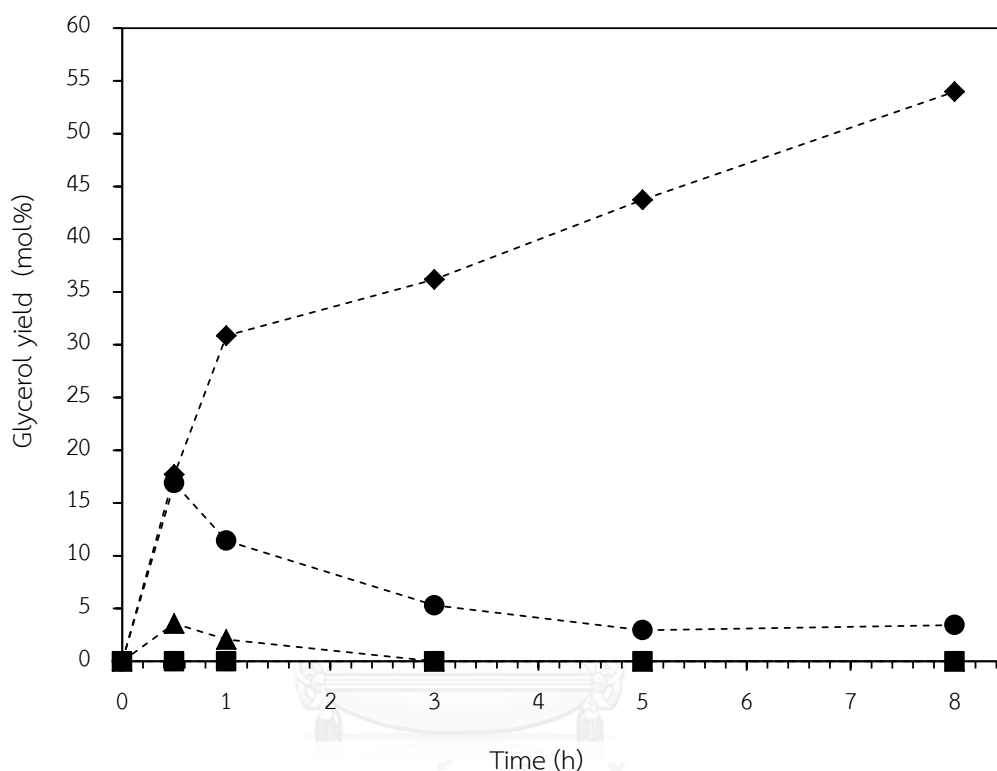
When a catalyst was added in the reaction, the glycerol yield and the H-SL selectivity were decreased, and the formation of GL and LGO was promoted. In case of sulfuric acid, the selectivity to H-SL (5%) was decreased, while the GL and LGO selectivities were increased to 34% and 58%, respectively. For the acidic ion-exchanged resin catalysts, Amberlyst 36 wet gave the glycerol yield higher than Amberlyst 15. It should be due to a higher moisture content of Amberlyst 36 wet.

However, the selectivity to GL and LGO was promoted over Amberlyst 36 wet higher extent than Amberlyst 15. This result was explained by effect of acidity, which was higher for Amberlyst 36 wet than Amberlyst 15 (Table 4.1). As shown in Figure 4.10, the HUSY with microporous structure gives the lowest SK and LA conversion among the solid catalysts. Similarly to the blank test, H-SL was the major product (50%), and the glycerol yield was comparable. This result was ascribed to the mass transfer limitation that inhibited the reaction over the acid sites, and so the majority of reactants underwent the spontaneous reactions. Besides their similar activity (Figure 4.10), both HMS-SO<sub>3</sub>H and NR/HMS-SO<sub>3</sub>H gave a similar glycerol yield and product distribution. The effect of hydrophobicity derived from NR was unclear, probably because the reactants (SK and LA) have small molecules and higher polarity. Interestingly, the acidic mesoporous catalysts enhanced the LGO selectivity to 63%. So, they benefit the production of long-chain products via the esterification and ketalization. As mentioned above, SK was hydrolyzed by the water generated from the esterification of SK and LA, backward to glycerol and acetone. In this work, the formation of glycerol was observed in all runs. As shown in figure 4.12, the blank test gave the glycerol yield of 16 mol%. Adding the acid catalyst in the reaction decreased the glycerol yield due to the formation of larger products. GL and LGO were generated together with releasing water as by-product, which then hydrolyzed SK and other derivatives back to glycerol. Therefore, the origin of glycerol formed remained unclear. Besides its high activity, Amberlyst 15 gave the lowest yield of glycerol (3 mol%). This is desirable because it reflected a small loss of products. Based on these results, we can conclude that Amberlyst 15 was a suitable catalyst for the esterification of SK and LA.

#### *4.2.2.3 Effect of SK: LA molar ratio*

The esterification of LA with alcohol is a reversible reaction. Water is formed as a by-product. To achieve a high LA conversion, the backward must be minimized by either elimination of water formed during the reaction or using an excess amount

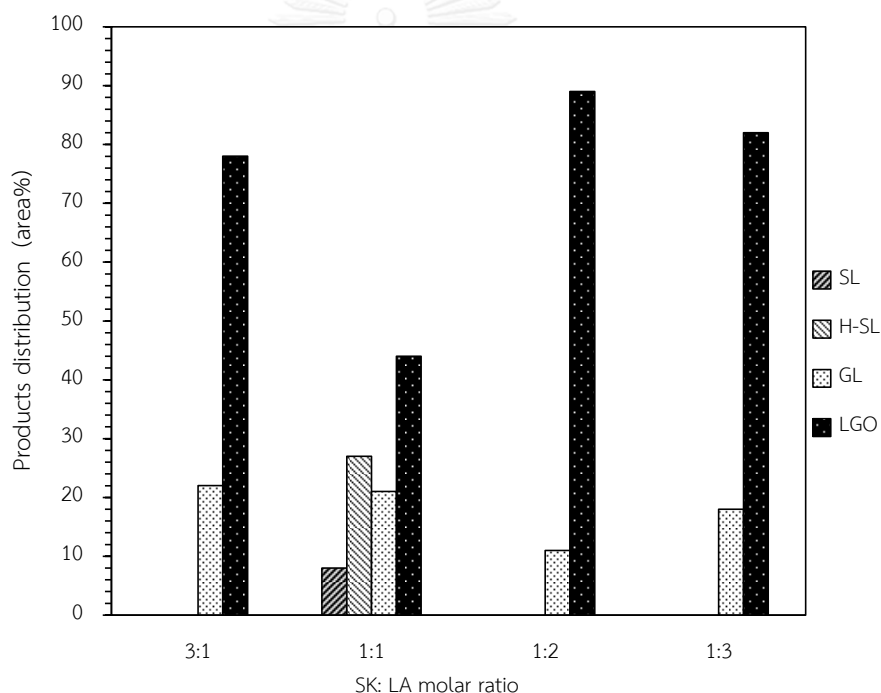
of alcohol [61]. In this part, the effect of SK: LA molar ratio on the SK and LA conversion and the products distribution were studied. The molar ratio of SK: LA was varied at 3:1, 1:1, 1:2 and 1:3. This approach would provide a solution for reducing the glycerol formation.



**Figure 4.15** The glycerol yield obtained from the esterification of SK and LA Amberlyst 15. A SK: LA molar ratio was varied at, (◆) 3:1, (▲) 1:1, (■) 1:2, and (●) 1:3. Other reaction conditions: catalyst loading, 5 wt.%; temperature, 120 °C.

Surprisingly, both of SK and LA conversion are achieved of 90–99 mol% for all of SK: LA molar ratio. Figure 4.15 shows the effect of SK: LA molar ratio on the glycerol yield attained from the esterification of SK and LA over Amberlyst 15. The formation of glycerol was dominant at the beginning of reaction. It indicates that the water generated from the esterification of SK and LA to produce SL mainly contributed the SK hydrolysis. At the 1:1 molar ratio, the glycerol yield decreased

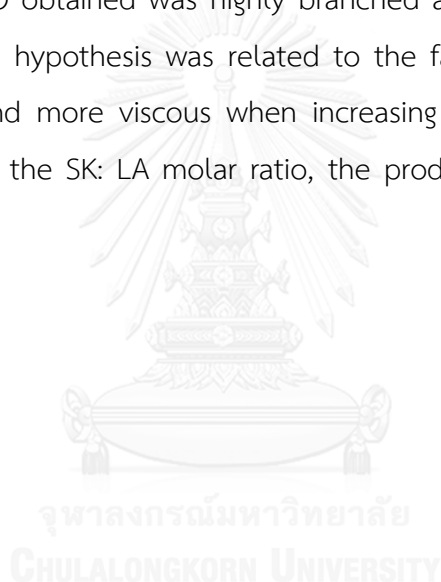
with time since it was consumed in the formation of GL and LGO. When the SK: LA ratio was increased to 3:1, the glycerol yield was enhanced. An increase in the amount of glycerol continued to 8 h, giving the glycerol yield of 54%. In this case, the water participating of the SK hydrolysis should be also derived from the formation of larger products, such as LGO. The presence of excess amount of SK was, moreover, a reason for the high yield of glycerol. On the other hand, the reaction at a low SK: LA molar ratio (1:2 and 1:3) decreased the glycerol yield less than 5%. This is because SK was consumed rapidly in the esterification with LA. However, the SL formed as the primary product was converted to H-SL, GL and LGO as revealed by the products distribution (Figure 4.16).



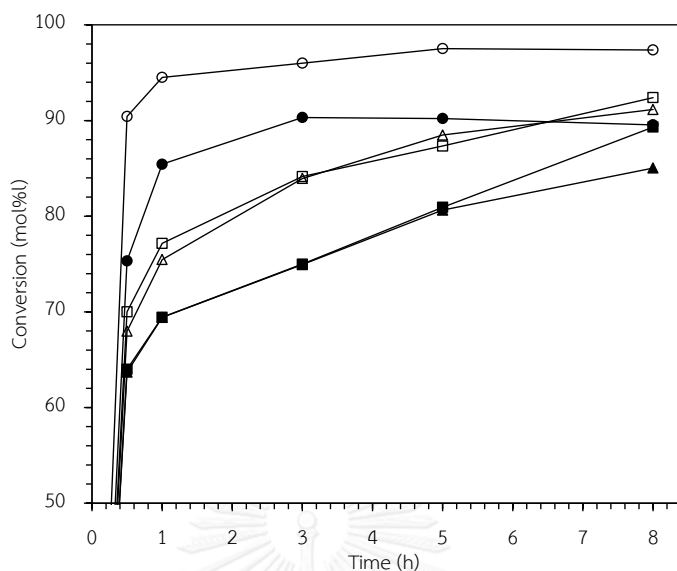
**Figure 4.16** Effect of SK: LA molar ratio on the products distribution obtained from the esterification of SK and LA over Amberlyst 15. Reaction conditions: catalyst loading, 5 wt.%; time, 5 h; temperature, 120 °C.

Figure 4.16 shows the effect of SK: LA molar ratio on the products distribution obtained from the esterification of SK and LA over Amberlyst 15. Reaction conditions: catalyst loading, 5 wt.%; time, 5 h; temperature, 120 °C. In all case, LGO was found

as the major product. Compared to the reaction with the SK: LA molar ratio of 1:1, either decreasing the ratio to 1:2 and 1:3 or increasing the ratio to 3:1 enhanced the formation of LGO to 78–89 % selectivity. However, since the oligomers were generated in association with the bifunctional groups of LA and glycerol with three hydroxyl groups, the LGO obtained from these two cases might have different chemical structure. As shown in Figure 4.15, using the 1:3 SK: LA ratio generated a large amount of glycerol. It was expected that the resulting LGO contained largely free hydroxyl groups or terminated with glycerol end groups (GET). On the other hand, glycerol was rarely available when the SK: LA ratio was decreased to 1:2 and 1:3. Possibly, the LGO obtained was highly branched and terminated with carbonyl ester of LA (KT). This hypothesis was related to the fact that the product mixture became yellowish and more viscous when increasing the initial LA concentration. Therefore, by varying the SK: LA molar ratio, the product with high LGO selectivity can be achieved.



#### 4.2.2.4 Effect of reaction temperature



**Figure 4.17** Effect of reaction temperature on the conversion of SK (open symbol) and LA (filled symbol) attained from the esterification of SK and LA over Amberlyst 15. Reaction conditions: SK: LA molar ratio, 1:1; catalyst loading, 5 wt.% respect to LA. The reaction temperature was varied at (triangle) 65 °C, (square) 80 °C, and (circle) 120 °C.

Esterification is an endothermic reaction. Increasing the reaction temperature is a way to enhance the reactants conversion and the products yield. However, Rammohan et al. [16] reported that the limit operation of Amberlyst-15 is 120 °C. Thus, the effect of reaction temperature was studied upto 120 °C to avoid the denature of Amberlyst 15. Figure 4.17 shows the SK and LA conversion obtained from the esterification of SK and LA at different temperature. At 65 and 80 °C, both of the SK and LA conversion were similar, about 80 and 88 mol%, respectively. The conversion of SK and LA increased to 98 and 90 mol%, respectively, and the reaction reached equilibrium in 1 h. At an elevated temperature, the kinetic energy of the reactant molecules was increased and the reaction was accelerated at a higher rate. In all cases, the SK conversion was higher than the LA conversion, indicating that not only the esterification, but also the hydrolysis of SK was promoted.



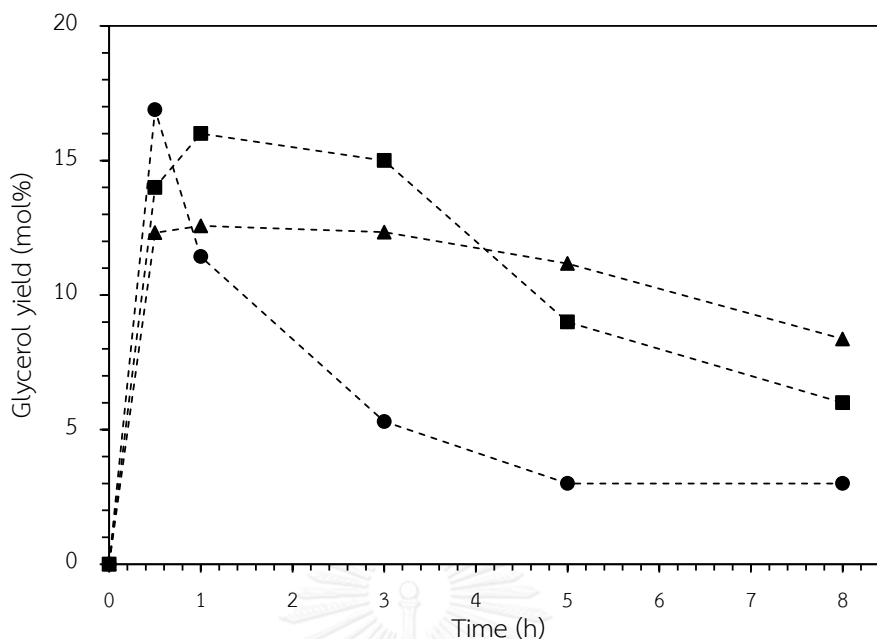


**Figure 4.18** The glycerol yield obtained from the esterification of SK and LA over Amberlyst 15 at (triangle) 65 °C, (square) 80 °C, and (circle) 120 °C. Reaction conditions: SK: LA molar ratio, 1:1; catalyst loading, 5 wt.% respect to LA.

Glycerol was detected in the reaction mixture at all reaction temperature. Figure 4.18 shows the effect of reaction temperature on the glycerol yield obtained from the esterification of SK and LA over Amberlyst 15. At the 5 h, The formation of glycerol was increased at higher temperature, and the highest glycerol yield of 17% was obtained at 120 °C. Since the esterification of SK and LA was promoted at high temperature Figure 4.17, a large amount of water was generated. As a result, the hydrolysis reaction to produce glycerol was enhanced. However, glycerol disappeared vary fast at 120 °C. At 5 h, the yield of glycerol remaining in the reaction mixture was decreased in the following order: 120 °C > 80 °C > 65 °C. It was explained by the transformation of glycerol to other products (LGO) as shown in Figure 4.19, which was also promoted at high temperature. This result indicates that the glycerol esterification required more severe conditions than the SK and LA esterification and SK hydrolysis. Consequently, the optimum reaction temperature was 120 °C because at this temperature the glycerol formation was minimized.

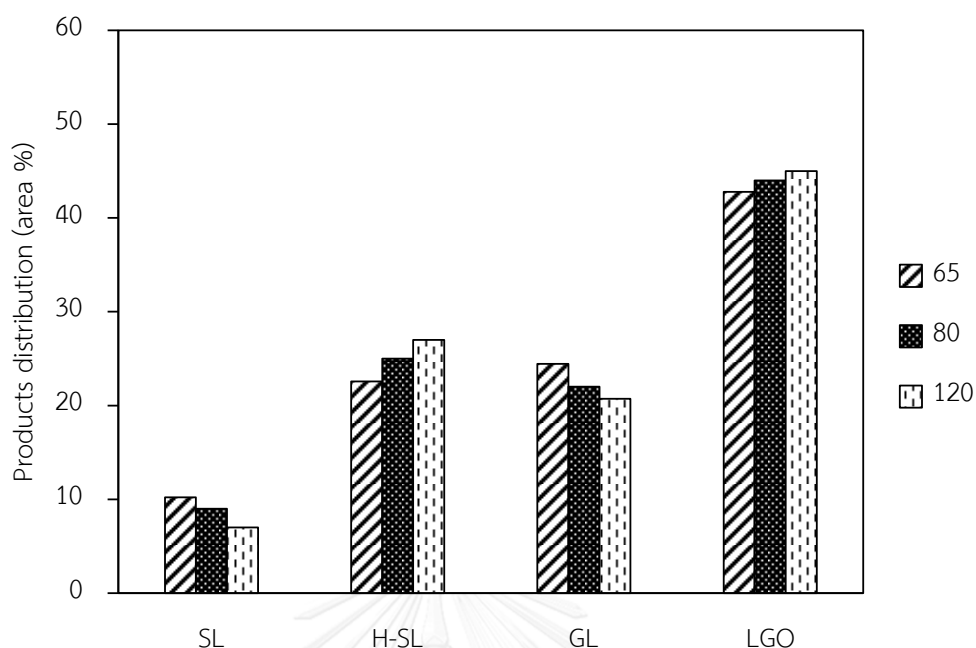


**Figure 4.19** The products distribution obtained from the esterification of SK and LA over Amberlyst 15. Reaction conditions: SK: LA molar ratio, 1:1; catalyst loading, 5 wt.% respect to LA. The reaction temperature was varied at at (▨) 65 °C, (■) 80 °C, and (▩) 120 °C.

#### 4.2.2.5 Effect of catalyst loading

The reactants (SK and LA) conversion and the reaction rate are strongly influenced by the catalyst loading level. In this work, Amberlyst 15 was chosen as the suitable catalyst for the esterification of SK and LA because it had a high acidity ( $4.7 \text{ mmol H}^+ \text{ g}^{-1}$ ), giving a high SK and LA conversion (Figure 4.20) and a low glycerol yield (Figure 4.21). The effect of catalyst loading on the esterification of SK and LA was varied from 1 to 8 wt.% with respect to LA in order to find the optimum catalyst loading. In the presence of Amberlyst 15 (at 3 to 8 wt.%), the small amount of SK remaining (less than 1 %) was detected in the products mixture. It can be concluded that SK was fully converted. Normally, the esterification of LA with alcohols occurs without any acid catalyst, owing to some acidity of LA itself that catalyzed the

reaction spontaneously [39]. In the blank test, the conversion of LA was 66 mol%, but SL as the primary product was not observed. SL was hydrolyzed to H-SL at high selectivity as shown in Figure 4.22. The addition of Amberlyst 15 enhanced the esterification. The LA conversion was enhanced upto 90% at 3 wt.% catalyst loading since the amount of acid site was increased. Further increasing the catalyst loading level did not affect the LA conversion. However, it was found that the reaction mixture became more viscous at an increased loading of catalyst. It indicates that the formation of oligomers was promoted under this condition. Based on the results obtained the catalyst loading of 3 wt.% respect to LA was the smallest catalyst amount required to the achieve the highest LA conversion and minimize the glycerol formation at 90 and 6 mol%, respectively. Moreover, increasing of catalyst loading (8 wt.%), LGO was observed as the main components around 80 % because high acidity. So, we can conclude that effect of catalyst loading is a strongly influence to control the product selectivity.

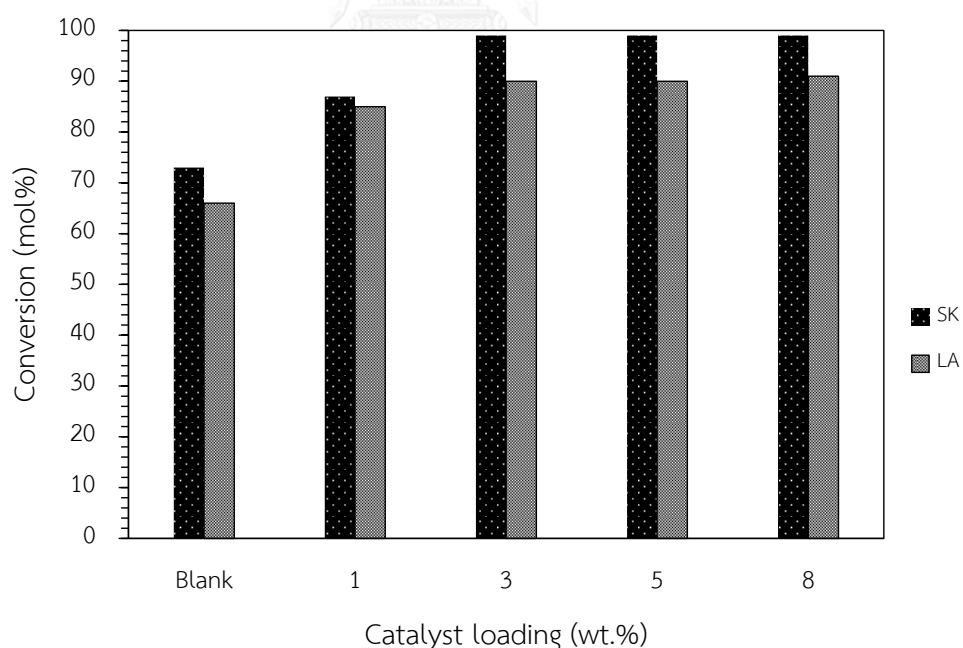


**Figure 4.20** Effect of catalyst loading on the SK and LA conversion obtained from the esterification of SK and LA over Amberlyst 15. Reaction conditions: SK: LA molar ratio, 1:1; temperature, 120 °C; time, 5 h.

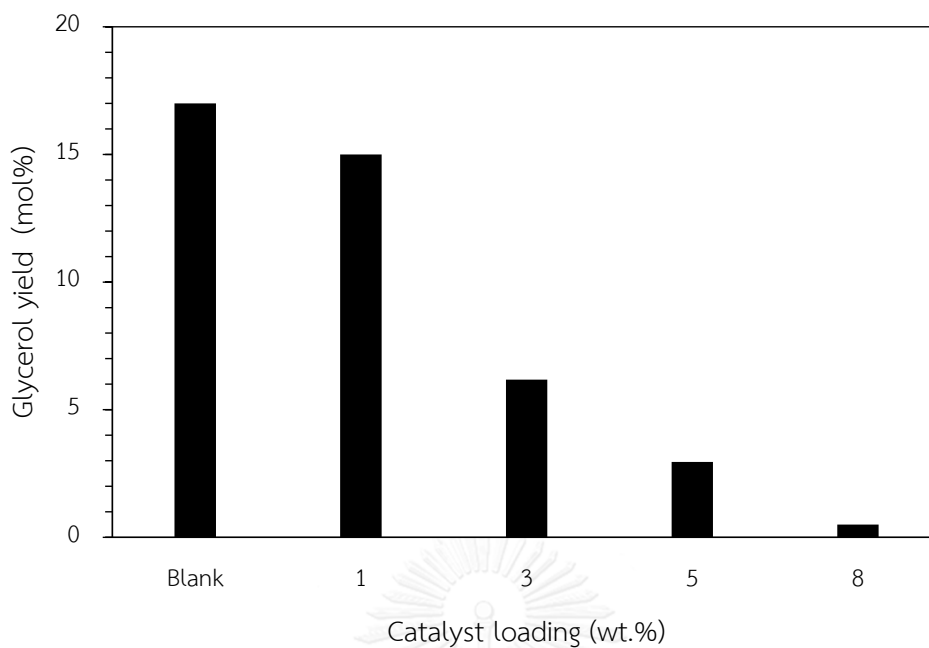


**Figure 4.21** Effect of catalyst loading on the glycerol yield obtained from the esterification of SK and LA over Amberlyst 15. Reaction conditions: SK: LA molar ratio, 1:1; temperature, 120 °C; time, 5 h.

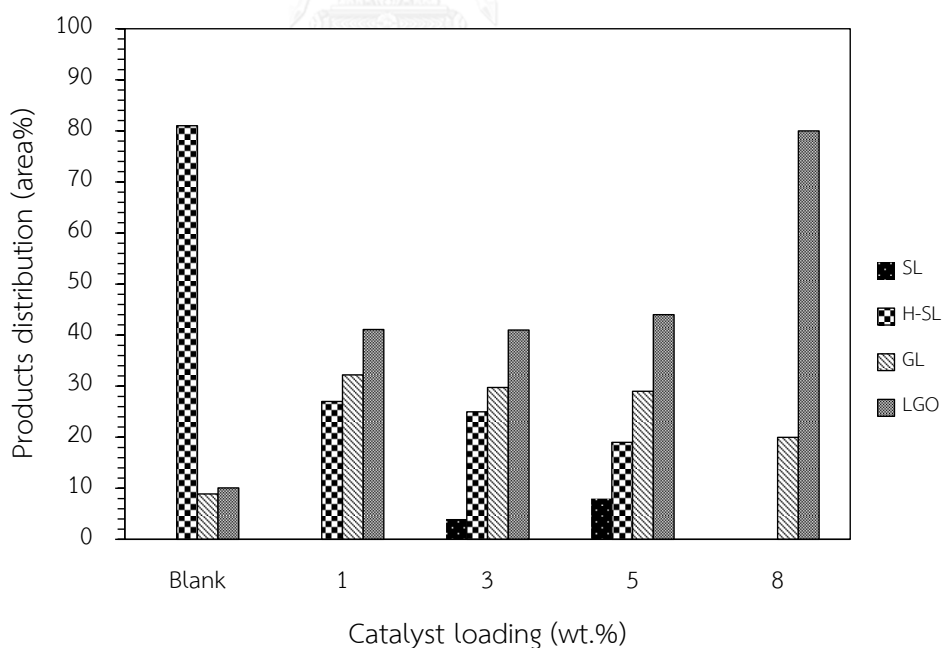


**Figure 4.22** Effect of catalyst loading on the products distribution obtained from the esterification of SK and LA over Amberlyst 15. Reaction conditions: SK: LA molar ratio, 1:1; temperature, 120 °C; time, 5 h.

#### 4.2.2.6 Elimination of water in the reaction

Because of water was generated during the reaction, elimination of water is required. In this case, zeolite 3A was added in the reaction of the esterification of SK and LA over Amberlyst 15 in order to absorb water. Reaction conditions: SK: LA molar ratio, 1:1; temperature, 120 °C; time, 5 h under 100 mbar. This case found that both of SK and LA are fully conversion (99 mol%) and the product mixture became highly viscous. Glycerol was found around 8 %. Moreover, other components (H-SL, GL and LGO) were found at 20, 7 and 74%, respectively.

#### 4.2.3 Plausible the reaction pathway

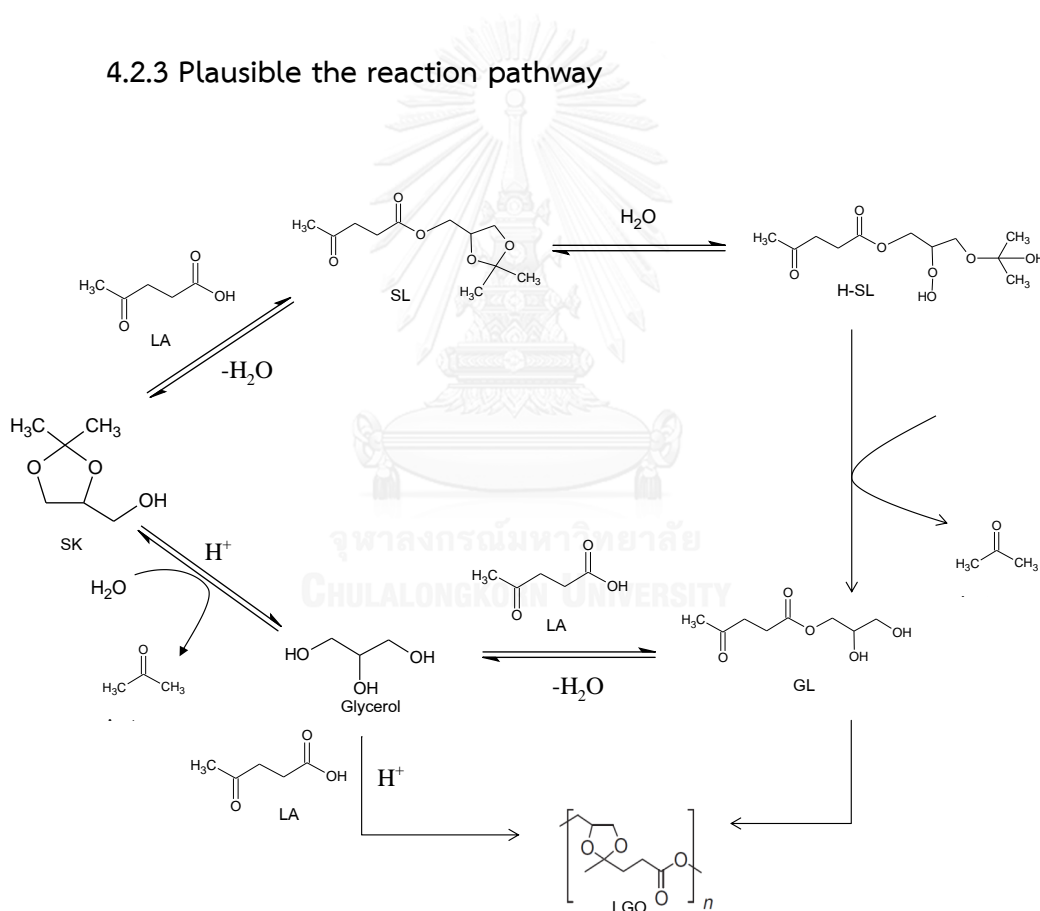


**Figure 4.23** The proposed reaction pathway in the esterification of SK and LA to various products.

Figure 4.23 illustrates the proposed reaction pathway of the esterification of LA and SK and its side reactions. SL is directly obtained as the primary product from

the esterification of SK and LA. Simultaneously, water is generated as a by-product from this reaction. Since the esterification is reversible in nature, the hydrolysis of ester product back to the reactants occurs to some extent [4]. However, glycerol was observed in the reaction mixture obtained under every condition, even when without any catalyst added. Therefore, the water generated takes place the hydrolysis of SK to glycerol and acetone. The SK hydrolysis can be catalyzed by the activity of LA, giving the glycerol yield of 17 mol%. In most cases, SL was rarely detected at the beginning of reaction. H-SL is a hemi-acetal of solkatal levulinate, which is formed as an intermediate from the hydrolysis of SL to GL. With no adding any catalyst, the H-SL selectivity was 81%. It can be concluded that the SL hydrolysis to H-SL is revealed to the water generated from the SK and LA esterification.

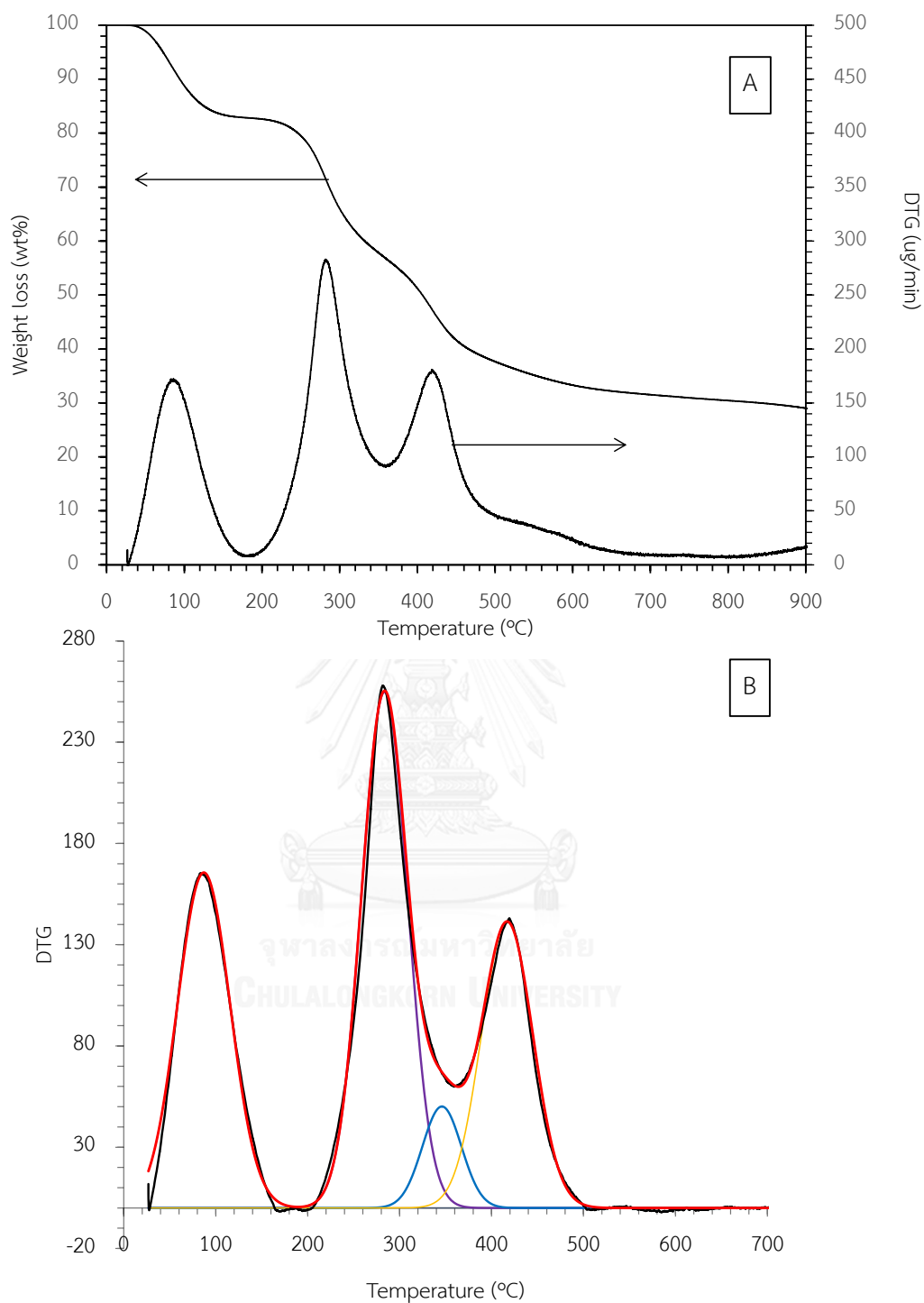
The formation of GL was favored when the acid catalyst was added into the reaction (Figure 4.11). An increase in the GL selectivity somewhat collaborated with a decrease in the glycerol yield and in the H-SL selectivity. Herein, there are two possible pathways for the GL formation. The first one is an acid-catalyzed conversion of H-SL to form GL and acetone. Another one is the esterification of glycerol with LA. Because LA is consisted of two functional groups in the same molecule, it can react with glycerol in two different reaction modes. The keto group of LA forms a Ketal by reacting with 1,2 or 1,3 hydroxyls of glycerol, while the acidic carboxyl group undergoes the esterification with glycerol. Therefore, LGO is generated via either the direct esterification of glycerol with LA or the transformation of GL with glycerol and LA. The resulting products are present as polymeric molecules of levulinic acid-glycerol ketal-ester oligomers (LGO) with different structure of terminal groups. The formation of LGO was enhanced when a large amount of acid catalyst and/or a high reaction temperature were used. The water generated from these reactions can take part in the hydrolysis reaction.

#### 4.2.4 Deactivation of Amberlyst 15 catalyst

Amberlyst 15 is a macro reticular polystyrene-based ion-exchange resin with strongly acidic sulfonic group. It is a powerful and selective acid catalyst for the esterification reactions due to a high acidity ( $4.7 \text{ mmol H}^{+1} \text{ g}^{-1}$ ) [35]. Herein, thermogravimetric/differential thermal analysis (TG/DTA) was used to study the thermal degradation behavior of organic compounds depositing on the surface of Amberlyst 15.

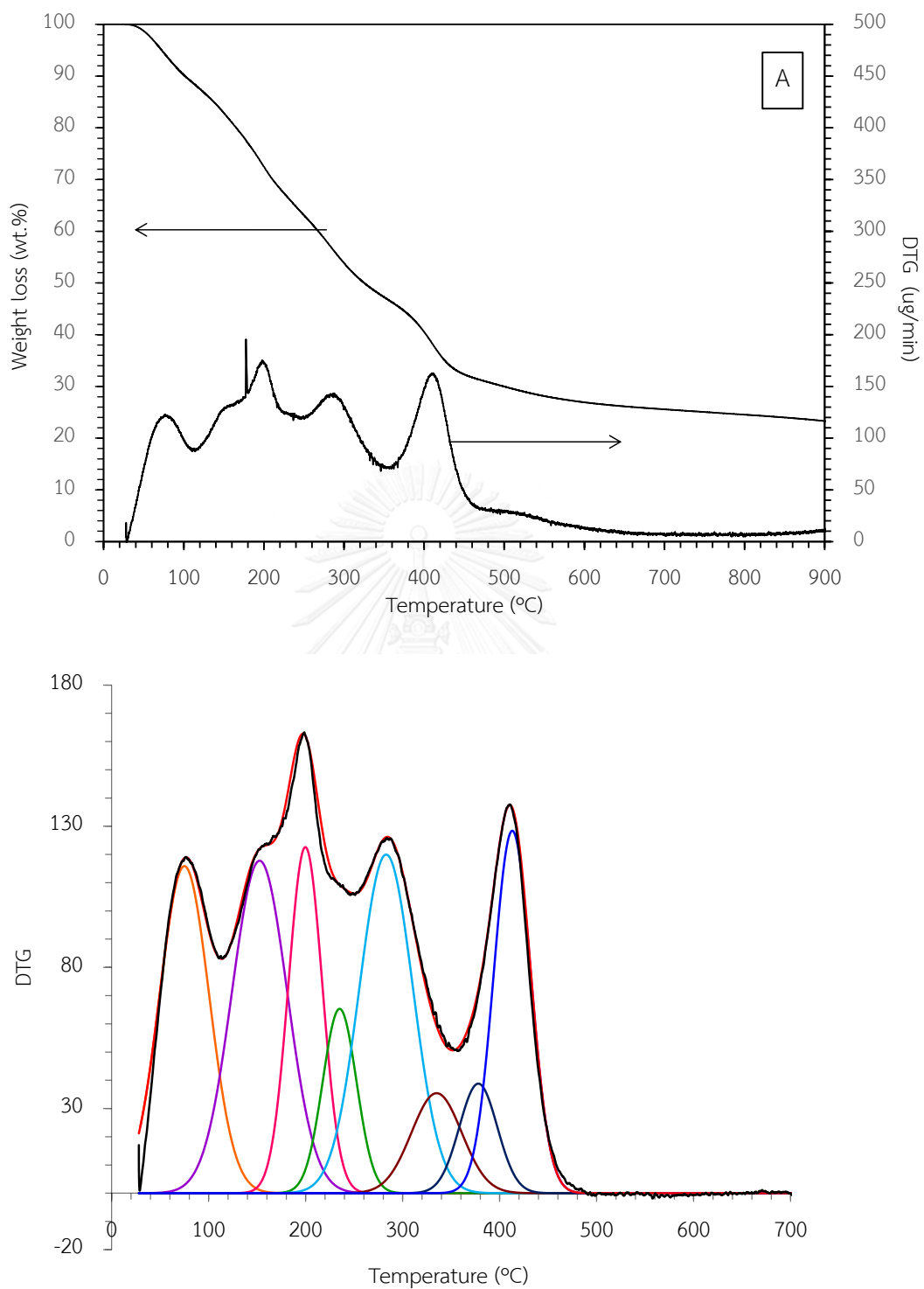
Figure 4.24 shows the weight loss and DTG curves obtained from the analysis of fresh Amberlyst15. The degradation of fresh Amberlyst 15 occurred in four steps. According to the literature [62-64], the loss of physisorbed water was observed below  $200 \text{ }^{\circ}\text{C}$ . The weight loss at  $278 \text{ }^{\circ}\text{C}$  was related to the decomposition of sulfonic acid groups. At  $350$  and  $425 \text{ }^{\circ}\text{C}$ , the polystyrene backbone was depolymerized, followed by degradation of divinyl benzene, respectively.

Figure 4.25 show the weight loss and DTG curves of spent Amberlyst 15. There were eight steps in the degradation of spent Amberlyst15. Besides the four decomposition steps observed for the fresh Amberlyst 15, the others were related to the decomposition of organic compounds presenting in the reaction mixture. The decomposition of SK and LA as reactant was found at  $146$  and  $197 \text{ }^{\circ}\text{C}$  [65-67], respectively. The weight loss at  $230 \text{ }^{\circ}\text{C}$  was ascribed to the decomposition of glycerol. The weight loss related to LGO was observed at  $385 \text{ }^{\circ}\text{C}$ . The total amount of reactants and products containing in the spent Amberlyst 15 was  $43 \text{ wt.}\%$ . Therefore, the deposition of organic compounds should be a cause of Amberlyst 15 deactivating.



**Figure 4.24** Weight loss and DTG curves of (A) fresh Amberlyst 15 and (B) deconvolution of DTG curve.





**Figure 4.25** Weight loss and DTG curves of (A) spent Amberlyst 15 and (B) deconvolution of DTG curve.

## CHAPTER V

### CONCLUSION AND RECOMMENDATIONS

#### 5.1 Conclusion

This study focused on the esterification of SK and LA over heterogeneous acid catalysts. Several solid catalysts (Amberlyst 15, Amberlyst 36 wet, HUSY zeolite, HMS-SO<sub>3</sub>H and NR/HMS-SO<sub>3</sub>H) were used to compare the catalytic performance. To achieve the higher conversion of SK and LA, the effect of reaction time, reaction temperature, catalyst loading, molar ratio of SK and LA were studied. SL was considered as a primary product. This compound was obtained from the reaction of SK and LA undergoes esterification. Generally, water is generated as a by-product of esterification. It is considered as an undesired product because it is a caused of reaction backward and ester hydrolysis. Interestingly, glycerol was found in all of experiments, it was obtained from SK hydrolysis. Thus, water elimination is required For the chemical structure identification, gas chromatography with mass spectroscopy (GC-MS) was used. Due to the water elimination difficultly, H-SL and GL were found in the products mixture. These compounds were formed by SL hydrolysis at the dioxolane ring. It can conclude that SK and its derivatives are not stable in water environment. Moreover, LA reacted with glycerol *via* ketalization to form oligomers. These compounds were investigated by <sup>13</sup>C nuclear magnetic resonance technique. There were three different end groups that terminated the oligomers, including keto terminal (KT), glycerol-ketal terminal (GKT), and glycerol-ester terminal (GET).

According to the screening of catalyst, Amberlyst 15 is a suitable solid acid catalyst because it enhances the SK and LA conversion, and minimizes the glycerol yield. Because of esterification is an endothermic reaction, increasing the reaction temperature is a way to enhance the reactants conversion and the products yield. However, Amberlyst 15 has operating limitation temperature at 120 °C so the reaction temperature should not higher than that temperature. Furthermore, the

optimum reaction conditions were 1:1 molar ration of SK and LA, catalyst loading of 5 wt.% respect to LA at 120 °C for 5 h.

### 5.1 Recommendations

The primary product (SL) was not found as a main component because water elimination difficultly. SK and SL were hydrolyzed and esterified to form other larger compounds, resulting in low product selectivity. Dean stark apparatus is suggested to solve this problem. Moreover, toluene is recommended as a solvent for water adsorption.



## REFERENCES

1. Werpy, T. and G. Petersen, *Top Value Added Chemicals from Biomass: Volume 1—Results of Screening for Potential Candidates from Sugars and Synthesis Gas*. U.S. Department of Energy, 2004. **1**: p. 1-67.
2. Climent, M.J., A. Corma, and S. Iborra, *Conversion of biomass platform molecules into fuel additives and liquid hydrocarbon fuels*. *Green Chemistry*, 2014. **16**(2): p. 516.
3. Démolis, A., N. Essayem, and F. Rataboul, *Synthesis and Applications of Alkyl Levulinates*. *ACS Sustainable Chemistry & Engineering*, 2014. **2**(6): p. 1338-1352.
4. Sah, P.P.T. and S.-Y. Ma, *Levulinic acid and its esters*. 1930. **52**: p. 4880-4883.
5. Schuette, H.A. and M.A. Cowley, *Levulinic acid II : The vapor pressure of its alkyl esters (C1-C6)*. 1931: p. 3485-3489.
6. Nandiwale, K.Y., S.K. Yadava, and V.V. Bokade, *Production of octyl levulinate biolubricant over modified H-ZSM-5: Optimization by response surface methodology*. *Journal of Energy Chemistry*, 2014. **23**(4): p. 535-541.
7. Suriyaprapadilok, N. and B. Kitiyanan, *Synthesis of Solketal from Glycerol and Its Reaction with Benzyl Alcohol*. *Energy Procedia*, 2011. **9**: p. 63-69.
8. Rodrigues, R., et al., *Solvent-free conversion of glycerol to solketal catalysed by activated carbons functionalised with acid groups*. *Catalysis Science & Technology*, 2014. **4**(8): p. 2293.
9. Rackemann, D.W. and W.O.S. Doherty, *The conversion of lignocellulosics to levulinic acid*. *Biofuels, Bioproducts and Biorefining*, 2011. **5**(2): p. 198-214.
10. Morone, A., M. Apte, and R.A. Pandey, *Levulinic acid production from renewable waste resources: Bottlenecks, potential remedies, advancements and applications*. *Renewable and Sustainable Energy Reviews*, 2015. **51**: p. 548-565.

11. Kamm, B., P.R. Gruber, and M. Kamm, *The Biofine Process – Production of Levulinic Acid, Furfural, and Formic Acid from Lignocellulosic Feedstocks*. Biorefineries – Industrial Processes and Products, 2006. **1**: p. 139-168.
12. Yan, L., et al., *Production of Levulinic Acid from Bagasse and Paddy Straw by Liquefaction in the Presence of Hydrochloride Acid*. CLEAN – Soil, Air, Water, 2008. **36**(2): p. 158-163.
13. Yan, K., et al., *Production and catalytic transformation of levulinic acid: A platform for speciality chemicals and fuels*. Renewable and Sustainable Energy Reviews, 2015. **51**: p. 986-997.
14. Redmon, B.C., *Process for the production of levulinic acid*. 1956.
15. Jinder Jow, Gregory L. Rorrer, and M.C. Hawley, *Dehydration of D-Fructose to Levulinic Acid over LZV Zeolite Catalyst*. Biomass 1987. **14**: p. 185-194.
16. Lourvand, K., *Partial Dehydration of Glucose to Oxygenated Hydrocarbons in Molecular-Sieving Catalysts*. 1995.
17. Schraufnagel, R.A. and H.F. Rase, *Levulinic Acid from Sucrose Using Acidic Ion-Exchange Resins*. Ind. Eng. Chem., Prod. Res. Dev., 1975. **14**(1): p. 40-44.
18. Hegner, J., et al., *Conversion of cellulose to glucose and levulinic acid via solid-supported acid catalysis*. Tetrahedron Letters, 2010. **51**(17): p. 2356-2358.
19. Buana, G., *Levulinic acid from lignocellulosic biomass*. 2007.
20. da Silva, C.X.A. and C.J.A. Mota, *The influence of impurities on the acid-catalyzed reaction of glycerol with acetone*. Biomass and Bioenergy, 2011. **35**(8): p. 3547-3551.
21. Rossa, V., et al., *Reaction Kinetic Study of Solketal Production from Glycerol Ketalization with Acetone*. Industrial & Engineering Chemistry Research, 2017. **56**(2): p. 479-488.
22. Perosa, A., et al., *Synthesis of the Fatty Esters of Solketal and Glycerol-Formal: Biobased Specialty Chemicals*. Molecules, 2016. **21**(2): p. 170.
23. Menezes, F.D.L., M.D.O. Guimaraes, and M.J. da Silva, *Highly Selective SnCl<sub>2</sub>-Catalyzed Solketal Synthesis at Room Temperature*. Industrial & Engineering Chemistry Research, 2013. **52**(47): p. 16709-16713.

24. Nanda, M.R., et al., *A new continuous-flow process for catalytic conversion of glycerol to oxygenated fuel additive: Catalyst screening*. Applied Energy, 2014. **123**: p. 75-81.
25. Deutsch, J., A. Martin, and H. Lieske, *Investigations on heterogeneously catalysed condensations of glycerol to cyclic acetals*. Journal of Catalysis, 2007. **245**(2): p. 428-435.
26. Roldán, L., et al., *Glycerol upgrading by ketalization in a zeolite membrane reactor*. Asia-Pacific Journal of Chemical Engineering, 2009. **4**(3): p. 279-284.
27. Pileidis, F.D., et al., *Esterification of levulinic acid into ethyl levulinate catalysed by sulfonated hydrothermal carbons*. Chinese Journal of Catalysis, 2014. **35**(6): p. 929-936.
28. Dharne, S. and V.V. Bokade, *Esterification of levulinic acid to n-butyl levulinate over heteropolyacid supported on acid-treated clay*. Journal of Natural Gas Chemistry, 2011. **20**(1): p. 18-24.
29. Gonzalez-Arellano, C., R.A.D. Arancon, and R. Luque, *Al-SBA-15 catalysed cross-esterification and acetalisation of biomass-derived platform chemicals*. Green Chem., 2014. **16**(12): p. 4985-4993.
30. Pierpont, A.W., et al., *Origins of the Regioselectivity in the Lutetium Triflate Catalyzed Ketalization of Acetone with Glycerol: A DFT Study*. ACS Catalysis, 2015. **5**(2): p. 1013-1019.
31. Manjunathan, P., et al., *Room temperature synthesis of solketal from acetalization of glycerol with acetone: Effect of crystallite size and the role of acidity of beta zeolite*. Journal of Molecular Catalysis A: Chemical, 2015. **396**: p. 47-54.
32. Castanheiro, J.E., et al., *Esterification of acetic acid by isoamylic alcohol over catalytic membranes of poly(vinyl alcohol) containing sulfonic acid groups*. Applied Catalysis A: General, 2006. **311**: p. 17-23.
33. Heveling, J., *Heterogeneous Catalytic Chemistry by Example of Industrial Applications*. Journal of Chemical Education, 2012. **89**(12): p. 1530-1536.

34. Liu, Y., E. Lotero, and J.G. Goodwin, *Effect of water on sulfuric acid catalyzed esterification*. Journal of Molecular Catalysis A: Chemical, 2006. **245**(1-2): p. 132-140.
35. Rammohan, P.T., S.; Shampa, K.; , *Amberlyst-15 in organic synthesis*. ARKIVOC p. 570-609.
36. Klaewkla, R., M. Arend, and W. F., *A Review of Mass Transfer Controlling the Reaction Rate in Heterogeneous Catalytic Systems*. 2011.
37. Dittmeyer, R. and G. Emig, *Simultaneous Heat and Mass Transfer and Chemical Reaction*. Handbook of Heterogeneous Catalysis, 2008: p. 1189-1261.
38. Tanabe, K. and H. W.F.;, *Industrial application of solid acid±base catalysts*. Applied Catalysis A: General 1999. **181**: p. 399-434.
39. Ehteshami, M., et al., *Kinetic study of catalytic hydrolysis reaction of methyl acetate to acetic acid and methanol*. Iranian Journal of Science & Technology, Transaction B, Engineering, , 2006. **30**(B5): p. 595-606.
40. Liu, X.Y., et al., *Preparation of a carbon-based solid acid catalyst by sulfonating activated carbon in a chemical reduction process*. Molecules, 2010. **15**(10): p. 7188-96.
41. Nuntang, S., et al., *Organosulfonic acid-functionalized mesoporous composites based on natural rubber and hexagonal mesoporous silica*. Materials Chemistry and Physics, 2014. **147**(3): p. 583-593.
42. Hu, X., et al., *One-Pot Synthesis of Levulinic Acid/Ester from C5 Carbohydrates in a Methanol Medium*. ACS Sustainable Chemistry & Engineering, 2013. **1**(12): p. 1593-1599.
43. Nandiwale, K.Y., et al., *Catalytic upgrading of renewable levulinic acid to ethyl levulinate biodiesel using dodecatungstophosphoric acid supported on desilicated H-ZSM-5 as catalyst*. Applied Catalysis A: General, 2013. **460-461**: p. 90-98.
44. Pasquale, G., et al., *Catalytic upgrading of levulinic acid to ethyl levulinate using reusable silica-included Wells-Dawson heteropolyacid as catalyst*. Catalysis Communications, 2012. **18**: p. 115-120.

45. Melero, J.A., et al., *Efficient conversion of levulinic acid into alkyl levulinates catalyzed by sulfonic mesostructured silicas*. Applied Catalysis A: General, 2013. **466**: p. 116-122.
46. Patil, C.R., et al., *Esterification of levulinic acid to ethyl levulinate over bimodal micro-mesoporous H/BEA zeolite derivatives*. Catalysis Communications, 2014. **43**: p. 188-191.
47. Fernandes, D.R., et al., *Levulinic acid esterification with ethanol to ethyl levulinate production over solid acid catalysts*. Applied Catalysis A: General, 2012. **425-426**: p. 199-204.
48. Yan, K., et al., *One-step synthesis of mesoporous H4SiW12O40-SiO2 catalysts for the production of methyl and ethyl levulinate biodiesel*. Catalysis Communications, 2013. **34**: p. 58-63.
49. Kuwahara, Y., T. Fujitani, and H. Yamashita, *Esterification of levulinic acid with ethanol over sulfated mesoporous zirconosilicates: Influences of the preparation conditions on the structural properties and catalytic performances*. Catalysis Today, 2014. **237**: p. 18-28.
50. Oliveira, B.L. and V. Teixeira da Silva, *Sulfonated carbon nanotubes as catalysts for the conversion of levulinic acid into ethyl levulinate*. Catalysis Today, 2014. **234**: p. 257-263.
51. Budarin, V.L., et al., *Versatile mesoporous carbonaceous materials for acid catalysis*. Chem Commun (Camb), 2007(6): p. 634-6.
52. Li, Z., et al., *Synthesis and characterization of sulfated TiO2 nanorods and ZrO2/TiO2 nanocomposites for the esterification of biobased organic acid*. ACS Appl Mater Interfaces, 2012. **4**(9): p. 4499-505.
53. Girisuta B. , Janssen L. P. B. M. , and H.H. J., *Kinetic Study on the Acid-Catalyzed Hydrolysis of Cellulose to Levulinic Acid*. Industrial & Engineering Chemistry Research, 2007. **46**: p. 1696-1708.
54. Mellmer, M.A., et al., *Selective Production of Levulinic Acid from Furfuryl Alcohol in THF Solvent Systems over H-ZSM-5*. ACS Catalysis, 2015. **5**(6): p. 3354-3359.



55. Amarasekara, A.S. and S.A. Hawkins, *Synthesis of levulinic acid-glycerol ketal-ester oligomers and structural characterization using NMR spectroscopy*. European Polymer Journal, 2011. **47**(12): p. 2451-2457.
56. Nuntang, S., et al., *Novel mesoporous composites based on natural rubber and hexagonal mesoporous silica: Synthesis and characterization*. Materials Chemistry and Physics, 2014. **143**(3): p. 1199-1208.
57. Wang, Y., et al., *Influence of Thermal Treatment of HUSY on Catalytic Pyrolysis of Polypropylene: An Online Photoionization Mass Spectrometric Study*. Energy & Fuels, 2016. **30**(6): p. 5122-5129.
58. Zanin, F.G., et al., *A one-pot glycerol-based additive-blended ethyl biodiesel production: a green process*. Bioresour Technol, 2013. **143**: p. 126-30.
59. Victor, A., I.N. Pulidindi, and A. Gedanken, *Levulinic acid production from Cicer arietinum, cotton, Pinus radiata and sugarcane bagasse*. RSC Adv., 2014. **4**(84): p. 44706-44711.
60. Cassel, S., et al., *Original Synthesis of Linear, Branched and Cyclic Oligoglycerol Standards*. European Journal of Organic Chemistry, 2001. **2001**(5): p. 875-896.
61. Vera L. P. Soares, et al., *New Applications for Soybean Biodiesel Glycerol, Soybean - Applications and Technology*. 2011: p. 151-172.
62. Ordonsky, V.V., et al., *Foam supported sulfonated polystyrene as a new acidic material for catalytic reactions*. Chemical Engineering Journal, 2012. **207-208**: p. 218-225.
63. Liu, F., et al., *High-temperature synthesis of strong acidic ionic liquids functionalized, ordered and stable mesoporous polymers with excellent catalytic activities*. Green Chemistry, 2012. **14**(5): p. 1342.
64. Fan, G., et al., *Amberlyst 15 as a new and reusable catalyst for the conversion of cellulose into cellulose acetate*. Carbohydr Polym, 2014. **112**: p. 203-9.
65. Moity, L., et al., *Glycerol acetals and ketals as bio-based solvents: positioning in Hansen and COSMO-RS spaces, volatility and stability towards hydrolysis and autoxidation*. Green Chem., 2015. **17**(3): p. 1779-1792.

66. Gómez-Siurana, A., et al., *TGA/FTIR study of tobacco and glycerol–tobacco mixtures*. *Thermochimica Acta*, 2013. **573**: p. 146-157.
67. Cyras, V.P., M.C. Tolosa Zenklusen, and A. Vazquez, *Relationship between structure and properties of modified potato starch biodegradable films*. *Journal of Applied Polymer Science*, 2006. **101**(6): p. 4313-4319.





## Appendix A

### The Calibration Curves of Solketal and Levulinic acid

The calibration curves were applied to analyze both of SK and LA conversion in the esterification. These curves were plotted by the data obtained from the GC chromatogram. Y-axis was the molar ratio of SK or LA, and standard solution while X-axis was the peak area ratio of SK or LA, and standard solution. This method used methyl undecanoate (C<sub>11</sub>) as the internal standard. Table A1 shows the molar ratio and peak area ratio for plot the calibration curve of SK. Table A2 shows the molar ratio and peak area ratio for plot the calibration curve of LA.

**Table A1** The molar ratio and peak area ratio of SK to internal standard for plot the calibration curve of SK

Molar ratio of SK to internal standard	Peak area ratio of SK to internal standard
4.3333	2.2290
3.4667	1.6908
2.6000	1.2600
1.7333	0.8168
0.8667	0.4601
0.0000	0.0000

**Table A2** The molar ratio and peak area ratio of LA to internal standard for plot the calibration curve of LA

Molar ratio of LA to internal standard	Peak area ratio of LA to internal standard
4.3333	2.4592
3.4667	1.9127
2.6000	1.3782
1.7333	0.9190
0.8667	0.4598
0.0000	0.0000

Figure A1 shows the calibration curve of SK which has  $R^2$  at 0.9968. And, Figure A2 shows the calibration curve of LA which has  $R^2$  at 0.9976. These calibration curve have the accuracy and able to use in the quantitative analysis.

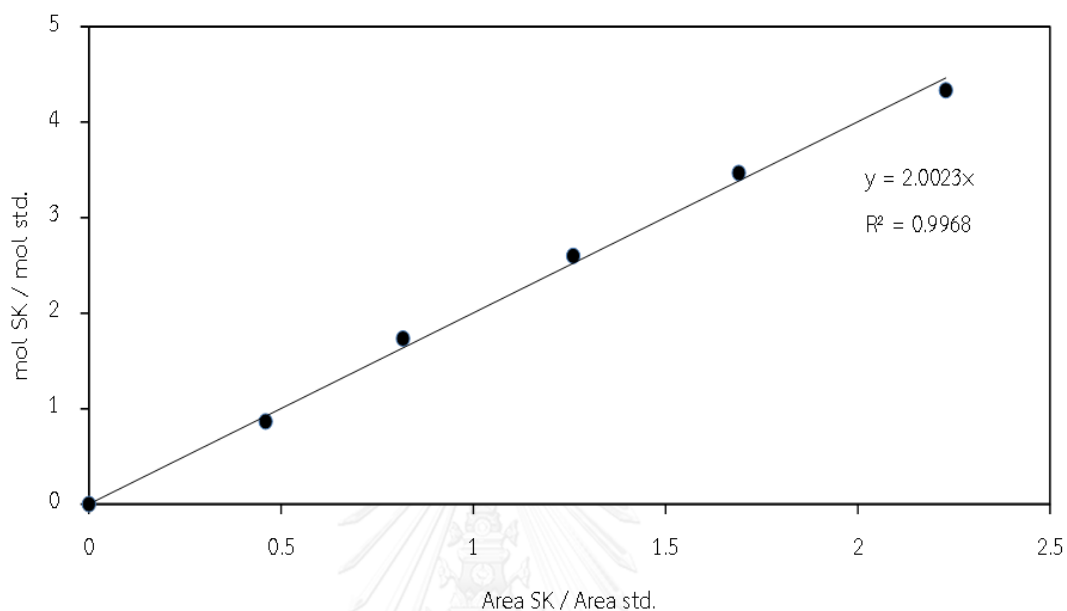


Figure A1 The calibration curve of SK

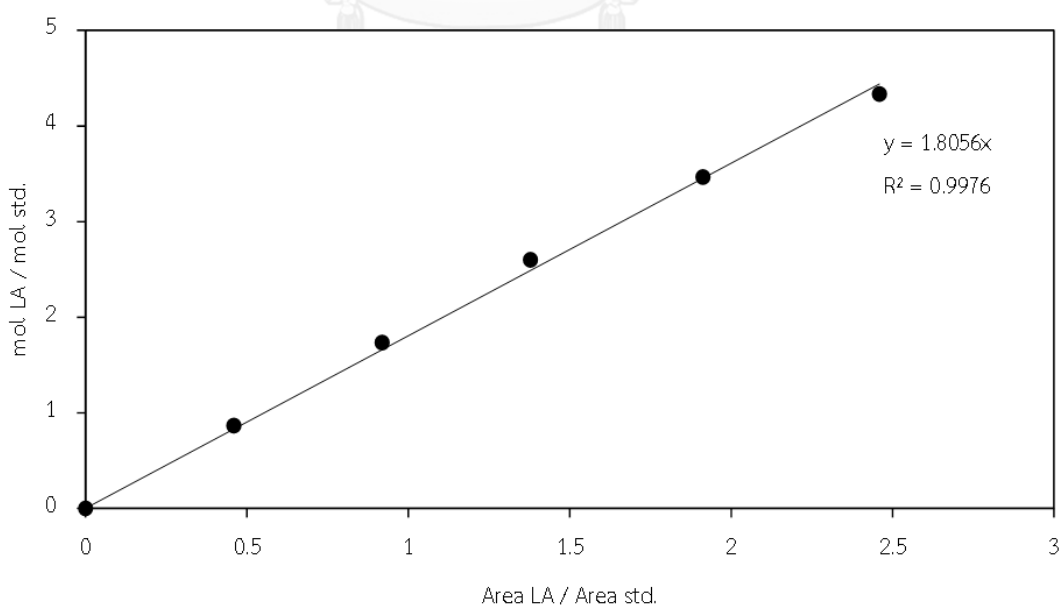


Figure A2 The calibration curve of LA

## Appendix B

### The Calibration Curves of Glycerol

The calibration curve of glycerol was applied to analyze the glycerol yield in the esterification. Y-axis was the molar ratio of glycerol and standard solution while X-axis was the peak area ratio of glycerol and standard solution. This method used methyl undecanoate (C<sub>11</sub>) as the internal standard. Table A1 shows the molar ratio and peak area ratio for plot the calibration curve of glycerol. Table B1 shows the molar ratio and peak area ratio for plot the calibration curve of glycerol. Figure B1 shows the calibration curve of glycerol which has R<sup>2</sup> at 0.9961

**Table B1** The molar ratio and peak area ratio of glycerol to internal standard for plot the calibration curve of glycerol

Molar ratio of glycerol to internal standard	Peak area ratio of glycerolto internal standard
0.0000	0.0000
0.8000	0.5146
1.6000	1.0257
2.4000	1.6193
3.2000	2.3001
4.0000	2.8606

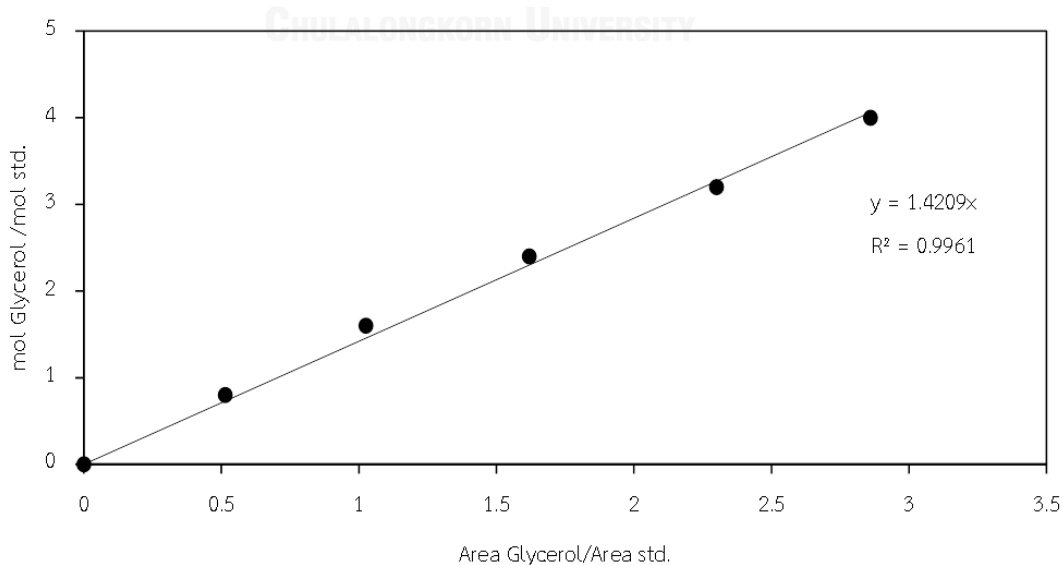


**Figure B1** The calibration curve of glycerol

## Appendix C

### Fragmentation Ions patterns

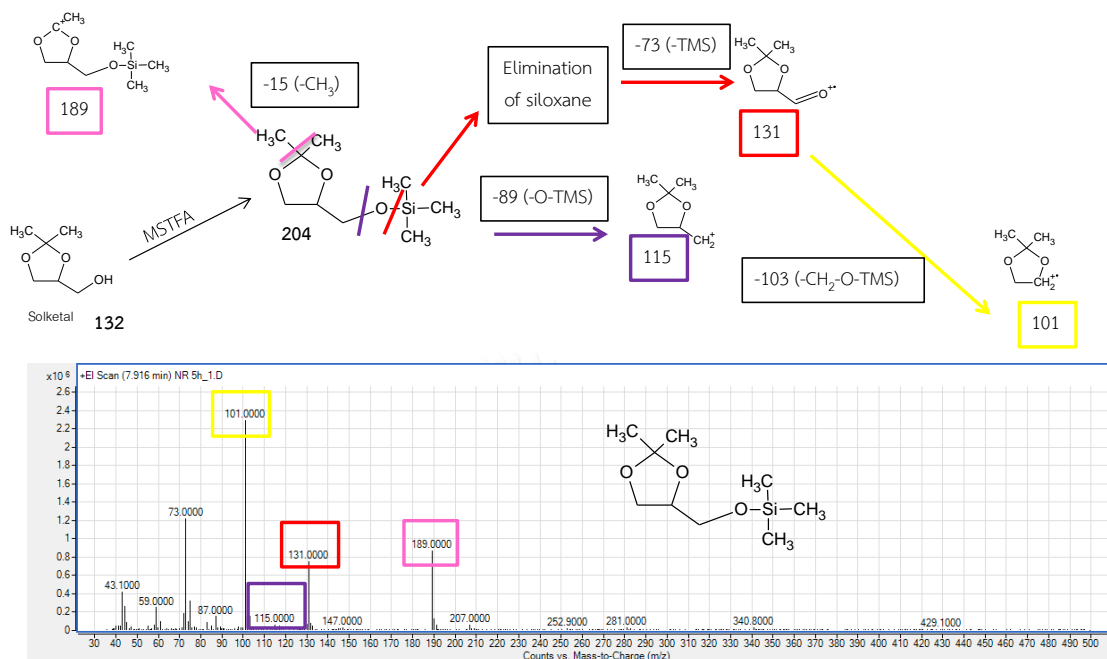


Figure C1 Fragmentation pattern of SK

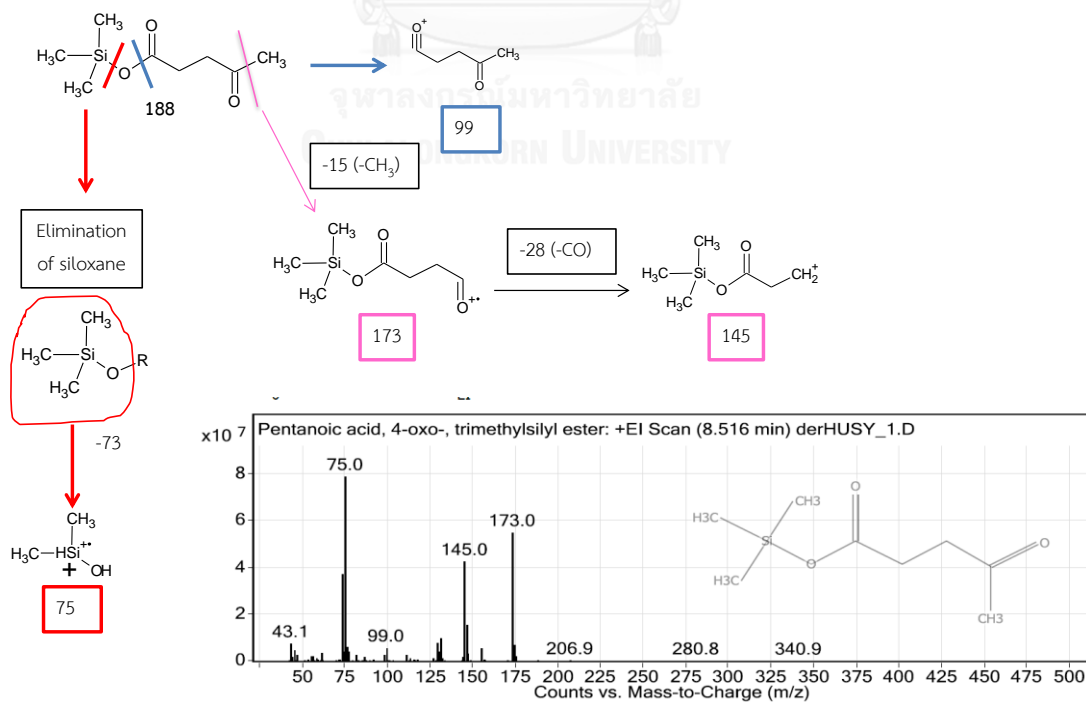


Figure C2 Fragmentation pattern of LA

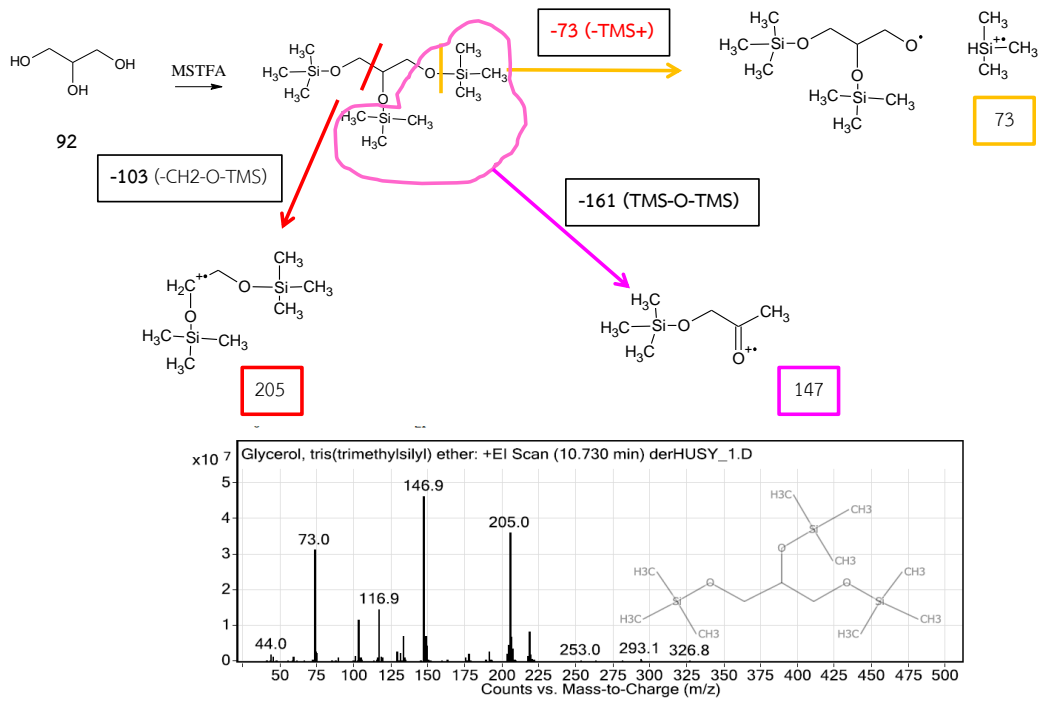


Figure C3 Fragmentation pattern of glycerol

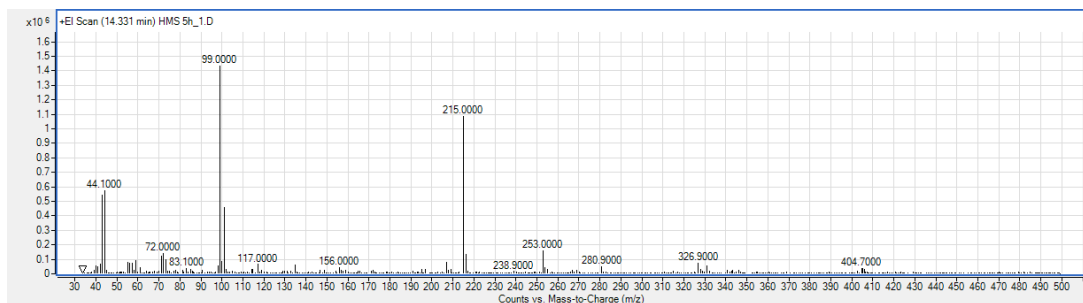
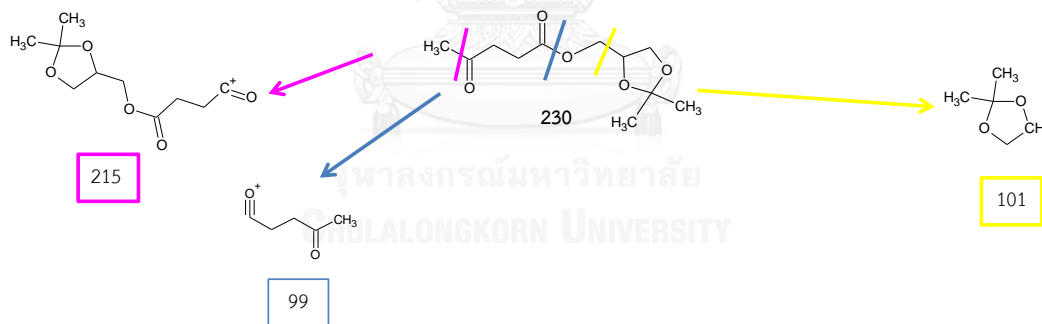


Figure C4 Fragmentation pattern of SL



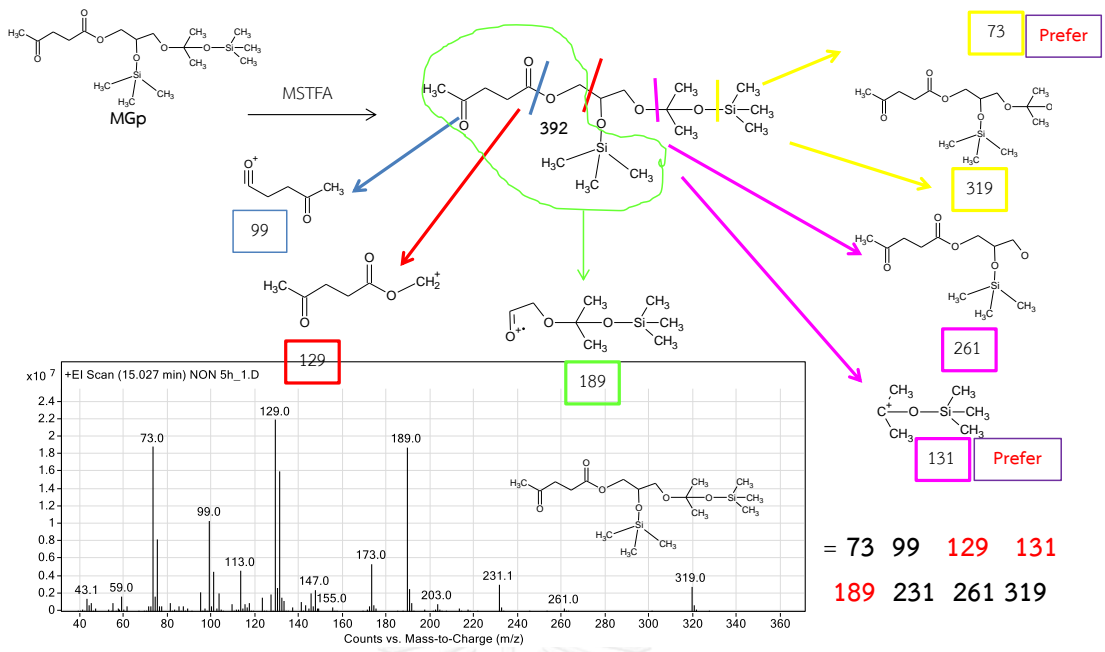


Figure C5 Fragmentation pattern of H-SL

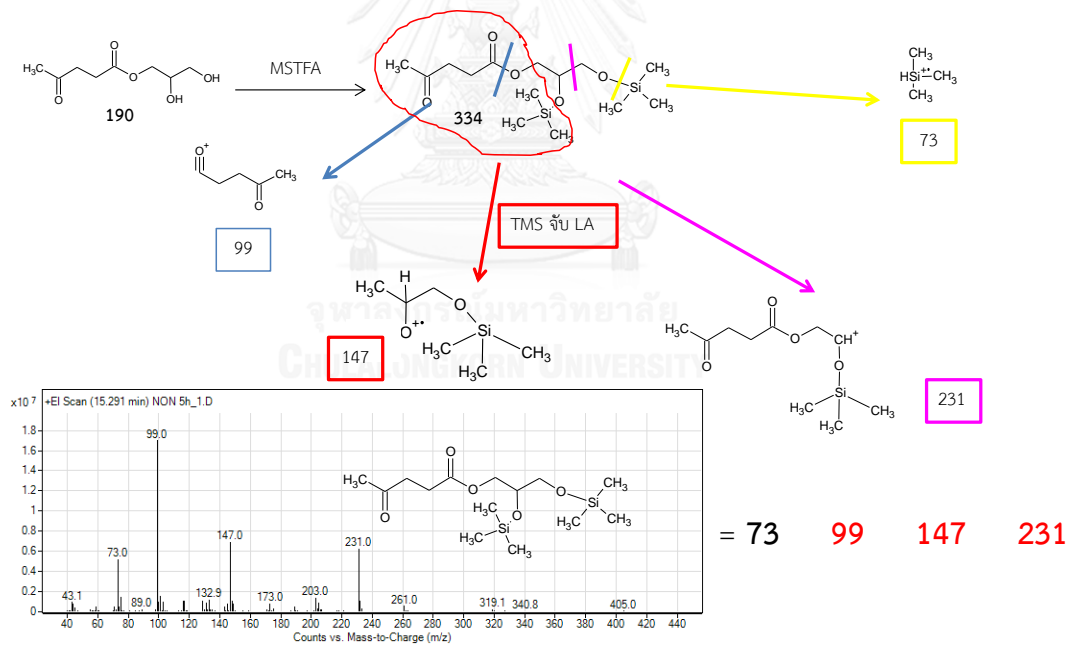


Figure C6 Fragmentation pattern of GL

## VITA

Mr. Sorrakan Sutinno was born on July 25th, 1989 at Bangkok, Thailand. He graduated high school from Nawamintrachunuthit Triamudomsuksanomkiao School. He graduated the Bachelor's degree of Science in Petrochemical Technology (International programme), King Mongkut's Institute of Technology Ladkrabang in 2012. He has continued to study in Master's degree, majoring in Petrochemistry and Polymer Science, Faculty of Science, Chulalongkorn University, Bangkok, Thailand since 2013 and finished his study in 2017.

Presentation: November 2015 “Esterification of Solketal and Levulinic Acid over Heterogeneous Acid Catalysts” with the oral presentation in The 5th TICHe International Conference 2015, Pattaya, Thailand which organized by Kasetsart University.

